

Breakdown and restoration of brain synchronization in blindness

Dissertation

Zur Erlangung des akademischen Grades

doctor rerum naturalium

(Dr. rer. nat.)

genehmigt durch die Fakultät für Naturwissenschaften
der Otto-von-Guericke Universität Magdeburg

von: Michal Bola, Magister in Psychologie
geboren am 29. März 1986 in Ciechanow (Poland)

Gutachter: Prof. Dr. Lutz Jäncke
Prof. Dr. Bernhard A. Sabel

engereicht am: 25. November 2014

verteidigt am: 24. März 2015

Abstract

Blindness is not only caused by problems of the eye's optics but it can be caused also by damage to the nervous system tissue. There are different diseases affecting the retina and optic nerve, including glaucoma, age related macular degeneration, and optic neuritis. Such vision loss is a "silent epidemic" with a prevalence of 160 million people worldwide.

Peripheral damage to the retina and optic nerve prevents visual information from reaching visual cortex where the visual input is processed. Consequently areas of the visual field retinotopically corresponding to the damaged tissue are blind (scotoma). But such lesions are typically diffuse and incomplete, and visual field areas corresponding to the uninjured tissue are preserved. Because such acquired partial blindness severely affects the patients' quality of life, we urgently need to understand the brain mechanisms of vision loss to eventually design better strategies of preventing and treating vision loss.

Vision loss is associated with anterograde degeneration of deafferented structures along the visual pathway, but there is also plasticity and adaptive reorganization of the damaged structure itself and its projection zones. Yet, the majority of studies investigated only micro-scale changes in early visual structures (e.g. lateral geniculate nucleus and V1) and little is known about the role of large-scale cortical networks and their reorganization in vision loss. Vision loss might disturb communication within the brain's neuronal network and disturbed network state may, in turn, hamper residual visual abilities. In this thesis I present three studies conducted to investigate the state of brain networks in vision loss and to characterize their role in perception.

In a first exploratory study (Study I) I studied temporal processing deficits in the "intact" visual field as a possible indicator of network-wide changes in brains of vision loss patients. Deficits in visual field regions quite distant from the scotoma have been observed and interpreted as a reflection of the global network impairment. In further experiments (Studies II and III) the electroencephalography (EEG) was used to record spontaneous, resting-state brain activity in patients with vision loss and control subjects. Spatial and temporal patterns of brain activity and functional connectivity were then related to visual perceptual capabilities of patients. I found that alpha band activity, specifically high alpha band (11-14Hz), is disturbed in patients and the extent of this disturbance correlates with vision measures. Alpha band disturbances include lower amplitude of oscillations, weaker

coherence, and altered small-world features of coherence networks (e.g. clustering and path length). Patients with vision loss were then treated with the application of alternating current stimulation (ACS) for 10 days to see if modulation the brain functional network through synchronization would improve vision. I found that ACS increased the alpha-band power and functional connectivity in patients and that greater post-ACS alpha increase was related to greater vision restoration (Study II). This further substantiates the role of the brain network state, particularly spontaneous alpha activity, as a biomarker of vision loss.

My findings indicate that the state of large-scale cortical networks might be crucial for visual perception. This is in line with earlier studies showing how perception depends on the instantaneous brain network state in normal vision and with studies where vision was improved by modulation of brain networks. Thus, the view of vision loss as a simple lack of bottom-up input might be oversimplified. I propose a new theoretical model of vision loss which explains that vision loss after a peripheral (optic nerve) lesion is a function of both, reduced (bottom-up) input and disturbed network state (top-down influences). This broader understanding has the potential to influence future efforts to prevent and restore vision.

Zusammenfassung

Erbindingen sind nicht nur Folge von Läsionen des optischen Apparates sondern können auch durch Hirnschädigungen bedingt sein. Verschiedene Erkrankungen betreffen die Retina oder die Sehnerven, zu nennen sind hier insbesondere die Glaukomerkrankung, die altersbedingte Makuladegeneration und Sehnerventzündungen. Sehverlust erreicht ein epidemisches Ausmaß mit einer weltweiten Prävalenz von 160 Millionen Menschen.

Periphere Schädigungen der Retina oder des Sehnerven behindern den Informationsfluss zum visuellen Kortex wo der visuelle Input verarbeitet wird. Aufgrund dessen sind jene Bereiche des Gesichtsfeldes von Erblindung betroffen (Skotome), die retinotopisch dem geschädigten Gewebe entsprechen. Diese Schädigungen sind jedoch typischerweise diffus und nicht vollständig und Gesichtsfeldbereiche, die dem unverletzten Gewebe entsprechen, bleiben erhalten. Da erworbene Teilerblindung die Lebensqualität der Betroffenen gravierend beeinträchtigen kann, ist ein verbessertes Verständnis der Mechanismen des Sehverlusts die Grundlage zur Entwicklung verbesserter Strategien zur Vorbeugung und Behandlung von Sehverlust.

Sehverlust geht mit einer anterograden Degenation der deafferentierten Strukturen entlang der Sehbahn einher, wobei auch Plastizität und adaptive Reorganisation der geschädigten Strukturen und deren Projektionsarealen beobachtet werden können. In der Mehrzahl vorliegender Studien wurden jedoch nur umschriebene Veränderungen in frühen visuellen Strukturen (Corpus geniculatum laterale, LGN und V1) untersucht. Über die Rolle räumlich ausgedehnter kortikaler Netzwerke und deren Reorganisation bei Sehverlust ist jedoch wenig bekannt. Bei Sehverlust kann die Kommunikation im neuronalen Netzwerk des Gehirns beeinträchtigt sein, wobei durch ein gestörtes Netzwerk auch wiederum die Nutzung der verbliebenen Sehleistung beeinträchtigt sein kann.

In dieser Arbeit stelle ich drei Studien vor, die mit dem Ziel durchgeführt wurden, den Zustand der Hirnnetzwerke bei Sehverlust zu untersuchen und deren Rolle für die visuelle Wahrnehmung zu charakterisieren. In einer ersten explorativen Arbeit (Studie I) wurden zeitliche Verarbeitungsdefizite im „intakten“ Gesichtsfeld als möglicher Indikator für Veränderungen in Hirnnetzwerken bei Patienten mit Sehverlust untersucht. Die in intakten Gesichtsfeldbereichen beobachteten Defizite wurden als Anzeichen einer globalen Beeinträchtigung des Hirnnetzwerkes interpretiert. In weiteren Experimenten (Studie II und

III) wurde das Elektroenzephalogramm eingesetzt, um spontane Hirnaktivität in Ruhe bei Patienten mit Sehverlust und Kontrollprobanden zu untersuchen. Räumliche und zeitliche Muster der Hirnaktivität und funktionellen Konnektivität wurden mit den Sehleistungen der Patienten in Bezug gesetzt. Ich konnte beobachten, dass die Aktivität im Alphaband, insbesondere im hohen Bereich (11-14Hz) bei Patienten beeinträchtigt ist, wobei das Ausmaß der Alphabandreduktion mit den Sehbeeinträchtigungen korreliert. Die Beeinträchtigungen des Alphabandes umfassen niedrigere Amplituden der Oszillationen, geringere Kohärenz und veränderte small-world Charakteristiken des Kohärenznetzwerkes (z.B. Gruppierung und Pfadlänge). Die sehbeeinträchtigten Patienten wurden mit Wechselstromstimulation (alternating current stimulation, ACS) über einen Zeitraum von 10 Tagen behandelt, um zu untersuchen, ob durch Modulation des funktionellen Hirnnetzwerkes durch Synchronisation die Sehleistung verbessert werden kann. Ich beobachtete, dass ACS die Power im Bereich des Alphabandes und die funktionelle Konnektivität stärkt, wobei ein höherer Anstieg der Alphapower nach ACS mit ausgeprägterer visueller Restitution einherging (Studie II). Dieses Ergebnis untermauert die Annahme, dass der Zustand des Hirnnetzwerkes, insbesondere die spontane Alphaktivität, als Biomarker für Sehverlust betrachtet werden kann.

Die Ergebnisse meiner Arbeit weisen darauf hin, dass räumlich ausgedehnte kortikale Netzwerke für die visuelle Wahrnehmung von entscheidender Bedeutung sind. Dies entspricht auch früheren Studien, die zum einen zeigten, dass die Wahrnehmungsleistung auch bei unbeeinträchtigtem Sehvermögen vom aktuellen Zustand des Hirnnetzwerkes abhängt und weiteren Studien zur Verbesserung der Sehleistung durch Modulation von Hirnnetzwerken. Somit sollte Sehverlust nicht in vereinfachter Weise ausschließlich als ein Verlust von bottom-up Input betrachtet werden. Ich schlage ein neues theoretisches Modell für Sehverlust vor, welches Sehverlust nach peripheren (Sehnerv) Läsionen als eine Funktion von sowohl reduziertem bottom-up Input als auch eines beeinträchtigten Zustands des Hirnnetzwerkes (top-down Einflüsse) betrachtet. Diese erweiterte Betrachtungsweise hat das Potential zukünftige Untersuchungen zur Vorbeugung und Wiederherstellung von Sehfunktionen zu beeinflussen.

Acknowledgments

I would like to express my gratitude to my supervisor and mentor, Prof. Bernhard A. Sabel, for his support and encouragement. Thank you for providing guidance at the beginning of my work, and space to independently develop my own ideas towards the end of my studies.

The experiments described in this thesis were conducted by researchers and technician working at the Institute of Medical Psychology before I joined the team and my contribution to the projects was data management and analysis, development of new data analysis techniques, as well as interpretation of results and writing of publications. Therefore, I would like to thank Dr. Carolin Gall, Anton Fedorov, Nicole Mäter, Sandra Heinrich, Antonia Borrmann, Lisa Ernst, and Eileen Poloski who organized and conducted studies and clinical trials in which the analyzed data were obtained.

When analyzing EEG data I collaborated with Prof. Herman Hinrichs (OvGU Neurology Department) and Dr. Christina Moewes (OvGU Computer Science Department).

I further would like to thank Dr. Sylvia Prillof and Steffi Matzke for their administrative assistance.

I greatly appreciated company of my colleagues, with whom I worked at the Institute of Medical Psychology for a longer or shorter time – Dr. Petra Henrich-Noack, Dr. Elena Sergeeva, Benedikt Steager, Younes Tabi, Ting Li, and Ying Gao.

Although when working on this thesis in the past four years I did not have enough time for my family and friends, I constantly experienced their support and encouragement for which I am very grateful.

Finally, thank you, Ola, for everything.

Abbreviations

ACS – alternating current stimulation
AMD – age-related macular degeneration
AOI – area of interest
ARV – areas of residual vision
DCS – direct current stimulation
DFA – detrended fluctuations analysis
EEG - electroencephalography
FIR – finite impulse response (filter)
fMRI - functional magnetic resonance imaging
GC – Granger Causality
HFD – Higuchi Fractal Dimension
HRP – high resolution perimetry
LGN – lateral geniculate nucleus (of the thalamus)
LPZ – lesion projection zone
MEG - magnetoencephalography
ON - optic nerve
PET – positron emission tomography
PLV – phase locking value
RT – reaction time
rtACS – repetitive transorbital alternating current stimulation
TMS – transcranial magnetic stimulation
V1 – primary visual cortex
VRT – vision restoration training

Table of Contents

1. Introduction.....	15
<i>1.1 Visual system damage.....</i>	<i>15</i>
1.1.1 Organization of the visual system.....	15
1.1.2 Perceptual consequences of visual system damage.....	16
1.1.2.1 “Sightblind” – perceptual deficits in the intact visual field.....	19
1.1.3 Neurophysiological consequences of visual system damage.....	21
1.1.3.1 Anterograde degeneration.....	22
1.1.3.2 Local plasticity.....	22
1.1.3.3 Effects on large-scale functional networks.....	23
1.1.4 Vision restoration.....	24
1.1.5 Vision loss: open questions.....	25
<i>1.2 Brain networks.....</i>	<i>25</i>
1.2.1 Communication in the brain.....	25
1.2.2 Brain connectivity networks.....	28
1.2.2.1 Structural and functional connectivity.....	28
1.2.2.2 Neuroimaging methods to study functional interactions.....	29
1.2.2.3 Brain spontaneous activity – the “resting-state” paradigm.....	30
1.2.2.4 Brain communication in pathological conditions.....	31
1.2.2.5 Graph theory.....	32
<i>1.3 Problem formulation and hypotheses.....</i>	<i>34</i>
2. Study I: Perceptual deficits in the “intact” visual field.....	37
<i>2.1 Study I: Introduction.....</i>	<i>37</i>
<i>2.2 Study I: Methods.....</i>	<i>38</i>
2.2.1 Ethics statement.....	38
2.2.2 Subjects.....	38
2.2.3 High Resolution Perimetry.....	39
2.2.3.1 HRP-based exclusion criteria.....	40
2.2.3.2 HRP analysis.....	40
2.2.3.3 Scotoma features and intact field RT.....	41
2.2.4 Statistics.....	42
<i>2.3 Study I: Results.....</i>	<i>43</i>

2.3.1 Intact field RT is higher in patients than in control subjects.....	43
2.3.2 RT is related to the functional state of the visual field.....	43
2.3.3 Local effect: intact field RT is related to the functional state of the immediate surround.....	43
2.3.4 Global effect: intact field RT is related to the scotoma size.....	44
2.3.5 Interhemispheric effect: intact field RT in quadrantanopia.....	45
2.4 Study I: Discussion.....	46
2.4.1 Perceptual deficits in the “intact” visual field of patients.....	47
2.4.2 Local effect of the visual system lesion.....	47
2.4.3 Global effect of visual system lesions.....	48
2.4.4 Clinical relevance of the intact field perceptual deficits.....	49
2.4.5 Conclusions.....	49
3. Study II: Breakdown of functional connectivity networks in blindness.....	51
3.1 Study II: Introduction.....	51
3.2 Study II: Methods.....	52
3.2.1 Patient consents.....	52
3.2.2 Subjects.....	52
3.2.3 Data acquisition.....	53
3.2.3.1 High Resolution Perimetry.....	53
3.2.3.2 Static perimetry, kinetic perimetry, and visual acuity.....	54
3.2.3.3 Questionnaires.....	55
3.2.3.4 EEG recordings.....	55
3.2.4 Electrical stimulation protocol.....	55
3.2.5 EEG data analysis.....	56
3.2.5.1 Preprocessing.....	56
3.2.5.2 Spectral power.....	56
3.2.5.3 Functional connectivity estimation.....	57
3.2.5.4 Graphs analysis.....	57
3.2.6 Statistical analyses.....	58
3.3 Study II: Results.....	59
3.3.1 Power spectra.....	59
3.3.2 Short-range functional connectivity.....	60
3.3.3 Long-range functional connectivity.....	61
3.3.4 Graphs analysis.....	62
3.3.5 Functional significance of EEG measures.....	63
3.4 Study II: Discussion.....	65

3.4.1 Visual system at rest can be studied by alpha band activity.....	66
3.4.2 No signs of compensatory plasticity.....	67
3.4.3 Altered functional network topology in vision loss.....	68
3.4.4 Perception is related to brain networks' state in patients.....	68
3.4.5 Neurophysiological effects of rtACS.....	68
3.4.6 Conclusions.....	69
4. Study III: Impaired temporal aspects of neural synchronization in blindness.....	71
4.1 Study III: Introduction.....	71
4.2 Study III: Methods.....	72
4.2.1 Subjects.....	72
4.2.2 Data acquisition.....	73
4.2.3 Data preprocessing and analysis.....	73
4.2.3.1 EEG preprocessing.....	73
4.2.3.2 Synchronization measures.....	74
4.2.3.3 Surrogate data.....	75
4.2.4 Analysis of synchronization dynamic.....	75
4.2.4.1 Synchronization stability.....	75
4.2.4.2 Higuchi Fractal Dimension (HFD).....	76
4.2.4.3 Detrended Fluctuation Analysis (DFA).....	76
4.2.4.4 Amplitude matched data.....	77
4.2.5 Statistical analyses.....	77
4.3 Study III: Results.....	77
4.3.1 Synchronization strength.....	77
4.3.2 Temporal stability of synchronization: active- and waiting-periods.....	78
4.3.3 Higuchi fractal dimension (HFD).....	78
4.3.4 Detrended fluctuation analysis (DFA).....	78
4.3.5 Comparison to surrogate data.....	78
4.3.6 Amplitude-matched data.....	79
4.3.7 Correlations with vision measures.....	79
4.4 Study III: Discussion.....	82
4.4.1 Temporal patterns – looking at brain activity from a new angle.....	83
4.4.2 Disturbance of temporal patterns as another aspect of diaschisis.....	83
4.4.3 Using EEG to study brain reorganization.....	84
4.4.4 Conclusions.....	84
5. General discussion.....	86

5.1 Brain visual network in vision loss - diaschisis.....	86
5.2 Plastic reorganization in vision loss.....	87
5.3 Spontaneous brain activity in neurological patients.....	88
5.4 Network synchronization and perception: areas of residual vision (ARV).....	89
5.5 Network synchronization and perception: "sightblindness".....	90
5.6 Network synchronization as a target for vision restoration treatments.....	91
5.7 Methodological considerations and limitations.....	92
6. Network-state dependent vision loss – a new theoretical model.....	94
7. References.....	97

List of Figures

Figure 1.1. Structure of the brain visual system.....	16
Figure 1.2. Visual field charts of patients.....	18
Figure 1.3. Anatomical basis of visual field loss.....	19
Figure 1.4. Theories of brain function and consequences of focal brain lesions.....	26
Figure 1.5. Communication through neuronal coherence.....	28
Figure 1.6. Graphs and graph theory measures.....	33
Figure 1.7. Different levels of brain activity analysis.....	34
Figure 2.1. RT and the functional state of the visual field area.....	44
Figure 2.2. Intact field RT and the functional state of the immediate surround.....	44
Figure 2.3. Intact field RT and the scotoma size.....	45
Figure 2.4. Intact field RT in quadrantanopia.....	46
Figure 3.1 Creating binary graphs from EEG data.....	58
Figure 3.2. EEG spectral power.....	60
Figure 3.3. EEG short-range coherence.....	61
Figure 3.4. EEG long-range functional connectivity.....	62
Figure 3.5. Baseline EEG coherence networks.....	64
Figure 3.6. Post-rtACS EEG coherence networks.....	65
Figure 3.7. Correlations between EEG and vision measures.....	66
Figure 4.1. Analysis of temporal dynamics of synchronization.....	74

Figure 4.2. Amplitude and temporal dynamics of local synchronization.....	80
Figure 4.3. Strength and temporal dynamics of distant synchronization.....	81
Figure 4.4. Analysis of amplitude-matched data.....	82
Figure 4.5. Correlation between EEG and vision measures.....	82
Figure 6.1. Vision loss is network-state dependent.....	96

List of Tables

Table 2.1. Description of the Study I patients sample.....	38
Table 3.1. Description of the Study II patients sample.....	53
Table 4.1. Description of the Study III patients sample.....	72

1. Introduction

1.1 Visual system damage

Humans rely on vision more than on any of the other senses. Consequently, blindness can lead to severe decline in quality of life (Gall et al., 2009) and is one of the most feared diseases in the elderly. Several conditions might lead to vision loss including glaucoma, age related macular degeneration (AMD), retinitis pigmentosa, diabetic retinopathy, and optic nerve and brain damage due to stroke or trauma. These diseases have in common that they do not affect the optic apparatus of the eye (cornea or lens), but they damage tissue of the retina and/or the brain. In the aging society prevalence of these conditions is on the rise and acquired blindness becomes an increasingly pressing problem. It affects not only the blind but also their caregivers, typically family members. Therefore, we urgently need to understand the mechanisms behind acquired blindness to more effectively prevent vision loss and to develop strategies of vision restoration.

1.1.1 Organization of the visual system

The visual system includes several anatomical structures organized hierarchically (**Fig. 1.1**). The light reflected off the objects in the environment is received by the retina in the eye and encoded as a sequence of action potentials which are transferred via the optic nerve, optic chiasm, and optic tract to the lateral geniculate nucleus (LGN) of the thalamus. From LGN visual information flows via the optic radiation to the primary visual cortex (V1). V1 processes basic features of the image and distributes the information to multiple extrastriate visual areas responsible for analysis of various features, e.g. color (V4) or motion (MT+). These areas, together with many other brain regions responsible for attention and multisensory integration create a large-scale brain network, giving rise to conscious perception. In contrast to serial and hierarchical structure of early processing stages (up to V1), processing of visual information in cortical networks is rather distributed, parallel, and recursive (van Essen et al., 1992; de Haan & Cowey, 2000).

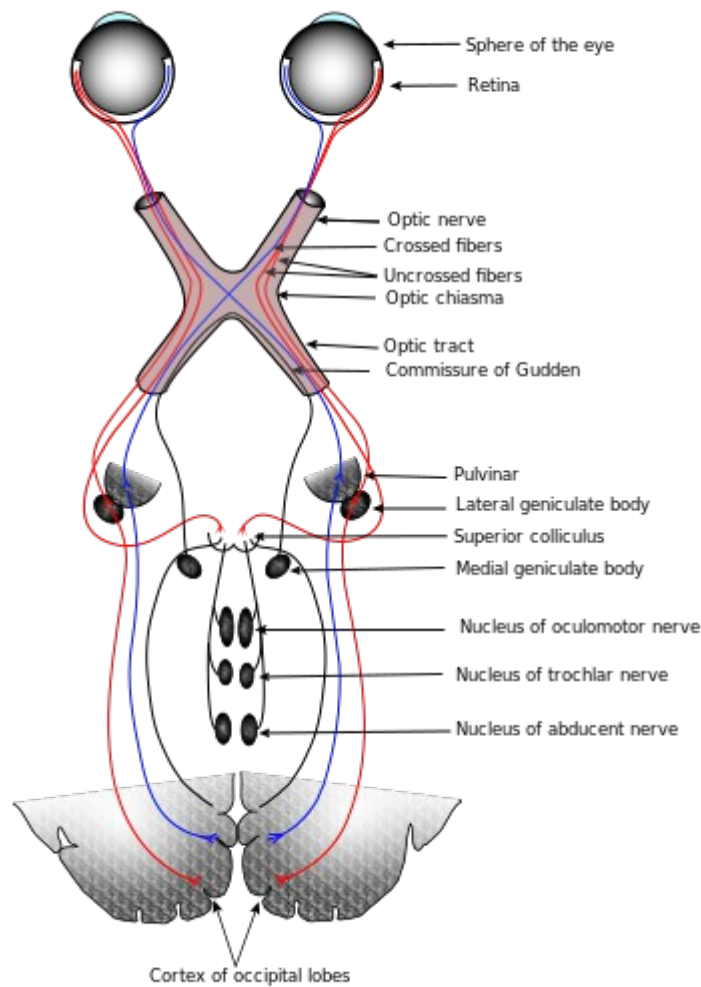


Figure 1.1. Structure of the brain visual system. Source: Wikipedia entry: visual system

Another important feature of the visual system is retinotopic organization of the early processing stages. The “retinotopic organization” indicates that the spatial structure of input is preserved, i.e. the objects which are close to each other in space are processed in nearby, corresponding regions of the visual cortex. In other words, the image of the environment is superimposed onto the visual cortex.

1.1.2 Perceptual consequences of visual system damage

In the present work patients suffering from lesions to the retina or optic nerve were studied. Such lesions are called “pre-chiasmatic” as retina and optic nerve are located before the optic chiasm (see: **Fig. 1.1**). Below I review what is known about the perceptual consequences of pre-chiasmatic visual system lesions.

To better understand perceptual effects of visual system damage it is important to know how vision loss is diagnosed and tested. Typically, acquired blindness is diagnosed with perimetry. Various types of perimetry methods exist, but the underlying principle of testing is the same - small stimuli are presented randomly over the visual field and patient's task is to respond to a stimulus presentation with pressing a button. Fixation should be kept at the same central position throughout the test to ensure reliable results. A visual field chart can then be created indicating visual field areas where vision is lost (no detections) and these where it is retained (**Fig. 1.2**).

The structure of the visual system, namely hierarchical and retinotopic organization, determines how perception is affected by pre-chiasmatic damage. Firstly, pre-chiasmatic lesions, occurring at the very beginning (periphery) of the visual pathway, prevent visual information from reaching primary visual cortex via retino-fugal projections. Such lesions are rarely complete and typically part of the visual cortex is deafferented but the other part continues to receive input. The deafferented visual cortex area is called the "lesion projection zone" (LPZ). Because of the hierarchical structure of the early visual system, the pre-chiasmatic lesion completely deprives LPZ of visual information, i.e. there is no "detour" or alternative pathway through which information might be routed to the cortex. Secondly, due to retinotopic organization of the visual system there is a close correspondence between the spatial pattern of anatomical damage and the spatial pattern of vision loss. In other words, whether perception in a certain visual field area is possible depends on the state of retinotopically corresponding neural tissue - the blind field corresponds to the damaged tissue and sighted field corresponds to the uninjured tissue. This principle actually led to discovery of retinotopic organization by Gordon Holmes who related topology of visual field defects to location of missile wounds in World War I soldiers.

As already mentioned brain lesions are typically not complete and clear-cut but rather partial and diffuse. Similarly, the neurodegenerative conditions like glaucoma or AMD do not affect the whole retina at once but rather lead to gradual, progressive neurodegeneration (Weinreb and Khaw, 2004). In both cases partially damaged tissue typically exists between intact and completely damaged retina/optic nerve areas and is perceptually manifested as "area of relative defect" in the visual field.

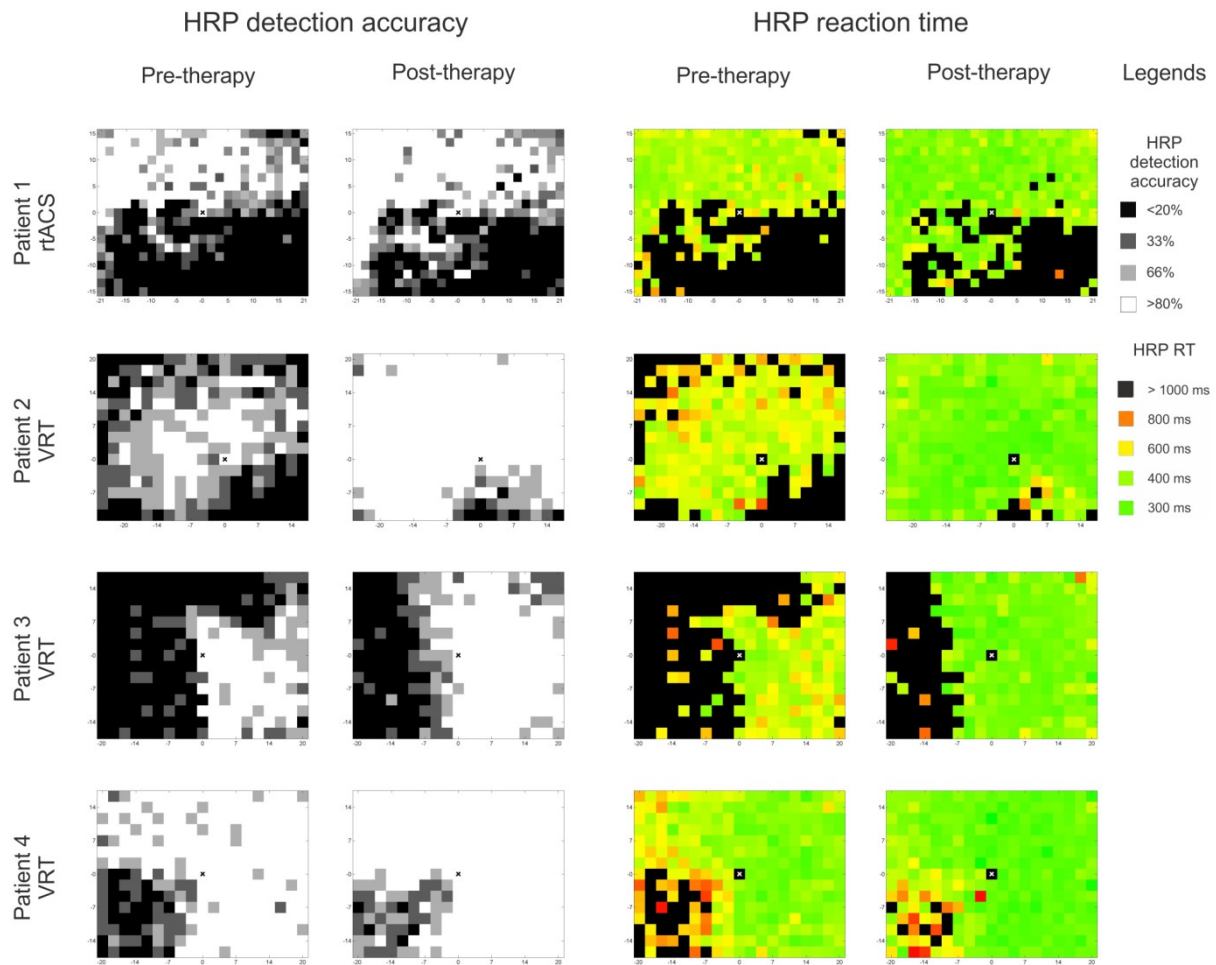


Figure 1.2. Visual field charts of patients. Patients 1 and 2 suffered from pre-chiasmatic lesion and patients 3 and 4 from post-chiasmatic lesion. Detection accuracy of stimuli presented in high resolution perimetry (HRP) is denoted by color: black represents absolute defect (0% detection), grey represents areas of residual vision (relative defect; detection >0% and <100%) and white represents intact field (100% detection). Reaction time (RT) is color-coded in RT charts. Patients were treated either with vision restoration training (VRT) or repetitive transorbital alternating current stimulation (rtACS). Pre- and post-treatment HRP data are presented.

Therefore, visual field of patients with visual system damage can be generally subdivided into three areas (**Fig. 1.2** and **Fig. 1.3**):

- i) *Scotoma (the blind field, absolute defect)* is the circumscribed visual field area where patient is completely blind, not able to see even high-contrast stimuli. The scotoma is believed to correspond to the completely damaged retinal/optic nerve tissue and to LPZ in visual cortex.
- ii) *Intact field (sighted field)* is the visual field region where patients' detection abilities are retained and it is believed to correspond to the uninjured tissue. It is

assumed that in the intact field all other perceptual capabilities, beyond simple detection, are normal as well.

- iii) Vision loss is typically diffuse meaning that there is no clear-cut border between the blind field and the intact field. Rather there is a transition zone where vision is unclear and unreliable, as indicated by partial detection or increased contrast threshold in perimetry. This transition zone is called relative defect or *areas of residual vision (ARV)*; Sabel et al., 2011a). ARV corresponds to the partially damaged tissue and partially deafferented visual cortex region. Because the damage is incomplete ARV hold potential for improvements of vision and for vision restoration.

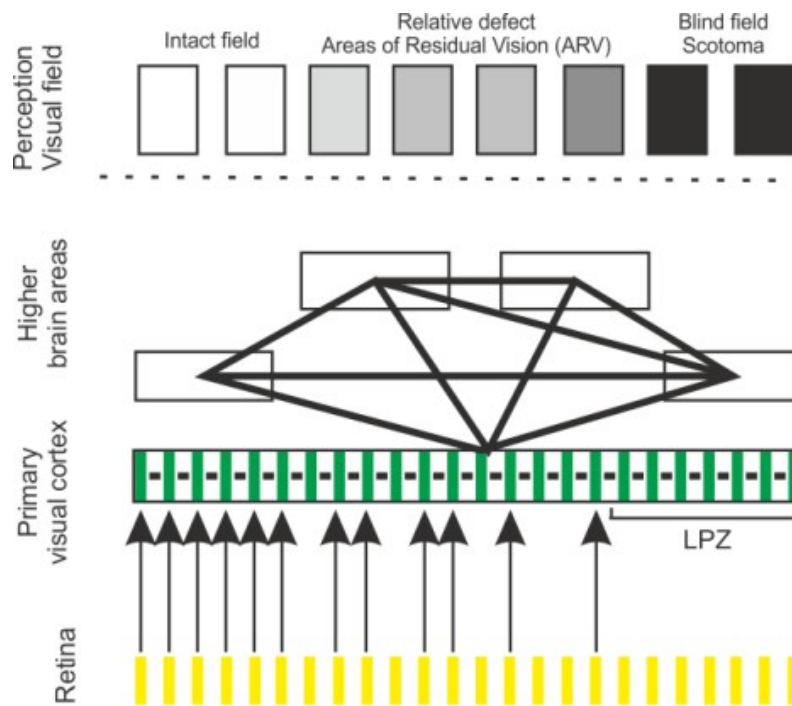


Figure 1.3. Anatomical basis of visual field loss. Visual field areas where vision is retained (intact field) or lost correspond to, respectively, uninjured and completely damaged retina/optic nerve. The diffuse nature of visual system lesions typically results in a transition zone where tissue is partially damaged and that is manifested as areas of residual vision (ARV; relative defect).

1.1.2.1 “Sightblind” – perceptual deficits in the intact visual field

In clinical work, and in most research studies, there are two general assumptions: (i) perception is completely abolished in the “blind” field and (ii) perceptual functions are “normal” in the intact field. But this is not always so. With regard to the former, the

discovery of the “blindsight” phenomenon shows that visual information can still be processed deep in the “blind” field, allowing patients to correctly detect the presence of stimuli without being aware of them (Pöppel et al., 1973; Weiskrantz et al., 1974). With regard to the latter, there is already some evidence that the presumably “intact field” might actually exhibit some subtle perceptual deficits which remain undetected by static perimetry.

Several experiments revealed that despite normal detection in perimetry there are actually subtle perceptual deficits in the “intact” field. For instance, patients who recovered from optic neuritis, despite exhibiting normal detection abilities in their visual field, are impaired in motion detection and temporal processing tasks (Raz et al., 2011, 2012). Also patients suffering from homonymous hemianopia due to unilateral post-chiasmatic damage exhibit perceptual deficits in the intact field (review: Bola et al., 2013b), including decreased contrast sensitivity (Hess and Pointer, 1989), impaired ability to detect targets on a noisy background (Rizzo and Robin, 1996), disturbed temporal aspects of visual processing (Poggel et al., 2011), and deficits in figure-ground segregation (Paramei and Sabel, 2008; Schadow et al., 2009). Importantly, in case of unilateral post-chiasmatic damage the hemisphere processing the intact visual field is certainly not injured and therefore intact field deficits cannot be ascribed to direct impact of the lesion. I reasoned that studying how the “intact” field deficits come about one might discover new pathophysiological mechanisms in the damaged visual system. Therefore, prior to investigating brain functional networks in vision loss using neuroimaging methods I focused on the “intact” field perceptual deficits using psychophysical approach. My findings were published in a research article (Bola et al., 2013a; Study I in this thesis) and in a review (Bola et al., 2013b). The work on the “intact” field deficits gave basis for hypotheses of involvement of large-scale brain functional networks in vision loss.

The term “blindsight” was coined to describe the phenomenon of residual perceptual capacities existing deep in the “blind” field (Pöppel et al., 1973; Weiskrantz et al., 1974; review: Cowey, 2010). Subtle perceptual deficits found in the “intact” visual field might be considered a flipside of “blindsight” and hence we termed this phenomenon “sightblind” (Bola et al., 2013b). “Sightblind” indicates that patients’ vision is actually more impaired than one would expect based on perimetry data alone. Interestingly, in subjects with chronic visual field loss objective measures of blindness (scotoma size measured by perimetry) are only modestly correlated with subjective vision loss quantified by vision-related quality of life

questionnaires (Gall et al., 2009; Müller et al., 2003). This indicates that the “sightblind” effect might partially account for the subjective visual impairment of patients – a hypothesis which might be tested by future studies. While subjective quality of vision is what ultimately matters for patients, to effectively restore vision we need to learn more about the neurophysiological mechanisms of vision loss.

1.1.3 Neurophysiological consequences of visual system damage

Brain lesions affect both structure and function of the brain. In this section I firstly provide a general description of possible effects local brain lesions can exert on neural circuits. Then I focus on reported effects specific to pre-chiasmatic visual system lesions.

The brain is a network where functioning of each area depends on input from other areas. Therefore, the impact of local, circumscribed lesion on brain functioning is twofold. Firstly, a lesion directly damages neural tissue and renders it dysfunctional. Secondly, a local lesion might indirectly disturb function and structure of distant regions which rely on input from the damaged one. This might be mediated by uni-synaptic or poli-synaptic chains of connections. Such impact on areas distant from the lesion is called *diaschisis* and it was first described by von Monakow (1914; review: Carrera and Tononi, 2014). Sensory damage leads to profound changes in the deafferented downstream brain structures, even if the brain itself remains uninjured (review: Chen et al., 2002; Merabet and Pascual-Leone, 2009), and therefore it provides a good example of diaschisis.

Further, there are two processes which might be triggered by local brain lesions – passive degeneration and active reorganization. Passive degeneration refers to progressive loss of neural tissue due to lesion or deafferentation. It might include loss of neurons, dendrites, synaptic spines, or any other structural elements. In vivo degeneration might be indicated for instance by decrease in tissue volume as measured by MRI (e.g. Boucard et al., 2009). Conversely, active reorganization (plasticity) refers to creation of new structural elements, e.g. spines or connections.

Finally, changes in the brain can be adaptive, i.e. advantageous for behavior, or maladaptive, which have detrimental effects (e.g. Sandmann et al., 2012). Yet, it is important to keep in mind here that correlating neurophysiological changes with behavioral observations do not inform us about the causal involvement of neural processes in behavior.

Below I review studies demonstrating these particular effects taking place in the visual system after visual system damage.

1.1.3.1 Anterograde degeneration

Previous studies revealed that patients suffering from vision loss due to glaucoma or AMD exhibit anterograde morphological degeneration of structures along the visual pathway, including optic nerve, optic tract, LGN, and optic radiation (Hernowo et al., 2011; Hernowo et al., 2013; Lee et al., 2014). Further, also in the early visual cortical regions like V1 and V2 the deafferented LPZ degenerates (Boucard et al., 2009; Plank et al., 2011; Bogorodzki et al., 2014; review: Gupta and Yücel, 2007). Interestingly, Hernowo et al. (2013) found reduction in frontal white matter volume in AMD patients which might indicate that vision loss might be associated with changes in areas far beyond the visual system.

1.1.3.2 Local plasticity

Effects of the pre-chiasmatic lesion are not limited to passive degeneration of downstream deafferented structures but there is also active reorganization (plasticity) of the visual circuits as reported by numerous studies. As already mentioned, local, circumscribed retinal lesion creates a LPZ in visual cortex, which receives no retinal input and corresponds to the blind visual field area. One would therefore not expect any stimulus-driven activity within LPZ. Indeed, a visual stimulus presented to the lesioned part of the retina cannot evoke a cortical response. But early electrophysiological studies in animal models revealed stimulus-driven activity in LPZ when the stimulus was presented in the vicinity of the retinal lesion close to the lesion border (Kaas et al., 1990; Gilbert and Wiesel, 1992; Calford et al., 2000; Waleszczyk et al., 2003). In other words, there is a shift of receptive fields of LPZ neurons. This was considered to be a sign of plasticity and reorganization. Specifically, plasticity of intrinsic V1 long-range connections growing into LPZ and sending activity from the LPZ border towards the LPZ center was hypothesized to be the mechanism. Further studies lend support to the hypothesis of reorganization, e.g. Palagina et al. (2009) visualized cortical activation spreading laterally from the intact field towards and into LPZ using voltage-sensitive dye imaging. Keck et al. (2008, 2011) employed two-photon imaging and showed that massive restructuring of synaptic spines takes places within LPZ. Yamahachi et al. (2011)

indeed observed axonal outgrowth towards the LPZ which provides structural underpinnings for the observed functional changes.

A number of studies were conducted to measure stimulus-driven activity of LPZ in human subjects suffering from retinal lesions, e.g. caused by AMD. These studies used non-invasive neuroimaging methods (fMRI) and provide a body of evidence supporting the hypothesis of reorganization within visual cortex in human subjects (Baker et al., 2005; Schumacher et al., 2008; Dilks et al., 2009; Liu et al., 2010).

However, it is important to note that others did not find signs of reorganization or plasticity. This includes electrophysiological studies in animal models (Smirnakis et al., 2005) as well as fMRI studies in patients (Baseler et al., 2011) which failed to record stimulus-driven activity within LPZ. Alternative explanations of the evoked LPZ activity, which does not require any plastic reorganization, were proposed, specifically unmasking of already existing silent long-range connections (review: Wandell and Smirnakis, 2009). Therefore, the question whether intrinsic reorganization within visual cortex takes place is not yet conclusively addressed and deserves further study.

1.1.3.3 Effects on large-scale functional networks

So far I discussed possible changes occurring on the micro-scale, i.e. *within* primary visual cortex. But apparently visual system damage leads also to macro-scale changes in functional activity and connectivity. These are defined here as alterations in areas and connections beyond V1. For instance, Werring et al. (2000) and Toosy et al. (2002) revealed that stimulus-evoked activity measured by fMRI is more extensive in patients who underwent an episode of optic neuritis. Specifically, while in control subjects only V1 was activated, in patients activation was found also in extrastriate visual regions. Toosy et al. (2005) proved that extrastriate reorganization occurring during and after optic neuritis episode is adaptive, i.e. it contributes to better vision in patients. Further, using resting-state fMRI Gallo et al. (2012) revealed that optic neuritis is related to changes in strength of functional connections between specific visual brain regions including both increases and decreases of functional coupling strength. Similar findings were reported by Dai et al. (2013) and Song et al. (2014) who investigated resting-state fMRI functional connectivity in glaucoma patients.

It is worth mentioning here that although few studies investigated reorganization of large-scale brain networks in patients blinded by visual system damage, a large body of literature exists concerning completely (congenitally) blind subjects (review: Pascual-Leone et al., 2005; Voss, 2013). In the completely blind large-scale brain networks undergo massive, multi-modal, and behaviorally relevant reorganization. Specifically areas processing visual information in sighted subjects in the blind are “invaded” by other senses. Importantly, subjects’ age at the onset of blindness is an important moderator of the reorganization. Those who lost sight after the critical period (i.e. in adulthood) are less likely to develop compensatory plastic changes in brain networks. For this reason adaptive plasticity is less likely to occur in patients blinded by glaucoma, AMD, or other optic neuropathies, which are typically diseases of the old. But a detailed review of the literature on the effects of complete blindness is beyond the scope of this thesis

1.1.4 Vision restoration

The motor system is considered a model for rehabilitation-induced neural plasticity. It has been shown that behavioral improvements in patients recovering from motor system lesions depend on the capability of the system to reorganize (Shepherd, 2001). Constant training leads to adaptive neural plasticity, i.e. the functions of the damaged regions are “relearned” by uninjured areas and networks resulting in behavioral improvements (review: Hallett, 2001). The extent of recovery depends on the initial state of neural circuits, i.e. if the damage is extensive patients are less likely to benefit from the treatment.

But the visual system was traditionally considered hierarchical and “hard-wired”, and therefore not likely to undergo significant plastic reorganization. Consequently, there was no justified hope that any rehabilitation strategy might restore vision after partial visual system damage. Only compensatory trainings teaching patient how to deal with the existing visual field defect, e.g. by scanning visual field and directing eye movements towards the blind field were considered feasible. But these types of training do not achieve vision restoration *per se*. Yet, studies reviewed in the previous section indicate that plasticity of the visual system does take place. Therefore, one can try to affect the visual system in such a way that adaptive changes occur, leading to restoration of vision.

Indeed, vision restoration can be achieved by repetitive training of stimulus detection in the damaged visual field (Kasten et al., 1998). Restoration is unlikely to happen deep in the

blind field but it can take place in the ARV and close to the defect border. Therefore, in vision restoration training (VRT) patients train detection in the border zone for 6 months which leads to enlargement of the intact field (see: **Figure 1.2**). The hypothetical mechanism of action was strengthening of bottom-up input to the visual cortex by repetitive stimulation (Sabel et al., 2011a). In a modified version of VRT patients' spatial attention was cued to the site of stimulus presentation, which resulted in even more pronounced therapeutic effects (Poggel et al., 2004). Similarly, presenting a stimulus designed to activate extrastriate areas deep in the blind field during VRT resulted in greater increase in the intact field size (Jobke et al., 2009). This suggests that combining bottom-up input with top-down influences might be the most effective way to restore visual function.

Recently, neurorehabilitation began taking advantage of the non-invasive brain stimulation techniques, like transcranial magnetic stimulation (TMS) and transcranial direct and alternating current stimulation (DCS and ACS, respectively). Again, these methods were firstly applied in the motor system (e.g. Hummel et al., 2005). But recently repetitive transorbital current stimulation (rtACS), with electrodes attached around the eyes, was shown to restore vision in vision loss patients (Sabel et al., 2011b). Supposedly, the current is exciting the retina causing synchronized firing and activating visual cortex. Repeated synchronous activation of retino-fugal pathway might cause strengthening of connections, similarly to VRT, and allow better perception. The increase in EEG alpha band power was reported as a neurophysiological effect of rtACS treatment (Sabel et al., 2011b; Schmidt et al., 2013) proving that rtACS affects cortical circuits.

1.1.5 Vision loss: open questions

The review of literature shows that several of studies investigated anatomical degeneration and local, micro-scale reorganization within V1. Yet, much less is known about the state of large-scale brain networks and their influence on perception in patients with vision loss. Numerous basic studies showed that instantaneous state of the brain networks (e.g. van Dijk et al., 2008) and top-down influences (review: Engel et al., 2001) affect perception. Also the studies on vision restoration prove that activating cortical networks, in addition to providing bottom up input, is beneficial for the restoration effects (Poggel et al., 2004; Jobke et al., 2009). My thesis describes studies conducted in order to learn about the state of functional brain networks in vision loss patients and to relate networks' activity to perception.

Therefore, in the remainder of this chapter I provide a short introduction into the topic of large-scale functional brain networks and describe methods available to study such networks in the human brain.

1.2 Brain networks

1.2.1 Communication in the brain

Traditionally, researchers investigating brain functions aimed to localize anatomical areas responsible for certain cognitive operations. The assumption here was that each brain region specializes in particular type of cognitive operation, e.g. vision or language, and that mapping functions to structures will reveal how the brain works. This approach can be traced back to neuropsychologists working in the XIX century, e.g. Paul Brocka and Carl Wernicke, who correlated anatomical location of brain lesions with behavioral deficits. More recently, the same principle underlies many neurophysiological studies in animal models investigating response of neural assemblies to external events, and PET or fMRI neuroimaging studies correlating activation patterns with cognitive tasks.

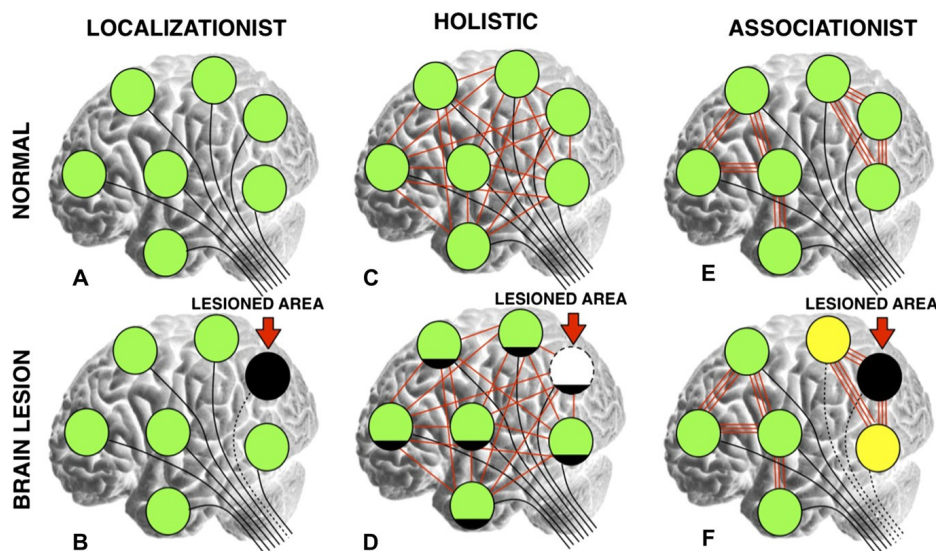


Figure 1.4. Theories of brain function and consequences of focal brain lesions. Localizationist theories assume that local brain lesion renders the damaged area dysfunctional, but other brain areas are considered intact. Conversely, holistic approach assumes that cognitive functions are results of the whole network activity and that local lesion affects all other brain areas. In associationist theory cognitive functions are rather performed by modules thus local lesion affects other areas within the same module but does not interfere with functioning of areas belonging to other modules. Adapted from: Catani et al., 2012.

Neuroimaging provided a great deal of information about functioning of the human brain by investigating local patterns of activity. Yet, recently neuroscience has witnessed a paradigm shift in a sense described by Thomas Kuhn (1962) - while early studies focused on patterns of *activation* of neurons and brain regions more recent approach emphasizes patterns of *communication*. Although particular neurons (e.g. in V1) are still believed to code for specific features of the stimulus and particular brain areas to perform specific operations complex functions of our mind are no longer thought to emerge from activity of such single elements. This new theoretical framework allows posing new questions, reinterpretation of the previous findings, and new methodological developments.

The importance of neural communication was studied by the group of Wolf Singer on the level of single neurons (review: Singer and Gray, 1995). Membrane potentials of neurons have an intrinsic tendency for oscillatory activity reflecting rhythmically changing excitability. Neurons can be effectively driven by external input only within a short time window (i.e. at the peak of the oscillatory cycle). Action potentials from one neural assemble might affect the other only if they arrive at the peak of the oscillations, but they have no effect when they arrive at the trough (Fries, 2005; **Fig. 1.5**). Therefore, neurons coding for different features of a percept need to synchronize phase of their oscillatory activity in order to communicate and bind the features into a unified and coherent percept. The “communication through neuronal coherence” allows great flexibility as particular neurons might be dynamically included or excluded from the synchronized assembly by synchronizing/desynchronizing their phase to the phase of the whole assembly.

The same principle holds also at the coarser spatial scale. Distant brain regions conducting specific, basic cognitive operations need to synchronize phase of their oscillatory activity to allow effective communication. Large-scale phase-synchronized brain networks integrate information from local brain centers and are nowadays believed to give rise to perception and cognition (review: Varela et al., 2001; Siegel et al., 2012). Phase synchronization as the binding mechanism allows great flexibility making it feasible to establish and dissolve large-scale functional networks on the timescale of tens to hundreds of milliseconds. These principles have been repeatedly tested in studies involving visual processing. Once the visual information reaches visual cortex it is processed in parallel by several cortical streams and connections between multiple areas need to be activated in concert to create a unified perceptual experience (review: Engel et al., 2001; de Haan and

Cowey, 2011; Siegel et al., 2012). Brain networks dynamically integrate information in space and time, binding different elements of the percept but also coordinate vision with attention (Siegel et al., 2008) and multisensory integration (Hipp et al., 2011).

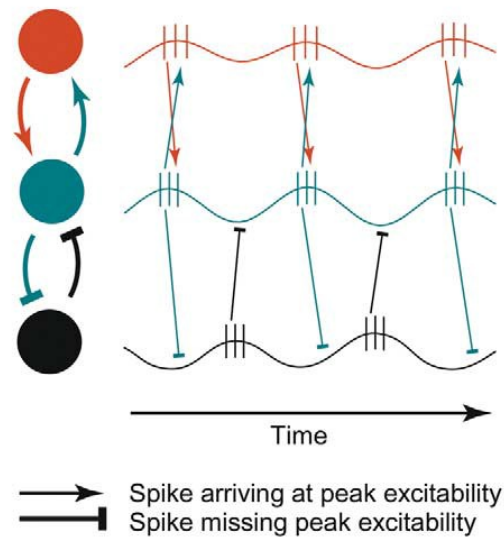


Figure 1.5. Communication through neuronal coherence. Red and blue neurons are synchronized “in phase” which allows effective communication as action potentials arrive when neurons are in an excitable state. But blue and black neurons are synchronized “out of phase” and that prevents communication between them as action potentials arrive when neurons are not easily excitable. Adapted from: Fries (2005).

Finally, the focus on brain communication helped to appreciate the distant effects of focal brain lesions. Although the diaschisis mechanism was postulated at the beginning of the XX century, only recently have clinicians begun to identify specific impairments in brain communication related to pathological conditions (review: He et al., 2007a; Carrera and Tononi, 2014). Below I provide a brief review of the concepts and methods which can be employed to better understand impaired visual system communication after visual system damage.

1.2.2 Brain connectivity networks

1.2.2.1 Structural and functional connectivity

Communication within brain networks depends on anatomical connections created by axons and dendrites which are the structural basis for functional interactions. Brain anatomical connectivity is dense and extensive, e.g. in the visual system around 40% of all

possible connections are realized (Felleman and van Essen, 1991). Nowadays anatomical connectivity can also be studied noninvasively in human subjects using diffusion tensor imaging (DTI). Yet, the focus of my thesis is on functional rather than structural connectivity.

Phase synchronization is the most widely used measure of functional interactions in electrophysiology. But development of novel neuroimaging methods, e.g. PET and fMRI which measure brain activity indirectly, called for a new definition of functional interactions. A concept of “functional connectivity” was proposed by Friston (1994; 2011) and defined as a statistical relation (correlation) between activity time-courses of two distant sources. Here, it is assumed that if activity of two sources covaries in time, no matter whether it is phase, amplitude, or any other feature of the signals, then the sources are “functionally coupled”, i.e. they exchange information. Because functional connectivity is defined as any statistical relation there are various measures used to quantify functional connections. Which method is used depends on the research question and on the data acquisition method. In fMRI studies Pearson correlation coefficient between BOLD time courses is typically calculated (e.g. Biswal et al., 1995). M/EEG signals might be analyzed in a frequency-dependent manner using coherence or phase locking value (PLV; Lachaux et al., 1999) as measures of phase synchronization. Most of the measures quantify undirected connectivity, meaning they detect relationship but not the direction of influence. A “directed functional connectivity” is estimated by Granger Causality (GC; review: Bressler and Seth, 2010), which provides information about the influence one source has on another.

1.2.2.2 Neuroimaging methods to study functional interactions

Analysis of functional connectivity requires recording time courses of brain areas activations. The most widely used method to study brain activity and interactions in human subjects is fMRI, which measures neural activity indirectly, by estimating associated changes in blood flow. fMRI is characterized by excellent spatial resolution, but relatively poor temporal resolution. It is thus not suited to detect transient, dynamic changes.

In contrast, the EEG directly measures the electrophysiological activity of interest. It is characterized by superb temporal resolution, able to detect changes in activation in the range of milliseconds. Yet, the disadvantage of EEG is poor spatial resolution caused mainly by the volume conduction problem, i.e. electric fields spread through the tissue and activity of a local source is recorded at many distant electrodes. Further, EEG is not able to detect activity of

subcortical sources. Thus, when analyzing functional connectivity it is important to keep in mind limitations of the chosen neuroimaging method.

The great advantage of EEG is that oscillatory activity of the brain can be recorded and analyzed in a frequency-resolved manner. The EEG signal is generally characterized by $1/f$ spectrum and contains various frequencies which are believed to have different functional meaning (review: Buzsaki and Draguhn, 2004; Siegel et al., 2012). For instance the gamma band (30Hz to 80Hz) is hypothesized to represent local processing of percepts' features (Fries et al., 2007) and the beta band (15Hz to 30Hz) was traditionally associated with sensory-motor functions. But recently a hypothesis of beta maintaining the status quo in neural circuits (i.e. when anticipating a stimulus) was put forward (Engel and Fries, 2010). The alpha band was proposed to represent an idling of cortical circuits but more recently it is believed to represent active inhibition of possibly interfering information (Palva and Palva, 2007). When a subject is resting with eyes closed alpha activity is abundant over occipital (visual) cortex and it appears to be generated by visual circuits and thalamo-cortical interactions (Hughes and Crunelli, 2005). Numerous methods exist to assess functional connectivity between signals in a frequency-resolved manner, e.g. they estimate interaction for each frequency separately. When employing such methods behavioral significance of functional interactions in specific frequencies can be explored.

1.2.2.3 Brain spontaneous activity – the “resting-state” paradigm

The majority of neuroscience studies focused on the response evoked in the brain by a stimulus or a task. Yet, in the past 20 years we have witnessed an increasing interest in spontaneous, intrinsic brain activity. Apparently, even in the absence of any overt task the brain exhibits strong activation. Researchers investigating event-related responses treated such intrinsic activity as noise. But spontaneous activation patterns are highly organized, both in the spatial and temporal domain (review: Fox and Raichle, 2007) – an observation which did not comply with the “intrinsic noise” hypothesis. Rather, the brain is organized into a set of networks, some of them are activated during task performance (task-positive networks) and others are deactivated (task negative networks, e.g. default mode network). These networks are reproducible within and between subjects. Further, resting-state activity is related to behavior in healthy subjects and in patients (review: van den Heuvel et al., 2010), stressing the fact that it contains valuable information about brains' state and capabilities.

Studying intrinsic activity has changed our understanding of how the brain works. The brain is no longer considered to be driven mainly from the outside. Rather external input and task-related processing merely modify (perturb) the spontaneous network activity. Therefore spontaneous, resting-state activation patterns constitute a good predictor of perception and action (review: Harmelech and Malach, 2013).

1.2.2.4 Brain communication in pathological conditions

Efficient brain communication is essential for perceptual, cognitive, and motor processes. Thus, it is hardly surprising that various pathological conditions are related to disrupted brain communication. Patients suffering from neuropsychiatric (review: Uhlhaas and Singer, 2012) or neurological disorders (review: Grefkes and Fink, 2011) exhibit disturbed functional activity and connectivity patterns when performing certain perceptual and cognitive tasks. Considering patients with focal brain lesions, neglect patients exhibit impaired functional connectivity in the attention networks during performance of attentional task, and degree of connectivity impairment is related to severity of the neglect syndrome (He et al., 2007b). Similarly, stroke in the motor system disrupts directed functional connectivity in the motor network during performance of a hand movement task (Grefkes et al., 2008). Specifically, in patients there is an excessive inhibitory influence of the uninjured hemisphere on the injured hemisphere and the inter-hemispheric inhibition is correlated with behavioral capabilities of patients.

Recently, the resting-state paradigm is extensively used in clinical neuroscience as even patients who are not able to perform cognitive tasks might take part in the resting-state experiments. Further, intrinsic brain activity was shown to be more rich and variable than task-related activity, possibly representing activity of greater number of neural circuits. Thus, resting-state data might be a more sensitive biomarker of brain pathologies. Indeed, in stroke patients inter-hemispheric (but not intra-hemispheric) resting-state fMRI functional connectivity was associated with behavioral deficits (Carter et al., 2010). Similarly, in trauma patients recovery of resting-state magnetoencephalography (MEG) functional connectivity was related to recovery of function, e.g. verbal fluency (Castellanos et al., 2010). Further, resting-state EEG functional connectivity recorded in the acute phase allows predicting the behavioral state of a patient in the chronic phase (Assenza et al., 2013).

Therefore, intrinsic activity holds valuable diagnostic and prognostic information and studying disrupted brain communication patterns might bridge the gap between studies of molecular changes and clinical symptoms (review: Pievani et al., 2011). Importantly, changes in functional connectivity caused by treatments were typically correlated with behavioral improvements. But now the functional connectivity pattern itself becomes a target for neurological treatments. Neural communication can be modulated with non-invasive brain stimulation methods (TMS, ACS, DCS) and there is a growing body of evidence that modulating brain communication might result in recovery or facilitate the effects of simultaneous training (review: Hummel and Cohen, 2006). This proves the causal role of functional interactions in brain diseases.

Recording brain activity and estimating functional connectivity can inform us about the strength of pairwise interactions between brain sources. But networks, including brain networks, exhibit also emergent topological properties which cannot be reduced to just the sum of pairwise interactions. To reveal the topological properties a network needs to be analyzed with measures developed within graph theory – a branch of mathematics devoted to studying complex networks.

1.2.2.5 Graph theory

In graph theory networks and complex systems are represented as graphs containing *nodes*, being elements of the system, and connections between nodes called *edges*, representing interactions between the elements (**Fig. 1.6**). Various natural and man-made systems can be represented as graphs and many of them exhibit non-trivial topological properties (review: Newman, 2003). Considering social systems, each person is represented as a node and presence of a relationship (e.g. friendship) is represented as an edge. Similarly, brain areas and functional interactions might be represented as nodes and edges, respectively. Once the system is represented as a graph, several topological properties might be estimated which inform us about the structure of the system or patterns of interactions within the system.

Graph theory has only recently been introduced to neuroscience, but it has rapidly gained popularity and there is a burgeoning literature on characterizing brain networks with graph measured. Initially, the brain anatomical connectivity was studied within the graph theory framework. Anatomical networks, as many other systems observed in nature, exhibit

the “small-world” modular structure (Watts and Strogatz, 1998; Hilgetag et al., 2000; Sporns and Zwi, 2004). “Small-world” architecture (**Fig. 1.6**) allows segregation of information into functionally distinct, highly clustered modules (e.g. visual, auditory, motor systems) and, at the same time, integration between modules/subsystems. This kind of topology is also believed to represent the optimal balance between brain information processing capabilities and cost (in terms of energy and space) of maintaining extensive connectivity, particularly long-range connections (Bassett et al., 2010).

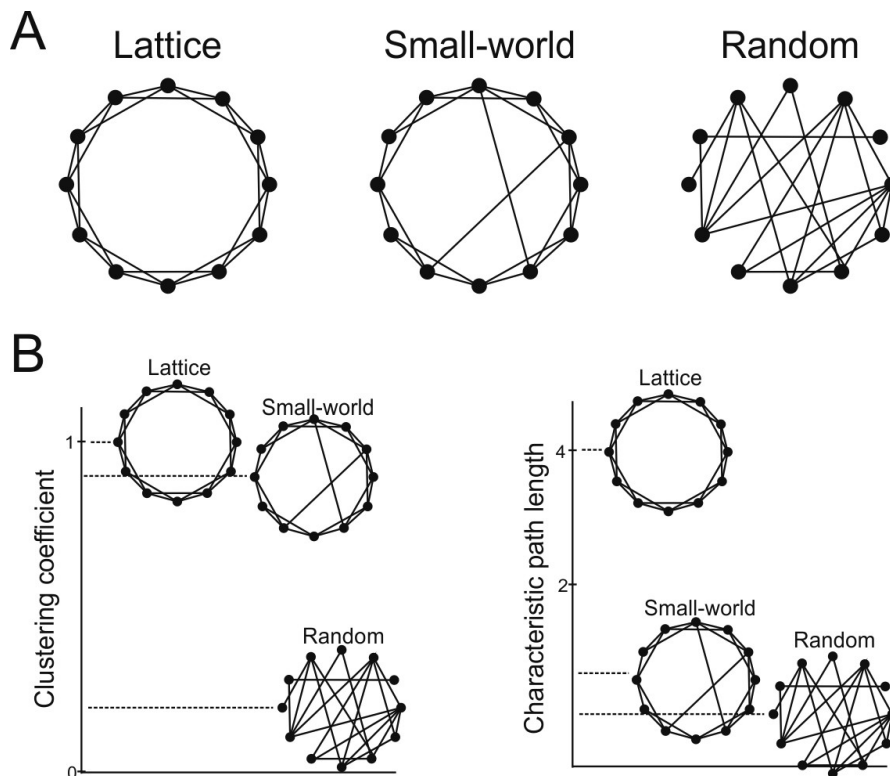


Figure 1.6. Graphs and graph theory measures. Black dots are *nodes* of a graph and lines between nodes are *edges*. Three types of networks are presented in A. Highly clustered lattice network, small-world network, and random network. In B typical values of two basic graph measures, clustering coefficient and characteristic path length, for the three canonical networks are presented. The small-world network is characterized by high clustering and at the same time low path length and this combination of features makes it an optimal pattern for information processing.

Similarly, studies investigating functional connectivity networks confirmed the small-world structure of micro- (Yu et al., 2008) and macro-scale functional networks (MEG: Stam, 2004; fMRI: Salvador et al., 2005). The topological properties of functional networks proved functionally relevant as they change during development (Boersma et al., 2011) and predict individual cognitive performance (van den Heuvel et al., 2009; Langer et al., 2012). Recently,

graph measures have been increasingly used in clinical neuroscience to track disease-related changes in network topology. A number of studies have been conducted on network changes in Alzheimer's disease (Stam et al., 2009) or traumatic brain injury (Castellanos et al., 2010; Caeyenberghs et al., 2012), and also after focal brain tumor (Bartolomei et al., 2006) or stroke (Wang et al., 2010).

Therefore, graph theory has contributed to our understanding of brain changes during brain development and degeneration. It is not only local tissue loss that affects behavior. Rather, impairments of communication between brain areas and, on a more abstract level, changing network topology which might facilitate or hamper information processing efficiency, are important as well (**Fig. 1.7**).

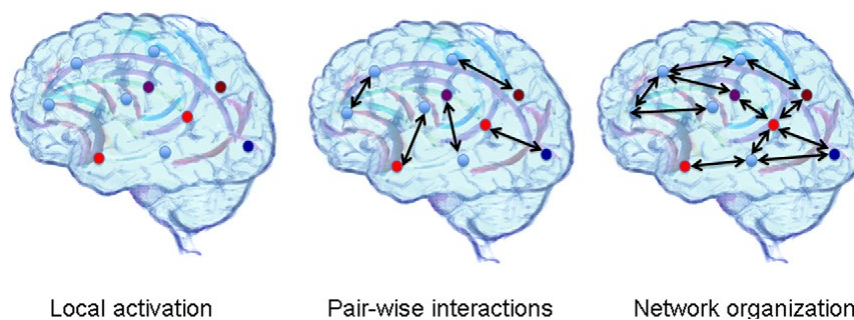


Figure 1.7. Different levels of brain activity analysis. Brain function can be analyzed on different levels, ranging from local activation, through pairwise interactions between local regions, to the level of whole brain network organization. Adapted from: Stam and van Straaten, 2012.

1.3 Problem formulation and hypotheses

The goal of the present series of studies was to elucidate brain mechanisms of vision loss and restoration in patients with visual system damage.

Loss of vision after retina or optic-nerve damage is conceived to be the direct consequence of the missing bottom-up (retinofugal) input. Indeed, a pre-chiasmatic lesion prevents bottom-up input from the retina from reaching visual cortex and therefore leads to blindness in the corresponding visual field regions. Because of the hierarchical and retinotopic organization of the visual system, and supposedly bottom-up character of visual processing, the scotoma is considered the only consequence of the damage and no physiological effects outside lesion the projection zone are expected. Consequently, the scotoma is believed to be

the only cause of patients' subjective loss and, since the anatomical damage is irreversible, there is no hope for vision restoration.

But simple activation of primary visual regions is not enough to create a percept. Despite the hierarchical structure of the early processing stages visual perception is not just a simple bottom-up process. Once the visual information reaches visual cortex it is processed in parallel by several cortical streams and connections between multiple areas needed to be activated in concert to create a unified perceptual experience (review: Engel et al., 2001; de Haan and Cowey, 2011; Siegel et al., 2012). Brain networks dynamically integrate information in space and time, which is the basis for binding of different elements of the percept and for integration of vision with other functions such as attention (Siegel et al., 2008), and multisensory integration (Hipp et al., 2011).

Yet, little is known about the functional state of brain networks in patients suffering from vision loss. Apparently, anterograde degeneration affects downstream visual regions (Boucard et al., 2009) and functional activity and connectivity of brain visual networks are altered (Toosy et al., 2005; Dai et al., 2012). Yet, the hitherto conducted studies measured brain functional activity and connectivity only indirectly, using fMRI. Thus, it is still not clear how vision loss changes communication within brain visual networks and, most importantly, how these changes affect perception.

Here we studied behavioral and EEG data from patients with vision loss. Behavioral data informed us about patients' perceptual capabilities while EEG provided insights into spatio-temporal patterns of brain networks synchronization. We aimed to address the following questions:

- i) Is the scotoma the only consequence of visual system lesion or is visual processing also impaired in regions beyond the "blind" field (**Study I**),
- ii) are *spatial* patterns of brain activity and functional connectivity disturbed in patients (**Study II**),
- iii) are *temporal* patterns of brain activity and functional connectivity disturbed in patients (**Study III**),

- iv) are *spatial* and *temporal* patterns of activity and functional connectivity related to perceptual capabilities of patients and to vision restoration (**Study II and III**)

We hypothesized that due to the prolonged sensory deprivation the functional state of brain visual networks is disturbed which, in turn, will be reflected by abnormal spatial and temporal patterns of activity and connectivity. Further, because the state of brain networks affects perception, we expected patients with more disturbed synchronization to exhibit worse perceptual functioning. Therefore, disturbance of brain functional networks likely causes perceptual deficits beyond the scotoma, i.e. in the “intact” visual field.

2. Study I: Perceptual deficits in the “intact” visual field

Published in:

Bola M, Gall C, Sabel BA. (2013a). The second face of blindness: processing speed deficits in the intact visual field after pre- and post-chiasmatic lesions. *Plos One*. DOI: 10.1371/journal.pone.0063700

Bola M, Gall C, Sabel BA. (2013b). “Sightblind”: perceptual deficits in the “intact” visual field. *Frontiers in Neurology* 4:80. DOI: 10.3389/fneur.2013.00080

2.1 Study I: Introduction

Vision loss is typically diagnosed based on detection accuracy in perimetry. The visual field region where patient is able to detect stimuli is considered to be intact. But traditional perimetry methods only test the most basic function of the visual system, i.e. reception. Here we employed data from HRP, which is a computer based perimetry and records reaction times (RT) of patients’ responses. We reanalyzed HRP data from a large sample of patients with the focus on RT as a measure of visual processing speed in the intact visual field. Patients were compared to an age-matched control group to test whether processing speed deficits exist in the intact field.

As not much is known about the mechanisms of intact field deficits, the main aim of the present study was to define features of the visual field defect related to the degree of the deficit. Structural damage on the border of the lesion or disrupted short-range interactions may cause perceptual problems. Therefore, processing speed should be more severely impaired in the intact field adjacent to the scotoma. At the same time the scotoma might also affect the whole visual field in a non-specific and non-retinotopic manner. We tested these hypotheses by relating RT to topological features of the visual field defect.

Of note, the focus of this thesis is on patients with pre-chiasmatic visual system damage. Yet, in Study I patients with post-chiasmatic damage were included as well, as a separate group, and their data are also presented here.

2.2 Study I: Methods

2.2.1 Ethics statement

This study was conducted according to the Declaration of Helsinki and it was approved by the ethics committee of the Otto von Guericke University of Magdeburg. Written informed consent was obtained from all participants prior to the experiments.

2.2.2 Subjects

We retrospectively analyzed data on patients' visual fields using a database consisting of 53 patients with pre-chiasmatic and 98 patients with post-chiasmatic damage. To be included subjects had to meet the following criteria: (i) chronic visual system damage (>6 months after damage); (ii) presence of residual vision as detected by HRP; (iii) sufficient fixation ability; and (iv) compliance with the experimenters' instructions. Based on additional exclusion criteria (see below) we excluded 13 pre- and 6 post-chiasmatic subjects. The analyzed groups (pre-chiasmatic, n=42; post-chiasmatic, n=92) were matched according to age and gender (see: **Table 2.1**).

Table 2.1. Description of the Study I patients sample. Groups did not differ significantly in age, fixation accuracy, and proportion of the absolute visual field defect. However, visual fields in the pre-chiasmatic sample were overall more diffuse, as indicated by a significantly higher proportion of relative defects which was accompanied by a lower proportion of the intact field.

	Pre-chiasmatic	Post-chiasmatic	p
<i>N</i>	42	92	
Gender (F/M)	15/27	32/60	0.91
Age (years)	54.9	56.10	0.71
Fixation accuracy (%)	97±0.004	96±0.002	0.19
False positive rate (%)	0.82±0.18	0.38±0.04	0.06
Intact field (%)	48±4	58.4±1	0.007
Relative defect (%)	21.8±2	7±0.5	<0.001
Absolute defect (%)	30±4	34.5±1	0.21
Diffuseness (%)	52.1±4	19.5±1	<0.001

Most patients in the post-chiasmatic group suffered from stroke (n=83) and a minority from trauma (n=5) and tumor (n=4). In the pre-chiasmatic group etiologies were more variable, including: arteritic anterior ischemic optic neuropathy (AION, n=13), optic nerve inflammation (n=7), idiopathic optic nerve atrophy (n=6), tumor (n=5), retinal artery occlusion (n=4), non-arteritic anterior ischemic optic neuropathy (NAION, n=2), glaucoma (n=2), trauma (n=2), optic nerve atrophy in Bechterews disease (n=1).

We compared the processing speed of both patients groups to a normative sample from the Tölz Temporal Topography study which used the same methodology of visual field testing (Poggel et al., 2012). The mean age of pre- and post-chiasmatic subjects was 54.9 yrs. and 56.1 yrs., respectively. The age of the normative data group was 50-59 yrs. (n=14; 8 female). Both patient groups were gender-matched to the normative group (chi-square(1,54)=1.99, p=0.158; chi-square(1,10)=2.58, p=0.108).

2.2.3 High Resolution Perimetry

All patients were tested with HRP. We chose to reanalyze HRP data as this method has been used for many years in our laboratory in different studies which provided the database for our study. Moreover, HRP provides an excellent spatial resolution and enables reaction time recording and analysis. Details of HRP are described elsewhere (e.g. Poggel et al., 2011).

Briefly, HRP measurements were conducted in a darkened room, where patients were seated in front of a 17" monitor with a chin-rest and forehead-holder. In this manner the eyes were kept at a constant distance of 42 cm from the screen. Supra-threshold, white light stimuli were presented continuously on dark grey background, within a grid of 25x19 or 19x15 sectors, covering $\pm 20^\circ$ horizontally and $\pm 15^\circ$ vertically of subjects' visual field. In each block one stimulus per sector was presented. The order of stimulus positions and the length of inter-stimulus intervals (ISI; from 1000 to 2000ms) were random so that patients could not predict when and where the stimuli were presented. A fixation point placed in the middle of the screen served as reference to set up the screen in the optimal height (keeping the patients' eyes at the level of the fixation point). In order to control subjects fixation, during the testing an isoluminant color change of the fixation point was presented 80 times per block. Subjects were instructed to maintain fixation at all times and press the space bar on the keyboard whenever a light stimulus was detected or a color change of the fixation point (fixation control) occurred. At 1000ms after presentation of a light stimulus or fixation control the next

trial started, beginning with a random ISI, followed by a stimulus presentation or another fixation control. RT values faster than 150ms and slower than 1000ms were treated as “false positives”. These cut-offs were used as this allows sufficient time to respond to the stimuli and effectively prevents guessing. RT upon “hits” were saved and analyzed as an indicator of visual processing speed.

Detection accuracy in every sector averaged over blocks of three repetitions was used as a criterion to define whether a given sector of the visual field belonged to the “intact” area (100% stimuli detected, shown in white in the visual field charts), mild relative defect area (66% stimuli detected, light grey), moderate relative defect (33% stimuli detected, dark grey) or absolute defect area (0% stimuli detected, black).

2.2.3.1 HRP-based exclusion criteria

Detection accuracy of the color change at fixation was taken as an indicator of fixation stability. We excluded subjects with fixation accuracy below 90% which resulted in the exclusion of 7 pre-chiasmatic subjects (7/53) and no subjects (0/98) from the post-chiasmatic group.

Additionally, we conducted all analyses (data not shown) also with a more strict fixation criterion by excluding subjects with fixation accuracy < 95%. This resulted in the exclusion of 15 subjects (15/53) from the pre-chiasmatic group and 28 subjects (28/98) from the post-chiasmatic group. This analysis led to essentially similar results than those of the more liberal exclusion as described below. However, the stricter fixation accuracy criterion reduced variability among subjects and therefore decreased the strength of correlations.

Furthermore, we excluded subjects with false positive rates >5% which resulted in the exclusion of four subjects (4/46) from the pre-chiasmatic and six subjects (6/98) from the post-chiasmatic group. After applying all exclusion criteria the final sample to be analyzed consisted of 42 pre-chiasmatic subjects and 92 post-chiasmatic subjects (see: **Table 2.1**).

2.2.3.2 HRP analysis

For every subject the size of each visual field functional “state” (intact, relative defect, absolute defect) was determined and expressed as percentage of HRP sectors belonging to each state. Both analyzed groups (**Table 2.1**) did not differ with respect to the extent of the

absolute defect areas ($t(1,132)=1.25$, $p=0.21$), fixation accuracy ($t(1,132)=1.31$, $p=0.19$), and false positive rate ($t(1,132)=1.89$, $p=0.06$). However, post-chiasmatic patients had significantly larger intact areas ($t(1,132)=2.73$, $p=0.007$), and smaller relative defect areas ($t(1,132)=3.56$, $p<0.001$). Thus, both groups differed with respect to the structure of the visual field defect: while pre-chiasmatic lesions typically led to more diffuse defects with broader transition zones (relative defects), post-chiasmatic subjects are characterized by a higher probability of clear-cut scotoma borders. To more explicitly quantify the “diffuseness” of the scotoma we calculated the proportion of relative defect sectors in the scotoma by using the formula:

$$\text{relative defect size}/(\text{relative defect size} + \text{absolute defect size})$$

This indicator was also significantly different between groups ($t(1,132)=3.82$, $p<0.001$).

2.2.3.3 Scotoma features and intact field RT

The main aim of the study was to define factors associated with processing speed in the patients' intact field. To this end we firstly studied the topography of RT, namely whether processing speed is similar across the whole intact field, or if there are some regions which are more deficient than others. We hypothesized that RT might be slower especially in areas adjacent to the scotoma because the local, lateral interactions are disturbed. The most straightforward approach to test this hypothesis was to define the lesion border of each patient and then analyze intact field RT as a function of the distance to the border. However, due to a high variability of visual field topography, especially in the pre-chiasmatic group, it was difficult to objectively define the scotoma border position. Therefore, we decided to analyze RT of intact sectors as a function of the number of defective sectors located within a 5-degree surround because this size approximates the receptive field size in the human early visual cortex (Nurminen et al., 2009). Because in this analysis we were not interested in interhemispheric effects, only spots positioned on the same side of the vertical meridian were considered. All intact sectors for each particular subject were then divided into four categories: (i) 0% defective sectors in the surround; (ii) 1%-25% defective sectors in the surround; (iii) 26%-50% defective sectors in the surround; (iv) more than 50% of defective sectors in the surround. Then, the average RT for each category was subjected to statistical analysis.

Secondly, to study global (non-retinotopic) effects of the scotoma, we conducted correlations between RT and scotoma size. We hypothesized that subjects with larger scotomata might be more impaired in intact field processing. To address this issue the size of the defective visual field was correlated with the averaged RT in the intact visual field. Because central sectors of the visual field occupy a larger cortical representation than peripheral regions, the HRP visual field charts were transformed according to the cortical magnification factor (CMF) as defined by Qiu et al. (2006). This was done to avoid over- or underestimating the functional impact of defects in the periphery versus the central visual field. However, when comparing correlations involving the CMF-corrected versus non-corrected proportion of the defect field, it was noted that the CMF correction had only a minor effect on our study results.

Thirdly, to study interhemispheric influences, a sub-population of post-chiasmatic patients was studied that suffered a loss of vision in only one quadrant (n=16; 8 female). The mean age in this subgroup was 52 ± 4 yrs. and the results were compared to the normative sample with an age-range of 50-59 yrs. (n=14; 8 female). Groups were gender-matched (chi-square(1,28)=0.153, p=0.696). This subgroup analysis allowed to investigate RT within three “intact” quadrants that are subject to different kinds of influences depending on their location and distance in relation to the scotoma: (i) the adjacent quadrant (lower or upper) in the same hemisphere which is possibly influenced by intrahemispheric interactions; (ii) the adjacent quadrant in the contralateral hemisphere which is possibly influenced by the loss of interhemispheric connections caused by the lesion in the mirror-symmetric position; and finally (iii) the diagonal quadrant in the contralateral hemisphere that we expected to be influenced the least by the lesion.

2.2.4 Statistics

To compare the pre- and post-chiasmatic patient groups with normative data from the Tölz Temporal Topography Study (Poggel et al., 2012) a t-test for independent samples was applied. To compare gender distribution chi-square test was used. To investigate effects of visual field features on RT we used repeated measures ANOVA with within-subject factor being the visual field feature. We tested three visual field features: detection accuracy (3 levels), accuracy in the surround (4 levels), and visual field quadrant (3 levels). Post-hoc tests

were Bonferroni corrected. The relationship between scotoma size and RT was analyzed with Spearman correlation coefficient.

Values are presented as mean \pm standard error of the mean (SEM). The two-tailed significance criterion was set at $p < 0.05$. Greenhouse-Geisser correction was applied when necessary. All analyses were carried out in Matlab 2011b (Mathworks) and SPSS 21.

2.3 Study I: Results

2.3.1 Intact field RT is higher in patients than in control subjects

Firstly, we compared intact field RT of both patients groups, pre- and post-chiasmatic, to normative data of healthy subjects (347.2 ± 4 ms) in the Tölz Temporal Topography Study (Poggel et al., 2012). In both, pre-chiasmatic (469.4 ± 10 ms; $t(1,41) = 12.18$, $p < 0.001$) and post-chiasmatic patients (437.4 ± 6 ms; $t(1,91) = 13.8$, $p < 0.001$) RT was significantly longer than in the control group.

Further, intact field RT of patients was compared to control group, but including only RT of intact sectors with completely intact 5 deg. surround. Still, both groups of patients, pre-chiasmatic (439.8 ms, $t(1,35) = 10.62$, $p < 0.001$) and post-chiasmatic (429.7 ms, $t(1,91) = 14.61$, $p < 0.001$), exhibited longer RT than control subjects.

2.3.2 RT is related to the functional state of the visual field

In both patient groups RT was found to be related to the visual field functional state, i.e. defect depth (**Fig. 2.1**, pre-chiasmatic: $F(2,39) = 84.02$, $p < 0.001$; post-chiasmatic: $F(2,94) = 134.24$, $p < 0.001$). All post-hoc comparisons between three visual field states were significant with $p < 0.001$.

2.3.3 Local effect: intact field RT is related to the functional state of the immediate surround

RT at any tested position in the intact visual field depends on the functional state of its immediate surround (**Fig. 2.2**; pre-chiasmatic: $F(3,29) = 77.24$, $p < 0.001$; post-chiasmatic: $F(3,73) = 68.47$, $p < 0.001$). All post-hoc comparisons between intact sectors with different surround states were significant ($p < 0.001$). This shows that processing speed deficits are not

uniformly distributed but intact visual field regions are more impaired when located in the vicinity of the scotoma.

Scatterplots of single cases (**Fig. 2.2, B**) show the association between RT of a particular HRP sector and the proportion of defective sectors in its surround. However, the inter-subject variability of RT is still rather high suggesting that additional, global factors have an impact on processing speed in the intact visual field.

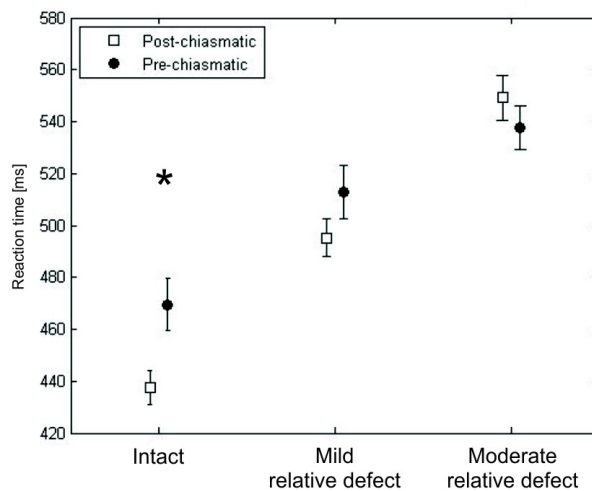


Figure 2.1. RT and the functional state of the visual field area. In both groups, pre-chiasmatic and post-chiasmatic, RT depends on the functional state of the visual field sector, as defined by HRP detection accuracy. Processing speed upon detected stimuli was higher in the relative defect regions than in the intact field.

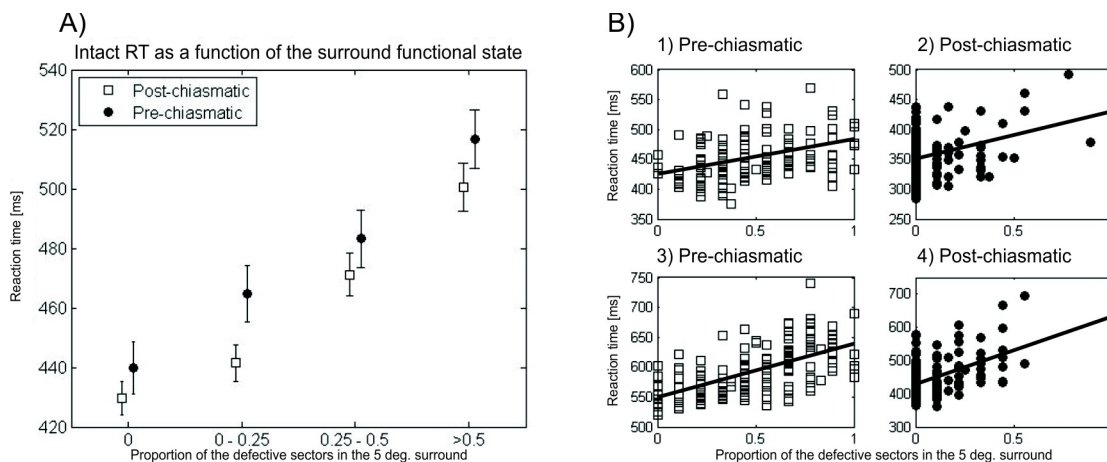


Figure 2.2. Intact field RT and the functional state of the immediate surround. Group analysis (A) and single cases as representative examples (B) are shown. Functional status of

the immediate neighborhood, defined as the percent of defective sectors in the 5-degree surround, partially explains within-subject variability of RT in patients with pre-chiasmatic (case 1 and 3) and post-chiasmatic lesions (case 2 and 4). However, between-subject RT variability is still substantial.

2.3.4 Global effect: intact field RT is related to the scotoma size

Larger defective visual fields were associated with longer RT averaged over the whole intact field in both groups, pre-chiasmatic ($r=0.63$, $p<0.001$) and post-chiasmatic ($r=0.28$, $p=0.006$) (Fig. 2.3). These correlations were also significant when only the absolute defect area (proportion of black sectors only) was considered (pre-chiasmatic: $r=0.53$, $p=0.001$; post-chiasmatic: $r=0.23$, $p=0.022$). However, it might be argued that the “local effect” contributes mainly to these correlations as the mere presence of a larger defective field implies a greater proportion of the intact field located in the vicinity of the defect. To refute this possibility the RT of all intact sectors were z-normalized for the proportion of defective sectors in the 5-degree surround. In line with our hypothesis, correlations with normalized RT were weaker but still significant for pre-chiasmatic ($r=0.35$, $p=0.022$) and post-chiasmatic patients ($r=0.27$, $p=0.008$), which proves that a local influence alone cannot explain longer RT in patients with greater defect size.

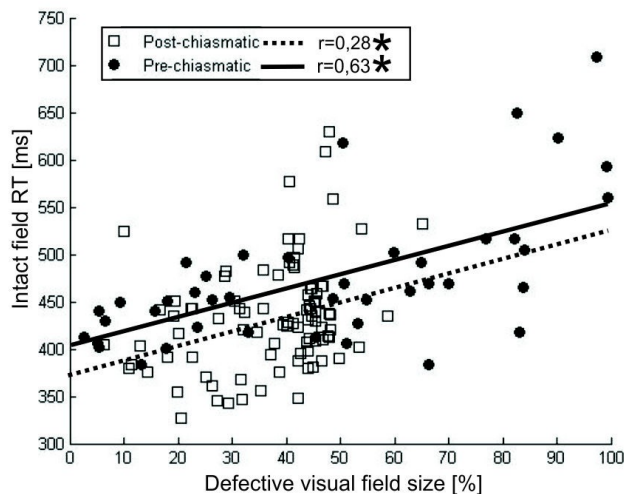


Figure 2.3. Intact field RT and the scotoma size. In both groups, pre-chiasmatic and post-chiasmatic, a significant correlation was found between the size of the scotoma and the intact field RT. This indicates that subjects with a larger defect field are more impaired in the intact field as well.

2.3.5 Interhemispheric effect: intact field RT in quadrantanopia

In a subsample of post-chiasmatic patients with quadrantanopia (n=16) the three intact visual field quadrants were defined according to their location in relation to the scotoma (**Fig. 2.4**). All three intact quadrants exhibited significantly higher RT than subjects from the normative sample (347.2±4ms). This was true for the adjacent quadrant in the defect ipsilateral hemisphere (421.4±17ms; $t(1,15)=4.25$, $p=0.001$), the adjacent quadrant in the contralateral hemisphere (392.5±10ms ; $t(1,15)=4.32$, $p<0.001$), and the diagonal quadrant in the contralateral hemisphere (391.1±10ms; $t(1,15)=4.19$, $p<0.001$; all tests Bonferroni corrected). Secondly, we found that RT differed in the three intact quadrants as a function of the relative position to the scotoma ($F(2,13)=8.95$, $p=0.007$). Mean RT in the adjacent quadrant in the same hemisphere (421.4±17ms) was significantly longer than in the adjacent quadrant in the contralateral hemisphere (392.5±10ms; $p=0.040$) or the diagonal quadrant (391.1±10ms; $p=0.012$).

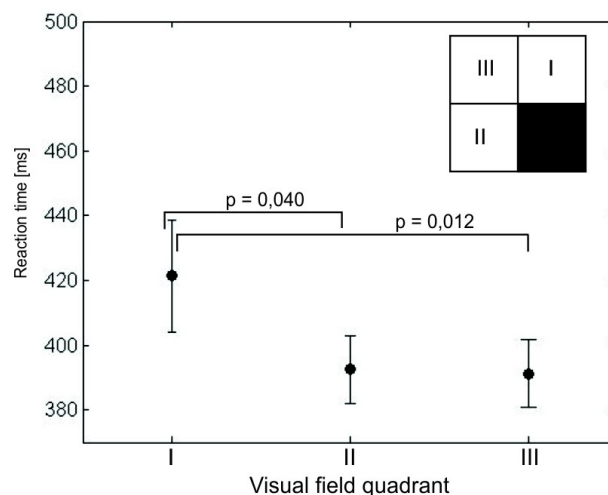


Figure 2.4. Intact field RT in quadrantanopia. RT was calculated for each of the three quadrants with respect to the position of each quadrant in relation to the scotoma: RT in the adjacent quadrant of the same hemisphere (I) was slower than in the adjacent (mirror-symmetric) quadrant of the contralateral hemisphere (II) and the diagonal quadrant (III). The inset is a simplified sketch of a visual field test showing an example of a lower right quadrantanopia to illustrate the position of the three “intact” quadrants. Processing speed in all three intact quadrants was impaired in comparison to healthy controls. Additionally, the intact quadrant located in the same hemisphere as the scotoma (I) was found to be more impaired than the two quadrants processed by the uninjured hemisphere (II and III). There was no evidence of symmetric transcallosal connectivity influences, since the quadrant mirror-symmetric to the scotoma (II) did not show more pronounced deficits than the diagonal quadrant (III).

2.4 Study I: Discussion

The present study demonstrates that visual processing speed, as indicated by reaction time (RT) to simple light stimuli, is impaired in the “intact” visual field of patients with visual system damage. Two correlates of processing speed in the intact visual field were identified. Firstly, RT in each tested position in the intact visual field is related to the functional state of its “local” surround: the more defective the surround the longer the RT. Secondly, the size of the scotoma matters: the bigger it is, the longer the average intact field RT, which indicates a “global effect” of the scotoma on the visual field and possibly a “network” dysfunction. From this we conclude that the visual system lesion might affect the “intact” visual field in a local (retinotopic) and a global (non-retinotopic) manner. The local effect accounts for the within-subject variability and topography of the intact field RT, whereas the global effect for inter-subject variability and general level of performance. This raises the question as to possible neurophysiological mechanisms underlying these influences.

2.4.1 Perceptual deficits in the “intact” visual field of patients

Perceptual deficits in the visual field parts believed to be intact were shown in subjects with visual system damage of different etiologies. Firstly, in patients with unilateral visual cortex lesions several perceptual functions such as contrast and contour perception were found to be impaired in the intact (seeing) field processed by the non-lesioned hemisphere (Rizzo and Robin, 1996; Paramei and Sabel, 2008; Schadow et al., 2009). Moreover, processing speed stands out as one of the main symptoms, since RT in the “intact” visual field of cortically lesioned patients was elevated in comparison to healthy subjects irrespective of the task (Rizzo and Robin, 1996; Paramei and Sabel, 2008; Schadow et al., 2009; Poggel et al., 2011; Cavezian et al., 2010). Likewise, in patients with optic neuritis, temporal processing and motion detection in the intact field were impaired, despite normal static perception (Raz et al. 2011, 2012). Here we confirm that in a simple detection task, patients with partial visual field loss exhibit processing speed deficits in the visual field area characterized by normal detection abilities. Further, evidence was found for both local and global, but not interhemispheric influences of the scotoma on temporal processing of the intact visual field.

2.4.2 Local effect of the visual system lesion

The intact field close to the scotoma is characterized by a slower processing speed when compared to the intact sectors with a relatively intact surround (**Fig. 2.2**). This factor is calculated for each visual stimulus position. This “local scotoma effect” accounts for within-subject variability and determines the topography of the impairment.

What are possible mechanisms of this local effect? Firstly, it has been postulated that in patients with visual field loss attention is not equally distributed across the visual field (Sabel et al., 2011a). Particularly, areas surrounding the scotoma lack attentional reinforcement, as patients might (unintentionally) use intact visual field areas located far from the blind field for everyday vision. If subjects indeed focus their attention far from the scotoma, processing in the intact field close to the scotoma border might be disturbed.

There are also several neurophysiological mechanisms that might be of relevance. Firstly, partial optic nerve damage or cortical tissue loss may lead to a reduced physiological signaling power and to a loss of firing synchrony of neuronal assemblies, thus increasing processing time. Secondly, there is an extensive remapping and reorganization of the visual field representation after pre- and post-chiasmatic damage as shown in animal model studies (Kaas et al., 1990; Gilbert and Wiesel, 1992; Calford et al., 2000; Waleszczyk et al., 2003), as well as fMRI studies in patients (Baker et al., 2005; Schumacher et al., 2008; Dilks et al., 2009; Liu et al., 2010). Such receptive field reorganization is believed to be mediated by mechanisms involving plasticity of intrinsic cortical horizontal connections but the perceptual consequences are vague. In this context a study by Dilks et al. (2007) showed that shapes presented in the intact quadrant adjacent to the scotoma (in the same hemispace) are distorted and often elongated toward and into the blind field. Presumably, reorganization demonstrated in animal models might produce this kind of spatial distortions. This is in line with our analysis of RT in quadrantanopia patients, revealing that the quadrant adjacent to the scotoma is most impaired in terms of processing speed (**Fig. 2.4**). Thirdly, receptive fields not only change their location but also become larger (Gilbert and Wiesel, 1992). It is still unclear how these changes affect perception. While an enlarged receptive field implies pooling of signals from larger regions of the visual field, thus increasing the probability of responding to stimuli, it may also introduce more noise. Future studies need to show if or when receptive fields plasticity is adaptive or maladaptive.

2.4.3 Global effect of visual system lesions

Besides local influences we also found evidence for a global (non-retinotopic) influence of the scotoma on the intact visual field. Specifically, a larger scotoma was associated with a greater RT deficit in the intact visual field (**Fig. 2.3**) suggesting that the amount of spared cortical tissue is related to the efficacy of intact field processing. This cannot be explained by local influences alone, because when the correlation analysis of scotoma size and intact field RT was repeated after RT normalization for the functional state of the surround, the correlation remained significant. Secondly, both groups of patients exhibited slower RT than healthy subjects when only intact sectors with completely intact surrounds were taken into account. Finally, a global effect was further substantiated by analysis of RT in quadrantanopia subjects. All three intact quadrants were impaired in comparison to healthy subjects, including the quadrant diagonal to the scotoma which is not influenced by any local interactions (see: **Fig. 2.4**).

Yet, given the extensive connectivity of the visual system (de Haan and Cowey, 2011) it is hardly surprising that a lesion or deafferentation of the primary visual cortex has a non-specific “global effect” on visual processing. Alterations in down-stream, higher cortical areas, not directly affected by the lesion, were already demonstrated in fMRI studies in human subjects (Raz et al., 2012; Dai et al., 2012; Toosy et al., 2005). However, the behavioral correlates of visual network alterations are still poorly understood. Our findings point towards deficits in visual processing speed as a possible, non-specific consequence of the visual system network changes induced by the lesion.

2.4.4 Clinical relevance of the intact field perceptual deficits

We propose that the intact visual field dysfunction, here temporal processing, has an impact on overall subjective vision in patients. Since the scotoma size does not always match well with the subjective vision loss, as measured by vision-related quality of life questionnaires (Gall et al., 2009; Müller et al., 2003), other factors than scotoma size may contribute to the patients’ subjective estimates of visual functions and the perceptual impairment in the seeing field may offer a possible explanation for this.

The question arises why so little is known about intact field deficits. We believe the main reason is that patients with visual system damage are usually diagnosed with standard perimetry using simple detection tasks which are “blind” with respect to higher perceptual and cognitive functions (e.g. feature binding, attentional selection), or dynamic perception (e.g.

motion detection). Therefore, to gain a better understanding of the subjective element of blindness, visual function beyond simple detection in a standard vision exam should be assessed to fully appreciate the objective and subjective elements of vision loss.

2.4.5 Conclusions

By analyzing RT in a simple perimetric light detection task we revealed that patients with visual field loss suffer processing speed deficits in visual field areas considered to be intact. In both groups, pre- and post-chiasmatic, visual system lesions have local (retinotopic) and global (non-retinotopic) effects on the intact field processing speed. Thus, visual system lesions have more far-reaching consequences for visual functions than previously expected, affecting the presumed “intact” visual field as well.

We expected that diaschisis and disturbance of large-scale cortical networks contribute to the intact field deficits and hamper subjective quality of vision in patients. Therefore, in the next study we investigated state of functional brain networks using EEG and related EEG measures to perception in patients.

3. Study II: Breakdown of functional connectivity networks in blindness

Published in:

Bola M, Gall C, Moewes C, Fedorov A, Hinrichs H, Sabel BA. (2014). Functional connectivity network breakdown and restoration in blindness. *Neurology*, 83, 542-551.

3.1 Study II: Introduction

In the second study we wished to address two research questions. Firstly, do peripheral visual system lesions, which do not directly damage the visual cortex, permanently alter *spatial* patterns of spontaneous cortical activity? Secondly, is the state of the functional connectivity network related to patients' perceptual capabilities? If state (synchronization) of the cortex is related to vision in patients this will further stress the point that vision loss is not only a bottom-up loss, but that also the visual system state and top-down influences are important. To test this hypothesis patients suffering from pre-chiasmatic visual system damage were compared to uninjured controls to define neurophysiological correlates of vision loss. Several measures quantifying activity of neural circuits based on EEG signal were used in order to obtain a full and comprehensive view of the brain networks state, including spectral power, coherence and Granger Causality, and graph measures. Patients EEG measures were (i) compared to these obtained from an age-matched healthy control group and (ii) correlated with vision measures (perimetry).

In the initial exploratory analysis I found alpha band activity and connectivity to be disturbed in patients. To strengthen the argument that resting-state alpha band activity is related to patients' vision I aimed to modulate the alpha activity and observe whether alpha

increase covaries with perceptual improvements. Therefore, rtACS, shown to strengthen alpha band synchronization and restore vision (Sabel et al., 2011b; Schmidt et al., 2013), was utilized. Further, the design of our study, involving comparisons at baseline (patients vs. controls) and investigation of rtACS effects (pre-ACS vs. post-ACS), allowed us to investigate the possible match of neurophysiological deficits exhibited by patients and rtACS induced effects. The conducted analyses indeed point towards resting-state alpha band activity and connectivity being a correlate of vision loss.

3.2 Study II: Methods

3.2.1 Patient consents

The study was approved by an ethical standards committee on human experimentation (institutional) and written informed consent was obtained from all patients participating in the study (consent for research). All patients were treated according to the Declaration of Helsinki.

3.2.2 Subjects

The study sample consisted of 15 patients (**Table 3.1**) with chronic pre-chiasmatic visual system damage and 13 control subjects without any neurological dysfunctions. Subjects were recruited and tested from 11.2006 to 03.2010 in Magdeburg. Both groups did not differ in age (patients: 50.5 ± 5 yrs; controls: 46 ± 5 yrs; $t(26)=0.68$, $p=0.50$) and any other demographic or vision-related measures.

Inclusion criteria for patient entry into the study were: (i) chronic visual system damage (>6 months of lesion age); (ii) sufficient fixation ability; and (iii) presence of residual vision detected by perimetry. Patient's diagnoses were taken from their medical records of the referring professionals. Medical records provided information about ophthalmological assessment and if available results of structural imaging of the brain. Two patients (IDs: 4, 10) had unilateral optic neuropathy (one eye remaining intact) and the rest of the patients had bilateral optic neuropathy. The patients were randomly assigned to either a sham ($n=8$) or rtACS group ($n=7$). The groups did not differ at baseline with respect to demographic and vision measures. One sham patient had to be excluded from post-rtACS analysis due to sedative drugs intake which was uncovered only after completing the experiment.

All patients were tested with perceptual tests and EEG before and after 10 days of daily non-invasive brain stimulation (baseline and post respectively). Measurements were done 1 or 2 days before the first and after the last stimulation session. Baseline data from patients were compared to data from healthy control subjects.

Table 3.1. Description of the Study II patients sample.

ID	Sex	Age	Lesion age [months]	Group	Etiology	Acuity		Static perimetry threshold [db]		Kinetic perimetry [deg]	NEI-VFQ
						Near R/L	Far R/L	Foveal R/L	Whole field R/L	Mean field size R/L	
1	W	47	509	Sham	ON atrophy after infection	1/1	0.8/0.8	29/26	17.8/16.41	60.3/60.3	85
2	M	20	53	Sham	Leber hereditary optic neuropathy	0.02/0.02	0/0	9/0	1.7/1.2	36.2/35.5	42
3	M	58	8	Sham	AION	1.4/0.4	1.2/0.24	24/16	17.4/9.35	55.8/46	92
4	W	24	51	Sham - excluded	Optic neuritis	1.4/1.4	1.2/1.2	30/28	22.3/15	59/56.9	91
5	W	68	14	Sham	AION	0.9/0.2	0.8/0.8	19/23	5/6	34/38	85
6	M	71	113	Sham	AION	0.5/0.13	0.4/0.17	21/20	10/16	54/58	76
7	M	73	170	Sham	Non-arteritic ischemic optic neuropathy	0.8/0.25	1.2/0.17	20/14	7/7	48/50	79
8	W	36	438	Sham	ON damage due to cerebral hypoxia during birth	0.8/1	0.4/0.8	26/30	12/14	37/47	89
9	W	49	6	rtACS	Resected tuberculoma sellae meningioma (WHOI)	0.9/0	0.8/0	22/0	4/0.4	13.3/9.4	26
10	W	36	17	rtACS	Optic neuritis	MD/1	MD/1.2	MD/27	MD/18.6	MD/59.4	92
11	W	44	32	rtACS	Optic neuritis	0/0.13	0/0.17	0/26	1/10	50/23	41
12	M	74	125	rtACS	AION	MD/0.9	MD/0.8	MD/24	MD/5.7	MD/37	92
13	M	67	23	rtACS	AION	0.06/0.04	0.17/0	15/0	0.4/3.9	47.9/43	46
14	W	62	175	rtACS	Glaucoma, ON atrophy	0.16/0.9	0.17/0.6	11/28	0.5/14	6.3/55.7	54
15	M	28	24	rtACS	Idiopathic ON atrophy	1.25/0.02	1.2/0	27/0	13/1	31/10	68

ON – optic nerve; MD - missing data.

3.2.3 Data acquisition

3.2.3.1 High Resolution Perimetry

Visual fields of patients were mapped monocularly with HRP before and after the rtACS. HRP measurements were taken in a darkened room, where patients were seated in front of a 17" monitor with the head positioned in a chin rest with a forehead-holder to keep the eyes at a constant distance of 42 cm, with the center of the screen at eye level. Supra-threshold, white light stimuli were presented on dark grey background, within a grid of size of 25x19 sectors, covering 40°x30° of subjects' visual field. In each testing block one stimulus

per sector was presented. The order of stimulus positions and the inter-stimulus intervals (ISI) were random so that patients could not predict when and where the stimuli were presented). In order to control subjects' fixation during testing, a central fixation stimulus was presented with isoluminant color changes from green to yellow to which the patients also had to respond 80 times per testing block. Subjects were instructed to maintain fixation at all times and press the space bar on the computer keyboard whenever a "target stimulus" was detected anywhere on the screen or when the fixation point changed colour. If the subject did not press the button within 1000ms after the target stimulus or fixation point colour change, the response was coded as "miss". These tasks were presented at random ISI. To control for random guessing all responses faster than 150ms and slower than 1000ms after the stimuli occurrence or fixation point colour change were treated as "false positives".

Detection accuracy in every sector averaged over 3 blocks was used as a criterion to define whether a given sector of the visual field belonged to the "intact" area (100% stimuli detected, shown in white in the visual field charts), mild (66% stimuli detected, light grey) or moderate relative defect (33% stimuli detected, dark grey) or absolute defect area (0% stimuli detected, black). For every sector where at least one valid response was given (button press > 150ms and <1000ms after the stimulus) averaged RT was calculated over all valid responses.

Three HRP measures were correlated with EEG measures. Firstly, detection accuracy averaged over all HRP sectors. Secondly, size of the intact field, being the proportion of intact sectors among all sectors. Thirdly, RT averaged over all intact sectors. Post rtACS change in HRP measures was calculated for every eye as percent of change over baseline:

$$\Delta HRP = ((post - pre) / pre) * 100,$$

where *pre* denotes patients result before and *post* after the rtACS treatment. When change in RT was calculated for intact sectors, only sectors being intact at baseline were considered (irrespective of their status post-rtACS). To correlate HRP and EEG measures, HRP results of both eyes were averaged.

3.2.3.2 Static perimetry, kinetic perimetry, and visual acuity

Visual fields were also measured with a Twinfield perimeter (Oculus, Lynnwood, WA). A video camera of the perimeter was used to evaluate eye movements, pupil size and fixation

ability. During static 30° perimetry 66 target stimuli (size: III/4mm², color: white, luminance: 318 cd/m²/0db, duration: 0.2 sec) were presented with a fast threshold strategy on a background with constant luminance of 10 cd/m². To verify proper fixation, four target stimuli were presented inside the blind-spot, these trials were later excluded from further statistical analysis. Measures derived from static perimetry were the foveal threshold, the mean threshold averaged across all tested positions excluding the blind spot, the number of absolute defects (misses of stimuli presented with maximum luminance), and the number of relative defects (stimulus detections at increased luminance above the physiological adequate threshold). In kinetic perimetry the target (0dB) was moved from the periphery towards fixation at a constant velocity of 2°/sec. The visual field border was then determined for all 24 meridians randomly. Visual acuity was measured monocularly with and without corrected refraction using a Snellen test chart at a distance of 6m for distance vision and the Landoldt-ring test at a distance of 40 cm for near vision.

3.2.3.3 Questionnaires

To quantify subjective vision patients filled out the National Eye Institute Visual-Functioning Questionnaire 39 (NEI-VFQ) and a composite score, excluding “general health” subscale, was calculated.

3.2.3.4 EEG recordings

EEG was recorded with BrainAmp amplifier (Brain Products, Munich, Germany) using 30 sintered Ag/AgCl electrodes mounted in an elastic cap according to the 10-10 system. Specifically we used the following electrodes: EOG, Fp1, Fp2, F7, F3, Fz, F4, F8, FC5, FC1, FC2, FC6, TP9, T7, C3, Cz, C4, T8, TP10, CP5, CP1, CP2, CP6, P7, P3, Pz, P4, P8, O1, O2. For the recording nose-tip reference was used and ground electrode was placed between Fz and Cz. The signal was acquired with sampling frequency of 5 kHz, high-pass (0.016 Hz) and low-pass (1000 Hz) filtered, and A/D converted (16 bit). Subjects were seated in a dimly lit room and asked to keep eyes closed during the recording.

3.2.4 Electrical stimulation protocol

To test whether change in alpha band activity and connectivity covaries with change in vision measures patients were treated with repetitive transorbital alternating current

stimulation (rtACS). The protocol has already been described elsewhere (Sabel et al., 2011b; Schmidt et al., 2013). Briefly, the rtACS was applied with four stimulation electrodes (sintered Ag/AgCl ring electrode) placed near the eyeball (“transorbital”) with eyes closed. The passive electrode was positioned on the wrist of the right arm. Multi-channel device (alpha-synch; EBS Technologies, Germany) was used generating weak current pulses firing bursts of 5 to 9 pulses. Current amplitude and frequency range were individually adjusted. Every stimulation session was preceded by diagnostic session. During diagnostic session (10 min) amplitude of the alternating current was increased stepwise (by 10 μ A per second) until the subject perceived phosphenes. The following stimulation (40 min) was given with amplitude clearly above the phosphene threshold (125%). For diagnostics 5 Hz stimulation was used, while during stimulation session a range of stimulating frequencies was used between 8Hz and 22Hz. The sham group received one 5Hz burst of pulses per minute during the diagnostic and stimulation sessions.

Patients and examiners performing visual diagnostic tests were blinded as to the group assignments of the patients. However, the neurologist performing rtACS stimulation and recording EEG was not blinded, as this was technically not possible.

3.2.5 EEG data analysis

3.2.5.1 Preprocessing

Analysis of the EEG data was carried out in MatlabR2011b and EEGLab (Delorme and Makeig, 2004). First 40 seconds of the EEG signal was chosen from each recording and the signal was re-referenced to the averaged reference. Then we applied high-pass (0.5Hz) finite impulse response (FIR) filter to exclude slow drifts, notch (50Hz) FIR filter to exclude 50Hz line, and low-pass (125Hz) FIR filter to prevent aliasing during the following down-sampling to 250Hz. Data were divided into 40 non-overlapping 1s long epochs, that were visually screened for artifacts and rejected in case of excessive oculographic or miographic activity. Mean number of epochs left after artifact rejection was 35 (min: 31; max: 37) in the patients group, and 36 (min: 32; max: 38) in the control group.

3.2.5.2 Spectral power

Power density was calculated with the Matlab *pwelch* function. It divides each epoch into 8 sections (50% overlap), each section is windowed with Hamming window, and 8 periodograms are calculated and averaged. Power density was averaged over all epochs for each subject. Power density was presented as normalized $10\log_{10}$ values. We investigated spectral power at two areas of interest (AOI): occipital (O1, O2) and frontal (FC1, Fz, FC2). The former AOI was placed over visual regions and far from the stimulating electrodes (although this is connected to the stimulation site anatomically via the optic nerve and optic tract). The latter AOI was placed far from the visual regions, but close to the stimulating electrodes (although it is not anatomically connected with the stimulation site). Thus, we expected lesion- and stimulation-related changes mainly at the occipital AOI.

For the EEG analysis we defined five spectral frequency bands: delta – 1-3Hz; theta - 3-7Hz; low alpha (alpha I) - 7-11Hz; high alpha (alpha II) – 11-14Hz; and beta - 14-30Hz.

3.2.5.3 Functional connectivity estimation

To investigate functional connectivity between brain regions we estimated coherence, indicating coupling between two signals as a function of frequency (Pereda et al., 2005). We calculated coherence for each pair of channels ij using the following formula:

$$C_{ij}(f) = \frac{|S_{ij}(f)|^2}{S_{ii}(f) S_{jj}(f)}$$

In this equation S denotes spectrum of signals from two EEG channels i and j , for a given frequency bin f . A Matlab function *mscohere* was used. Initially, a coherence adjacency matrix was obtained for each data epoch (29X29Xf) and then matrices were averaged over epochs to give a coherence estimate for each subject, and over frequency bins, to give a coherence estimate for each EEG band. Thereafter, three types of analyses were carried out: (i) short range coherence within the occipital AOI (between O1 and O2); (ii) short range coherence within the frontal AOI (between FC1, FC2, Fz); and (iii) long-range coherence, between occipital and frontal AOI (between [O1, O2] and [FC1, FC2, Fz]).

As strength of long-range coherence between occipital and frontal AOI differed between groups, we calculated Granger Causality (GC), a directed measure of functional

interactions in the frequency domain (Seth, 2010). This permitted us to confirm our initial result with an independent method, and secondly, to test the hypothesis concerning the direction of the influence. A freely available toolbox was used to calculate GC (Seth, 2010). We restricted this confirmatory analysis to long-range interactions between occipital and frontal AOI ([O1, O2] – [FC1, Fz, FC2]). Briefly, GC was implemented via multivariate autoregressive model (MVAR) fitted to every data epoch to model signal from 5 channels chosen as weighted sums of past values. To find an optimal order the Bayesian Information Criterion (BIC) was used. Model order was assessed for every data epoch and the median was taken as an indicator of optimal model order for the subject. Then the median of optimal model orders from all subjects was taken as a model order used for the analysis, which was 17 in our case. The fit of the MVAR model was assessed with the consistency test which expresses the portion of the data captured by the model as percentage. Model consistency did not differ between control (90.7 ± 2.2) and patients group (87.8 ± 2).

3.2.5.4 Graphs analysis

To analyze topology of the functional connectivity networks coherence estimates were converted into binary graphs consisting of nodes ($N=29$; representing EEG channels) and undirected edges (connections between nodes; see **Fig. 3.1**). An edge between two nodes exists when the coherence value for this particular pair of nodes exceeds the threshold T . The threshold T was adjusted on an individual basis, for every subjects and frequency band, to obtain equal number of edges per graph (**Fig. 3.5, 3.6**). In this manner graphs are not influenced by differences in the general level of synchronization between subjects and groups. Usually, the number of represented edges K is defined as a multiplication of the number of nodes N . We present data for $K=3N$, but the results were similar for $K=5N$.

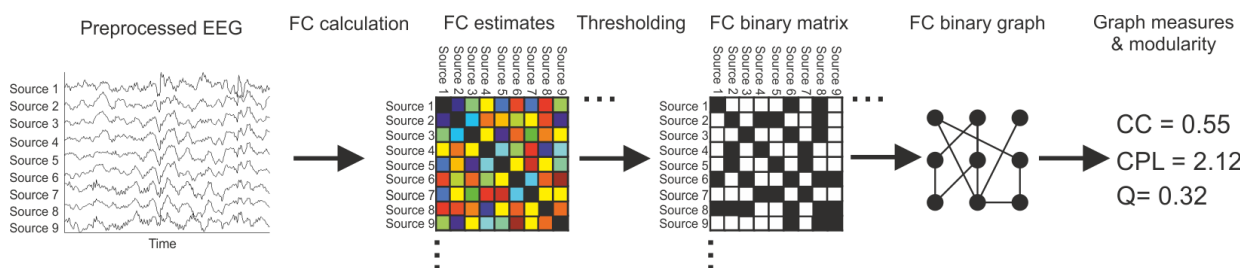


Figure 3.1 Creating binary graphs from EEG data. Preprocessed EEG data are used to estimate functional connectivity (FC; e.g. coherence) between all pairs of channels/sources. The strength of coupling is marked by color in the connectivity matrix. Then a threshold is

applied to create a binary connectivity matrix which can be represented as a graph. Various graph measures can be applied to characterize a binary graph.

Having obtained binary graphs for each subject and band, we used the Brain Connectivity Toolbox (Rubinov and Sporns, 2010) to calculate “small-world” measures for each node of the network. Firstly, clustering coefficient, indicating how many nodes connected to the node of interest is also connected to each other (how many neighbors of the node are neighbors to each other). Secondly, we determined the characteristic path length which is the average of the shortest paths between all nodes. Shortest path between nodes A and B is the minimal number of edges that have to be traversed to reach B from A. Both measures were averaged over all nodes in a network. The “small-world” network, believed to be optimal for information processing, is characterized by high clustering coefficient and low characteristic path length.

3.2.6 Statistical analyses

Data were analyzed in two steps. Firstly, the repeated measures ANOVA was applied to capture the effects of considered factors on the EEG measures. The factors we selected depended on the type of analysis. Between-subjects factor GROUP (baseline analysis: patients, controls; rtACS analysis: sham, rtACS), and within-subjects factor frequency BAND (delta, theta, alpha I, alpha II, beta) were always included. When analyzing spectral power and short range coherence within-subjects factor AOI (occipital, frontal) was included, whereas when analyzing GC within-subjects factor DIRECTION (occipital to frontal, frontal to occipital) was included. As we were interested mainly in between group differences, either between patients and control subjects, or between sham and rtACS groups, we report only effects including GROUP factor. Secondly, detailed comparisons of between groups differences were conducted with independent samples t-test. Concerning effects of rtACS the difference between EEG measures “post” and “pre” stimulation was calculated ($\Delta\text{EEG}=\text{EEG}_{\text{post}}-\text{EEG}_{\text{pre}}$) and subjected to statistical analysis.

To assess the relation between EEG and clinical variables, Spearman correlation coefficient was used. All statistical tests of significance used a criterion of 0.05 (two-tailed). Analysis was done in MatlabR2011b and SPSS 21 and displayed as mean \pm standard error of the mean (SEM).

3.3 Study II: Results

3.3.1 Power spectra

Patients exhibited lower spectral power than healthy controls and the between group difference depended on the area of interest (AOI; “group” x “AOI” interaction: $F(1,24)=7.25$, $p=0.012$; **Fig. 3.2**). Specifically, alpha II band power at the occipital AOI was lower in patients than in controls ($t(1,26)=2.60$, $p=0.015$). Furthermore, after rtACS the change in spectral power was greater in rtACS group than in sham group, which was modulated by AOI (“group” x “AOI” interaction: $F(1,10)=6.20$, $p=0.026$) and frequency band (“group” x “band” interaction: $F(4,4)=3.48$, $p=0.034$). Detailed comparisons showed that rtACS led to an increase of theta ($t(1,12)=3.35$, $p=0.006$) and alpha I power ($t(1,12)=2.52$, $p=0.027$) at the occipital AOI.

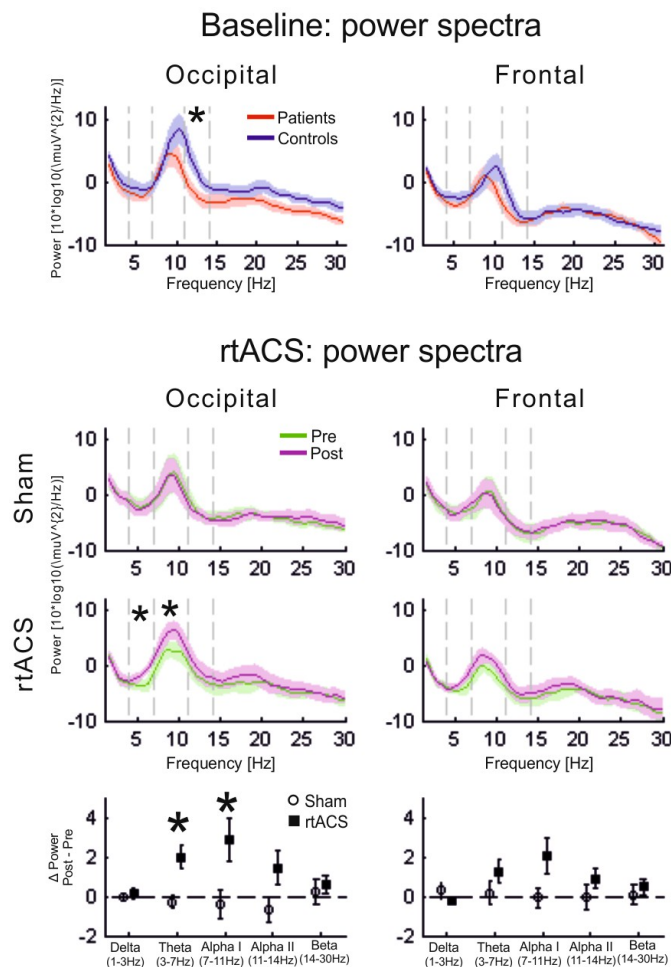


Figure 3.2. EEG spectral power. Baseline analysis indicates that patients exhibit lower power of alpha II band than control subjects. This was found at the occipital region (O1, O2) but not at the frontal area of interest (FC1, FC2, Fz). Further, 10-day rtACS stimulation

induced theta and alpha I entrainment at occipital location. Gray vertical lines indicate chosen frequency bands.

3.3.2 Short-range functional connectivity

Patients had lower short-range coherence than control subjects and the difference depended on the frequency band (“group” x “band” interaction: $F(4,18)=3.46$, $p=0.044$; **Fig. 3.3**). Between groups comparisons indicate that alpha II coherence at frontal AOI differed between groups ($t(1,26)=3.17$, $p=0.004$). After tACS greater increase in short-range coherence was observed in rtACS group than in sham group and the effect was dependent on the frequency band (“group” x “band” interaction: $F(4,4)=3.36$, $p=0.017$). Specifically, alpha I coherence increased at frontal AOI in rtACS group ($t(1,12)=3.71$, $p=0.003$).

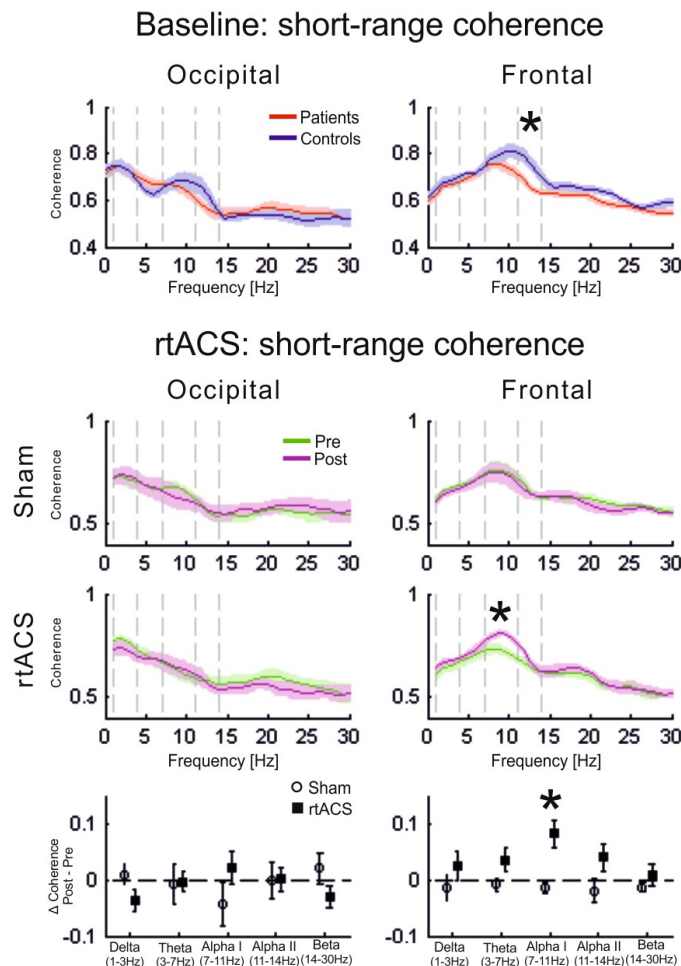


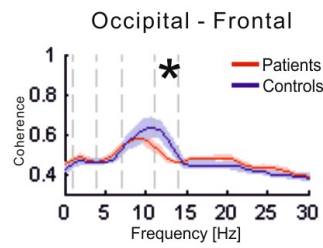
Figure 3.3. EEG short-range coherence. Short range coherence was defined as coherence within occipital (between O1 and O2) or frontal (Fz, FC1, FC2) areas of interest (AOI). In the frontal AOI patients had lower alpha II coherence than control subjects. Further, 10 day rtACS stimulation increased short-range coherence in the alpha I band in the frontal AOI.

3.3.3 Long-range functional connectivity

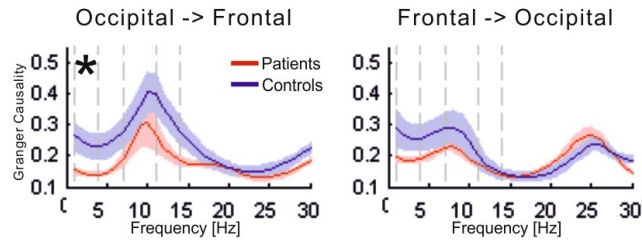
Long-range coherence was lower in patients than in control subjects and the effect depended on frequency band (“group” x “band” interaction: $F(4,18)=3.79$, $p=0.35$). Detailed analysis showed that patients had lower long-range coherence in the alpha II band than control subjects ($t(1,26)=2.20$, $p=0.042$, **Fig. 3.4**). Analysis of Granger Causality (GC) – a directed measure of functional interactions - demonstrated that long-range functional interactions were weaker in patients than in healthy controls (“group”: $F(1,26)=4.49$, $p=0.44$), specifically, patients had weaker occipital-to-frontal connectivity in the delta band ($t(1,26)=2.18$, $p=0.045$).

Analyzing effects of rtACS we found that neither the group effect (“group”: $F(1,12)=3.76$, $p=0.076$) nor the “group” x “band” interaction were significant ($F(4,4)=1.98$, $p=0.159$). Nevertheless, detailed comparisons showed that tACS strengthened long-range coherence in the alpha I ($t(1,12)=2.42$, $p=0.032$) and alpha II bands ($t(1,12)=2.47$, $p=0.029$).

Baseline: long-range coherence



Baseline: long-range Granger Causality



rtACS: long-range coherence

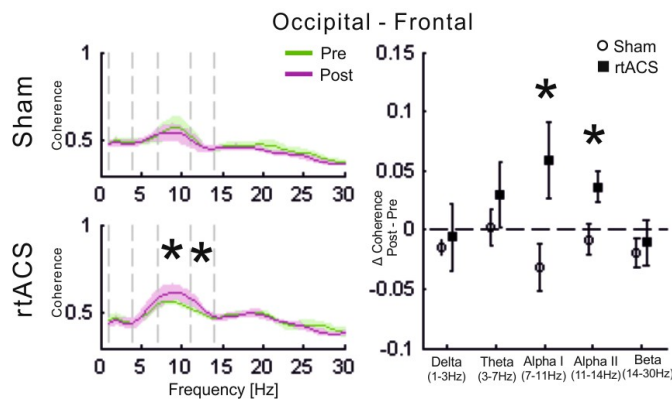


Figure 3.4. EEG long-range functional connectivity. Long-range functional connectivity was defined as coherence or Granger Causality (GC) between occipital and frontal areas of interest ([O1, O2] – [Fz, FC1, FC2]). Firstly, we found that at baseline, alpha II band long-range coherence was lower in patients than in control subjects. Secondly, using GC we confirmed weaker long-range connectivity in patients. However, GC indicated between-group difference in the delta band. Thirdly, rtACS strengthened long-range coherence in alpha I and alpha II bands, compensating for the deficit found at baseline.

3.3.4 Graphs analysis

Coherence results, converted into binary graphs, were further characterized with two graph measures: clustering coefficient and characteristic path length. Analysis of network clustering at baseline (**Fig. 3.5**) showed no group effect ($F(1,26)=0.78$, $p=0.38$) and no “group” and “band” interaction ($F(4,18)=1.47$, $p=0.21$). However, comparisons with t-tests indicate that alpha II functional connectivity networks of patients were less clustered than

those of controls ($t(1,26)=2.13$, $p=0.042$). We did not find any between groups differences in characteristic path length.

rtACS was found to influence network clustering in stimulated patients. The “group” effect (“group”: $F(1,12)=3.84$, $p=0.074$; **Fig. 3.6**) and the “group” x “band” interaction ($F(4,4)=2.51$, $p=0.053$) were not significant but specific comparisons indicated increase of clustering coefficient in theta ($t(1,12)=3.72$, $p=0.003$) and high alpha bands ($t(1,12)=2.28$, $p=0.041$). Concerning characteristic path length we did not find an effect of “group” ($F(1,12)=1.46$, $p=0.25$) or “group x band” interaction ($F(4,4)=1.25$, $p=0.30$), but t-test comparisons showed increases in alpha II band path length ($t(1,12)=2.56$, $p=0.025$).

3.3.5 Functional significance of EEG measures

At baseline higher local alpha I coherence at occipital AOI was related to greater size of intact visual field as measured by HRP ($r=0.53$; $p=0.043$; **Fig. 3.7**), to faster processing speed, as indicated by the intact field RT in HRP ($r=-0.58$, $p=0.025$), and to better detection in the fovea, as indicated by static perimetry threshold ($r=0.57$, $p=0.028$). Further, a post-rtACS increase in the local alpha II coherence at the occipital AOI was associated with increased detection accuracy in HRP ($r=0.57$, $p=0.035$), while an increase in long-range alpha II coherence was related to shorter intact field RT in HRP ($r=-0.56$, $p=0.049$). Correlations between EEG measures and near/far acuity, kinetic perimetry, and NEI-VFQ results were not found.

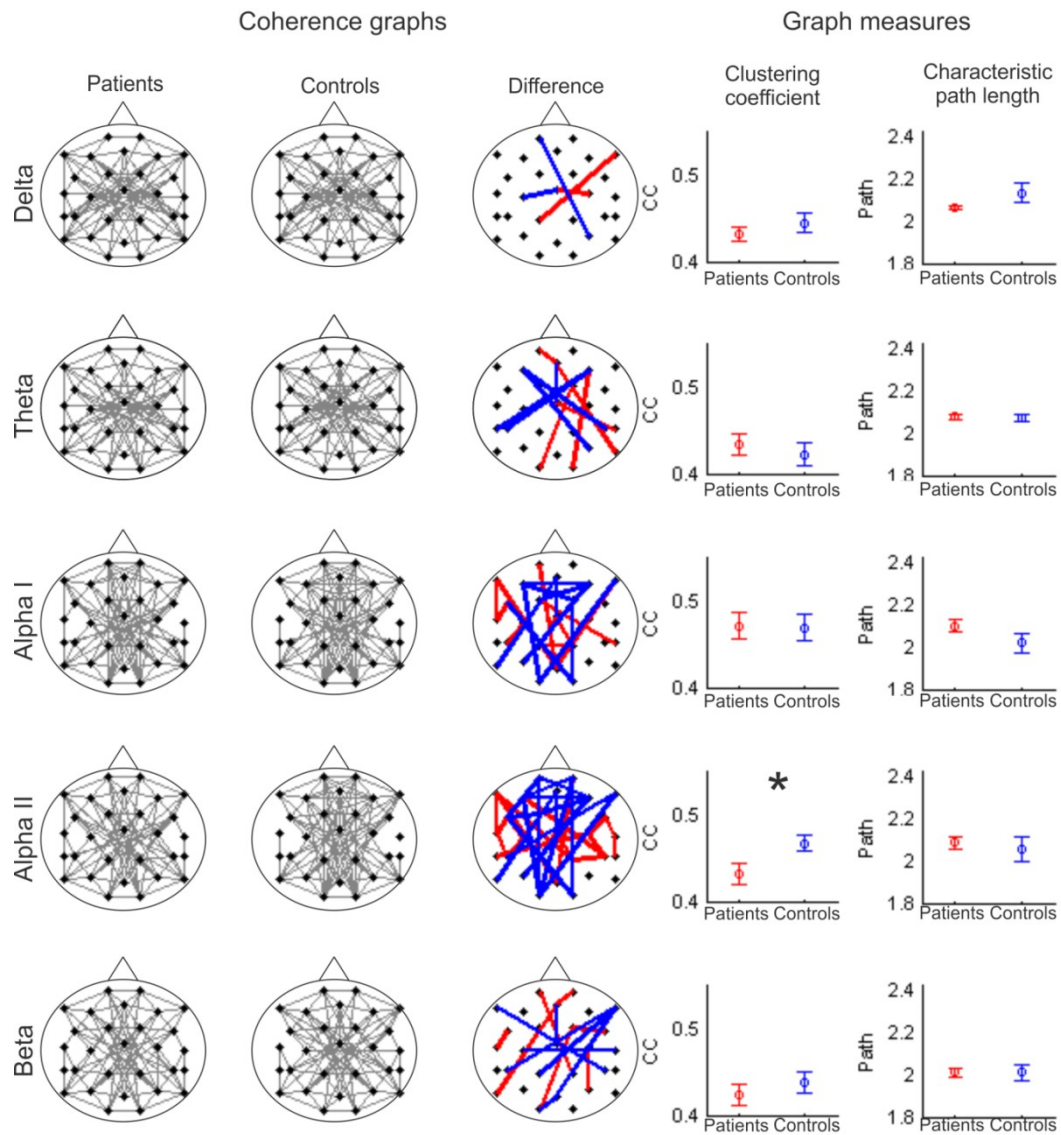


Figure 3.5. Baseline EEG coherence networks. The first three columns show coherence networks graphs with black dots representing standard EEG electrode positions, with frontal areas in the upper and occipital areas in the lower panel. All graphs contain the same number of edges (connections). The difference graphs (3rd column) display edges present in controls but missing in patients (blue) and edges missing in controls but present in patients (red). Close inspection reveals that the most pronounced between groups differences occur in the alpha II band, as graphs of patients show less edges between occipital and frontal nodes and in the frontal region, while they have more short range connections in the central area. Difference in the network topology is confirmed by analysis of clustering coefficient, indicating that networks of patients are less densely clustered.

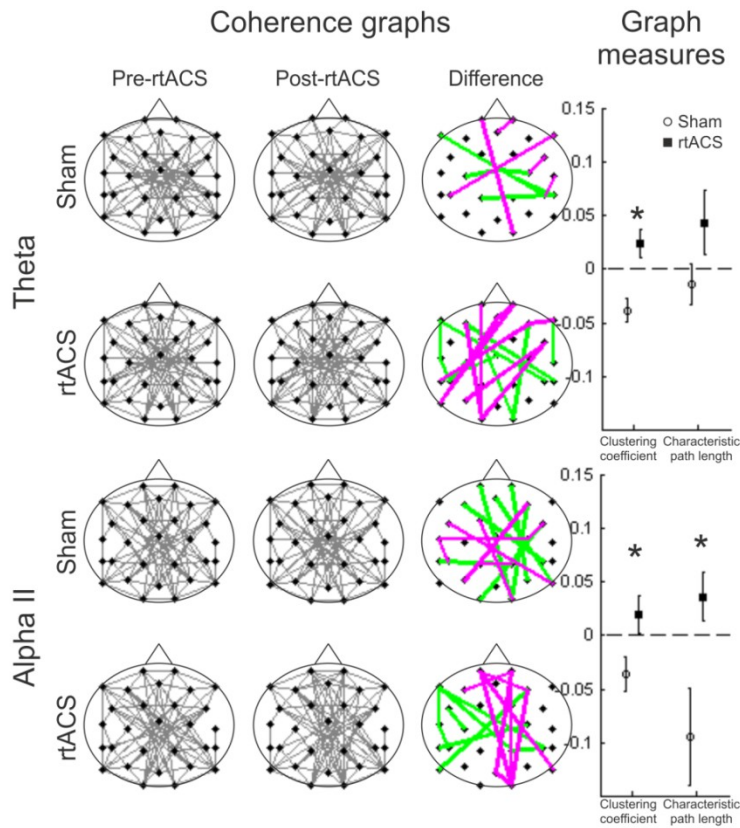


Figure 3.6. Post-rtACS EEG coherence networks. The convention is the same as in Fig. 3.5. The difference graphs (3rd column) display edges present pre- but missing post-treatment patients (green) and edges missing pre- but present post-treatment (violet). rtACS modifies network topology, as indicated by increase in clustering coefficient, modifying structure of patients networks towards patterns exhibited by healthy controls. Additionally, there was an increase in characteristic path length in the rtACS group after treatment.

3.4 Study II: Discussion

My study revealed that patients partially blinded by optic nerve damage exhibit a breakdown of resting-state alpha band power and functional connectivity. Loss of connectivity strength was related to visual perceptual capabilities. Specifically, in comparison to normally sighted controls, patients with pre-chiasmatic lesions had lower power of oscillatory activity, decreased strength of short- and long-range functional connectivity, and they exhibited less clustered patterns of the functional connectivity networks. Changes were found in a narrow frequency range, namely the high alpha band (alpha II, 11-14Hz). Further, a neuromodulation experiment with rtACS, previously shown to modulate alpha band activity (Sabel et al., 2011b; Schmidt et al., 2013), was utilized to manipulate the network synchronization and study its impact on visual perception. rtACS strengthened alpha band functional connectivity which was associated with perceptual improvements. This suggests

that the alpha band oscillatory activity in the resting state (at eyes closed) is a marker of both loss and restoration of visual perceptual capabilities in partially blinded patients.

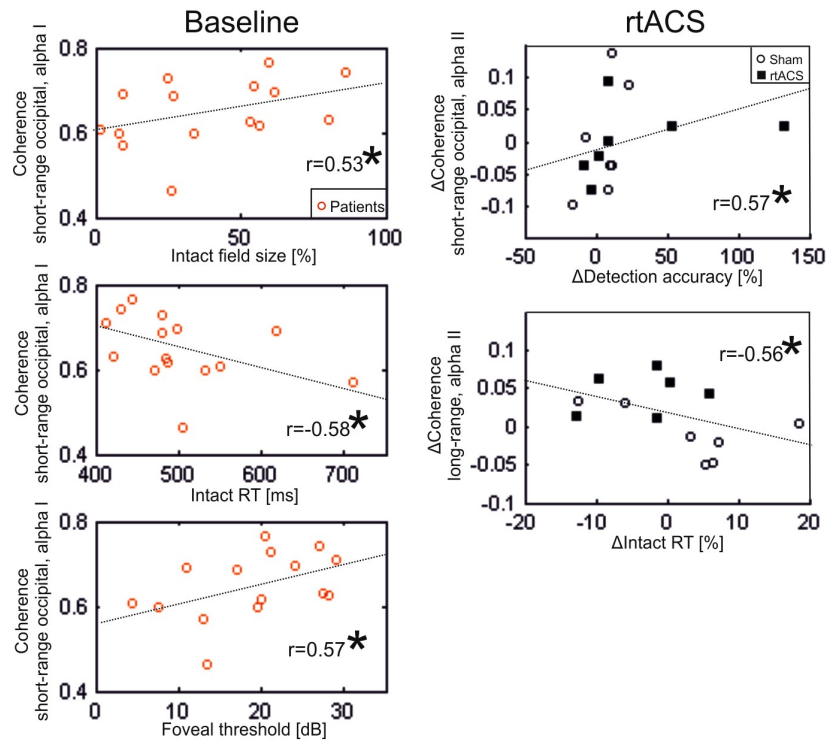


Figure 3.7. Correlations between EEG and vision measures. At baseline patients with stronger short-range alpha I coherence at occipital region had bigger intact fields, as measured by HRP, shorter RT to HRP stimuli in the intact field, and better foveal detection in static perimetry. Analyzing change in EEG and vision measures subjects with an increase in short-range alpha II coherence at occipital regions improved their detection abilities, and subjects with increase in long-range alpha II coherence improved their processing speed in the intact field as indicated by RT to perimetric stimuli.

3.4.1 Visual system at rest can be studied by alpha band activity.

Little is known about the scope of brain networks changes caused by visual system damage and, especially, about its functional effects. Our results support the hypothesis that peripheral visual system damage leads to permanent alterations in spontaneous cortical activity. This is in agreement with previous fMRI studies investigating resting-state connectivity in vision loss (Dai et al., 2012; Gallo et al., 2012). Specifically, patients exhibit lower power and decreased functional connectivity in the high alpha band and that connectivity strength is associated with the extent of vision loss.

How can this specific involvement of alpha band be explained? It is well-established that the visual system is not silent at rest but that brain visual circuits generate rhythmic oscillations in the 7-14Hz range called alpha rhythm. This phenomenon was already observed by Hans Berger in 1924 during his first EEG recordings. More recent analyses repeatedly point towards visual system circuits as the source of alpha activity (Hughes and Crunelli, 2005). Thus, considering on the new understanding of the role of spontaneous activity (see section 1.2.2.3), studying resting-state alpha band synchronization is a reasonable mean to probe functioning and efficiency of the visual system requiring no presentation of a visual stimulus. The advantage of this approach is that the interpretation of any EEG measure is not limited to one specific task, but the spontaneous activity of visual system might be a more fundamental measure of its integrity. Importantly, we recorded “eyes-closed” EEG in a dark room so that any between-groups differences could not be attributed to differences in the degree of visual input during EEG recording, i.e. the reduced retinal input to visual structures of the brain in patients could then not account for any brain activity changes. Therefore, decreased alpha band activity and connectivity likely indicate decreased functional efficiency of visual circuits which, although here manifested at rest, might be related to reduced abilities to process visual stimuli.

Further, our results provide support for the concept that the two alpha sub-bands, low- and high alpha, should be analyzed separately as they might serve different functional roles (review: Klimesch, 1999). But what specific roles low and high alpha band play in visual perception remains to be studied. We recognize it might be reasonable to define frequency bands based on individual alpha frequency (IAF), but in our sample some patients did not have a clear alpha band peak in the spectral domain, making it impossible to define IAF. In fact, the very loss of the alpha peak in such patients further argues for the alpha band activity is an important marker of visual perception.

3.4.2 No signs of compensatory plasticity

We did not find signs of “compensatory” plasticity in patients, defined as greater oscillatory power or connectivity strength when compared to normally-sighted subjects at baseline. Compensatory plasticity defined in such way was found in previous studies of subjects with pre-chiasmatic visual system damage (Dai et al., 2012; Werring et al., 2000; Toosy et al., 2005) and it is a well-established phenomenon in congenitally blind subjects

(review: Pascual-Leone et al., 2005). Yet, such definition of reorganization and compensatory changes might be too narrow and misleading, as compensation might come about in other unexpected forms. Therefore, further studies are needed to elucidate whether and in what form the neurophysiological compensatory processes occur.

3.4.3 Altered functional network topology in vision loss

Altered topology of alpha-band functional connectivity network was another marker of vision loss. Brain networks exhibit non-trivial spatial patterns of connections which can be assessed by graph measures (Rubinov and Sporns, 2010). The so-called “small-world” pattern, characterized by the existence of clusters of densely interconnected nodes and, at the same time, long-range connections between clusters, is hypothesized to be most optimal for information processing (Stam, van Straaten, 2012). The deviation from the small-world pattern is a hallmark of many clinical conditions including Alzheimer disease (Stam et al., 2009), brain tumor (Bartolomei et al., 2006), and traumatic brain injury (Caeyenberghs et al., 2012). In the present study we show that also in patients with vision loss the topology of functional connectivity networks is disrupted, specifically, high alpha band networks of patients were less densely clustered. Such topological changes might impact information processing, e.g. by making local segregation of visual information more difficult.

3.4.4 Perception is related to brain networks’ state in patients

Importantly, in our study functional connectivity was of relevance for perceptual abilities in patients. Therefore, we argue that not only local changes within and around the lesioned tissue - or the zone of primary deafferentation - determine the level of functional impairment, but also synchronization of the network (or lack thereof) might facilitate (or further hamper) perception in patients. Therefore, the disturbance of connectivity networks in patients might not only contribute to impaired vision at or near the zone of deafferentation, but it might also be the mechanism behind “sightblindness” (Bola et al., 2013b) – the phenomenon of perceptual deficits occurring in the “intact” regions of the visual field not directly affected by tissue loss (Bola et al., 2013a; Poggel et al., 2011; see section 1.1.2.1). Indeed, EEG coherence was related to reaction time to stimuli presented in the “intact” visual field, i.e. the stronger alpha-band coherence at rest, the faster RT in the intact field.

3.4.5 Neurophysiological effects of rtACS

Alpha oscillations can be entrained in healthy subjects (Zaehle et al., 2010) and in partially blind subjects (Sabel et al., 2011b; Schmidt et al., 2013) using ACS. Therefore, in the second part of our study, we aimed to modulate alpha band functional connectivity and observe whether changes in connectivity strength co-vary with changes in vision measures. rtACS indeed increased alpha coherence and modified network topology in our patient sample which is in line with previous studies on network effects of local brain stimulation (Polania et al., 2011; review: Shafi et al., 2012). Crucially, post-treatment strengthening of alpha band connectivity, with or without rtACS, was correlated with better perceptual functioning as shown by improved detection abilities and faster reaction times. This temporal co-variation strengthens our argument concerning the role of the alpha band in visual perception. However, the rtACS experiment was not aimed at determining rtACS efficacy, which requires prospective clinical trials which are currently ongoing, but it was rather used to check if alterations of synchronizations would be correlated with perceptual improvements. More details on clinical studies showing rtACS efficacy are found elsewhere (Sabel et al., 2011b; Schmidt et al., 2013).

The design of our study, involving comparisons at baseline (patients vs. controls) and investigation of rtACS effects (pre-ACS vs. post-ACS), allowed us to investigate the possible match of neurophysiological deficits exhibited by patients and rtACS induced effects. We show that some of the stimulation induced changes were observed in the alpha II band (long-range coherence, network clustering), and in lower frequencies, e.g. theta and alpha I (power, short-range coherence). Importantly, it was the change in alpha II coherence which correlated with the clinical improvement. Further studies on non-invasive stimulation techniques in vision restoration are needed to achieve a better match between neurophysiological deficits related to visual system damage (lack of alpha II) and neurophysiological effects of non-invasive stimulation.

3.4.6 Conclusions

Brain networks exhibit highly complex spatio-temporal patterns of activity. Here we showed that spatial patterns of brain functional activity and connectivity are disrupted in vision loss patients. Importantly, network activity at rest was related to perception in patients, i.e. stronger functional connectivity predicted better perception.

While the *spatial* aspect of brain networks has been extensively studied in health and disease, the *temporal* aspect of brain activity so far has received not much attention. In fact, to the best of my knowledge, it has never been studied in vision loss or any other sensory damage. Therefore, in the next study the same EEG data set as described in this chapter was reanalyzed to assess temporal patterns of activity.

4. Study III: Impaired temporal aspects of neural synchronization in blindness

The work presented in this chapter is currently submitted for publication:

Bola M, Gall C, Sabel BA. (2014). Brain network synchronization in blindness.

4.1 Study III: Introduction

The study described in the last chapter revealed disturbance of spatial patterns of brain functional activity and connectivity in vision loss patients. My next step was to explore the role of temporal dynamics of networks' activity in vision loss.

Prior studies of human visual system plasticity used fMRI to map changes of spatial patterns of local activations thought to indicate degeneration or plasticity (e.g. Baker et al., 2005; Schumacher et al., 2008; Dilks et al., 2009; Liu et al., 2010). Yet, neural activity is organized not only in space but also in time. Perceptual and cognitive operations are rapid and typically comprise several processes executed in parallel which makes temporal coordination essential. Even when no visual task is carried out, i.e. in the resting state, neural synchronization constantly fluctuates resulting in highly complex temporal patterns (Linkenkaer-Hansen et al., 2001; Stam and de Bruin, 2004; Nikulin and Brismar, 2004; Poil et al., 2008; Kitzbühler et al., 2009; He et al., 2010). Structural and functional changes in the neural circuits of vision are expected to affect complexity of temporal patterns and may thus comprise a plausible biomarker of brain pathology. Indeed, in various diseases the disruption of temporal patterns of brain activity were observed such as depression (Linkenkaer-Hansen et al., 2005), Alzheimer's disease (Montez et al., 2009), schizophrenia (Nikulin et al., 2012), epilepsy (Parish et al., 2004, Monto et al., 2007), and stroke (Zappasodi et al., 2014). High temporal complexity, in turn, might be identified with a rich repertoire of functional states needed to achieve sufficient flexibility of neural systems which support the emergence of perception and behavior (Goldberger et al., 2002).

I studied temporal dynamics of cortical synchronization with the following hypotheses: (i) due to prolonged sensory deprivation the spontaneous activity of visual network is disturbed and exhibits less complex, more random temporal patterns; and (ii) greater

complexity of temporal dynamics is associated with better vision in patients. Brain synchronization, both local (power) and distant (functional connectivity), was represented as time series with high temporal resolution. Three methods characterizing complexity of temporal patterns were applied to the synchronization time-series: length of synchronized/desynchronized periods, Higuchi Fractal Dimension (HFD), and Detrended Fluctuations Analysis (DFA). All three measures were compared between vision loss and control groups and correlated with perceptual capabilities as measured by perimetry

4.2 Study III: Methods

4.2.1 Subjects

The study sample consisted of 19 patients (**Table 4.1**) with chronic pre-chiasmatic visual system damage and 13 control subjects that had no neurological dysfunctions. Data of 15 patients were already analyzed by different methods and published elsewhere (Study I; Bola et al. 2014).

Table 4.1. Description of the Study III patients sample.

Nr	Sex	Age	Lesion age [months]	Etiology	Acuity		Static perimetry threshold [db]		Kinetic perimetry [deg]
					Near R/L	Far R/L	Foveal R/L	Whole field R/L	Mean field size R/L
1	M	20	53	Leber hereditary optic neuropathy	0.02/0.02	0/0	9/0	1.7/1.2	36.2/35.5
2	M	58	8	AION	1.4/0.4	1.2/0.24	24/16	17.4/9.35	55.8/46
3	W	24	51	Optic neuritis	1.4/1.4	1.2/1.2	30/28	22.3/15	59/56.9
4	W	68	14	AION	0.9/0.2	0.8/0.8	19/23	5/6	34/38
5	M	71	113	AION	0.5/0.13	0.4/0.17	21/20	10/16	54/58
6	M	73	170	Non-arteritic ischemic optic neuropathy	0.8/0.25	1.2/0.17	20/14	7/7	48/50
7	W	49	6	Resected tuberculoma sellae meningioma (WHOI)	0.9/0	0.8/0	22/0	4/0.4	13.3/9.4
8	W	36	17	Optic neuritis	MD/1	MD/1.2	MD/27	MD/18.6	MD/59.4
9	W	44	32	Optic neuritis	0/0.13	0/0.17	0/26	1/10	50/23
10	M	74	125	AION	MD/0.9	MD/0.8	MD/24	MD/5.7	MD/37
11	M	67	23	AION	0.06/0.04	0.17/0	15/0	0.4/3.9	47.9/43
12	W	62	175	Glaucoma, ON atrophy	0.16/0.9	0.17/0.6	11/28	0.5/14	6.3/55.7
13	M	28	24	Idiopathic ON atrophy	1.25/0.02	1.2/0	27/0	13/1	31/10
14	M	66	78	Glaucoma	0.5/0	0.6/0	24/0	17/0	57/16
15	M	68	163	Central retinal vein occlusion	0.9/0.05	0.8/0.12	23/2	12/4	58/39
16	M	47	64	NAION	0.05/1	0/1.5	0/26	3/5	33/45
17	M	53	6	AION	0/0.6	0/0.6	0/21	0/6	0/40
18	M	57	14	Idiopathic optic atrophy	0.25/0.25	0.4/0.4	21/23	13/13	59/60
19	M	63	60	AION	0.7/0.8	0.8/0.8	27/23	18/8	53/50

“MD” - missing data.

Patients and control subjects did not differ in age (patients: 53.4 ± 3 yrs., range [20 - 73]; controls: 46 ± 5 yrs., range [20 - 74]; $t(30)=1.28$, $p=0.20$). Four patients had unilateral optic neuropathy (one eye intact) and the others bilateral optic neuropathy. Inclusion criteria for patient entry into the study were the same as in Study II.

4.2.2 Data acquisition

Data set used in the Study II was reanalyzed here. For details of data acquisition procedures see methods sections Study II.

4.2.3 Data preprocessing and analysis

4.2.3.1 EEG preprocessing

Analysis of the EEG data was carried out in MatlabR2011b and EEGLab (Delorme and Makeig, 2004). The first 60 seconds of the EEG signal was used for analysis. The sampling frequency was 500Hz and the signal was re-referenced to the averaged common reference. Based on our previous results showing that alpha-frequencies are modified by vision loss (Study II; Bola et al., 2014), I focused our analysis on two alpha sub-bands: low alpha (alpha I; 7-9Hz), where I expected no differences between patients and controls, and high alpha (alpha II; 11-13Hz) where between groups differences were expected. Since my focus was on temporal dynamic I aimed to avoid extensive temporal integration caused by filtering. Therefore, the filter order of the band-pass FIR filter was set to two cycles of the lowest cut-off frequency (142 and 90 points for alpha I and alpha II respectively). Hilbert transform (Matlab function *hilbert*) was applied to band-pass filtered EEG signals to obtain discrete time analytic signals (**Fig. 4.1**).

For the present analysis I wanted to obtain continuous EEG signals of the same length from each participant. Therefore, I did not reject noisy parts of the EEG during preprocessing. Yet, it is unlikely that the results are contaminated by artefacts, as firstly, resting-state eyes closed was analysed which contains less eye- and muscle-related artefacts, and secondly, only the alpha band was analyzed which is typically neither contaminated by low frequency artefacts (e.g. eye movements) nor by high frequency artefacts (e.g. miographic activity).

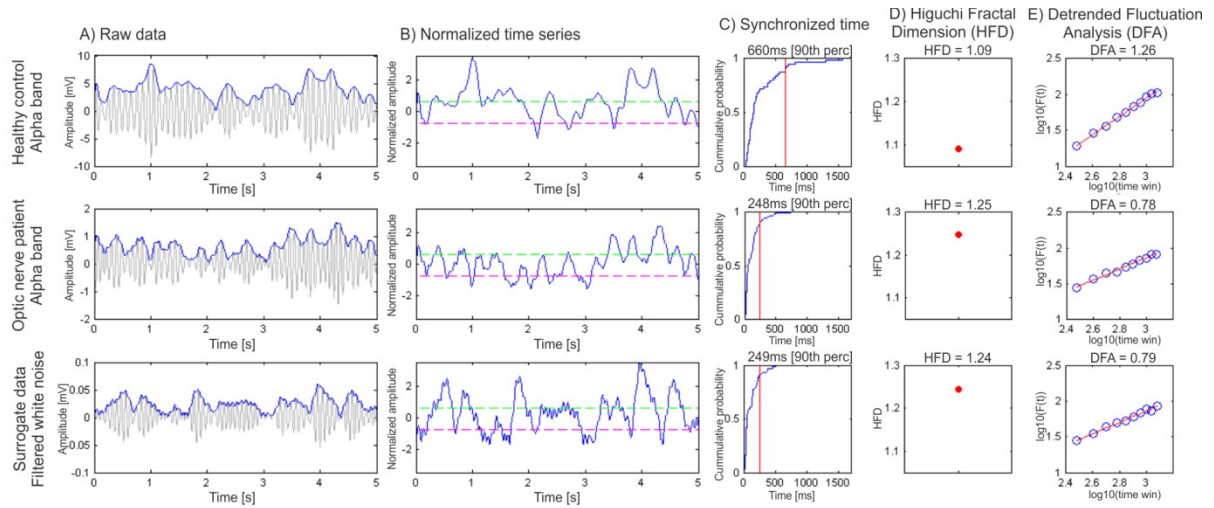


Figure 4.1. Analysis of temporal dynamics of synchronization. (A) Filtered alpha band oscillations are plotted in grey. An envelope of oscillations (in blue) was used as an index of synchronization strength. Note that healthy control, patient, and surrogate data exhibit different amplitudes. (B) For analyses of temporal dynamics envelopes were normalized by subtracting temporal mean and dividing by temporal standard deviation. For analysis of active- and waiting-periods for each envelope we set an upper and lower threshold (65th and 35th percentile, in green and magenta respectively). Every time the signal goes beyond the upper threshold or below the lower threshold I assume it enters active- or waiting-period, respectively. (C) Cumulative distributions of active-/waiting-periods' duration were created and 90th percentile was taken as a measure of active-/waiting-periods duration. (D) A second measure, HFD, indicates the tendency of the time series to fill the space between a straight line (HFD = 1) and a plane (HFD = 2). (E) The third measure, the DFA exponent, quantifies long-range temporal correlations in the envelopes, with higher values indicating stronger, more complex temporal correlations. High-alpha band activity of control subjects was characterized by occurrence of long active- and waiting-periods (C), lower HFD (D), and higher DFA exponents (E).

4.2.3.2 Synchronization measures

My analysis focused on the temporal dynamics of brain synchronization using two measures: (i) amplitude (power) of alpha-band oscillations and (ii) alpha-band functional connectivity between electrodes estimated by phase locking value (PLV; Lachaux et al., 1999). To obtain amplitude envelopes absolute values were taken from Hilbert-transformed signals. PLV, which measures variability of phase difference in a time interval, was calculated as follows:

$$PLV_t = \frac{1}{N} \left| \sum_{n=1}^N \exp(j(\varphi_{channel1}(t) - \varphi_{channel2}(t))) \right| ,$$

where N is the number of time points in a time window t and $\varphi_{channel}(t)$ denotes phase from a given channel for the window t .

PLV were calculated using a sliding window of 601 points (300ms) length which was shifted one point at a time to obtain maximal temporal resolution. To obtain estimates of PLV time courses for each electrode n , time courses of PLV between n and all other electrodes were averaged.

The mean amplitude of oscillations and PLV (**Fig. 4.2A**; **Fig. 4.3A**) was calculated as time-averaged amplitude envelope and time-averaged PLV.

4.2.3.3 Surrogate data

Filtering causes temporal integration of the signal and therefore might induce temporal correlations even in non-correlated time series. To control for this effect, white noise time-series of length equal to the analyzed EEG signals were created. To obtain surrogate data for alpha I and alpha II white noise was filtered with a band-pass FIR filter with cut-off and filter order the same as used for EEG data (7-9Hz and 142 points for alpha I; 11-13Hz and 90 points for alpha II). Filtered white noise was Hilbert transformed to obtain amplitude envelopes which were analyzed with three analysis methods described below.

4.2.4 Analysis of synchronization dynamic

All the methods used to study dynamic of amplitude/PLV time series were independent from time series amplitude. This way I was able to obtain biomarkers independent from the ones already reported (Study II; Bola et al. 2014).

4.2.4.1 Synchronization stability

Processing of information in the brain requires both flexibility and stability. To quantify temporal stability of synchronization I studied the periods when the brain lingers in a state of strong or weak synchronization (see: Montez et al. 2009; **Fig. 4.2B, C**; **Fig. 4.3B, C**). To this end for each time series two thresholds, lower and upper, were set based on percentile values. Lower threshold was defined as 35th percentile and upper as 65th percentile. All values above the upper threshold were considered to belong to an “active-period” (strong synchronization)

and all values below the lower threshold were considered to belong to a “waiting-period” (weak synchronization). Length of each synchronized- and waiting-period was calculated and their cumulative distributions calculated. In agreement with Montez et al. (2009), I noticed that the probability to linger in an active-/waiting-period was greater for EEG time series than for created surrogate data. In other words, the probability distribution obtained from EEG had a slowly decaying, long tail. Therefore, for each time series the 90th percentile of the active-/waiting-periods length was taken as an index of lingering time. By taking the 90th percentile I was able to capture the slowly decaying tail of the distribution. Repeating the analysis with different threshold values (e.g. 50th percentile lower and 50th percentile upper, 25th percentile lower and 75th percentile upper) led to similar between groups differences.

4.2.4.2 Higuchi Fractal Dimension (HFD)

The complexity of a signal was quantified using HFD (Higuchi, 1988; **Fig. 4.2D**; **Fig. 4.3D**). This method has been used to estimate dimensional complexity of physiological signals, including EEG (e.g. Accardo et al., 1997). Yet, we are not aware of any study applying it to amplitude envelopes and PLV time series. The mathematical details of the method can be found in Higuchi (1988). Briefly, HFD may be illustrated by the tendency of the time series to fill the space between a straight line (HFD = 1) and a plane (HFD = 2). Therefore a flat line, or a low frequency sine wave, is characterized by $HFD \approx 1$ and white noise by $HFD \approx 2$.

4.2.4.3 Detrended Fluctuation Analysis (DFA)

Finally, DFA was used to quantify long-range temporal correlations in synchronization time series (**Fig. 4.2E**; **Fig. 4.3E**). DFA has been introduced by Peng et al. (1994) and is used to analyze long-range temporal correlations in non-stationary physiological time series, including EEG power envelopes (Linkenkaer-Hansen et al., 2001) and functional connectivity (Stam and de Bruin, 2004). When calculating DFA I followed the pipeline proposed by Hardstone et al. (2012). Briefly, for each time series $[x]$ I calculated the cumulative sum to obtain time series profiles $[x_{prof}]$. A set of time windows was defined and for each window size $[t]$ the signal profile was divided into a set of separate segments $[w]$ of length equal to the window size $[t]$. Segments were created with 50% overlap. Each signal segment $[w]$ was detrended using least-squares fit $[w_{detrend}]$. Standard deviation of the detrended segment was

calculated ($\sigma(w_{detrend})$). Fluctuation function was defined as mean standard deviation for segments of the same size [$F(t)=\text{mean}(\sigma(w_{detrend}))$]. F was plotted for all windows sizes on logarithmic axes. The DFA exponent is the slope of the trend line and is estimated using linear regression. DFA exponent indicates whether a time series is anti-correlated (DFA<0.5), uncorrelated (DFA=0.5), positively correlated (0.5<DFA<1), or scale-free (DFA>1). The smallest window for analysis of amplitude envelopes was estimated to be 300 points based on procedure described by Hardstone et al. (2012) and it was used as the smallest window also in the PLV analysis.

4.2.4.4 Amplitude matched data

To prove that between-groups differences in temporal dynamics were not due to between-groups differences in amplitudes, an amplitude-matched data set was created (**Fig. 4.4**). In this analysis I focused on O1 and O2 electrodes only. For every subject I divided the 60s long signal into 10 equal epochs. To obtain a data set without differences in amplitude between controls and patients 5 epochs with the lowest amplitude were chosen for controls, while 5 epochs with highest amplitude were chosen for patients. I calculated HFD on the chosen epochs and compared between groups. This control analysis was done using HFD as, unlike synchronization stability measures and DFA, it does not require continuous data, e.g. data can be split into shorter segments.

4.2.5 Statistical analyses

Initially between groups comparisons were conducted separately for each electrode (see topographic maps in **Fig. 4.2, 4.3**). Then, for each frequency band, data were averaged over electrodes with significant between groups difference and plotted in a scatter plot. In several cases there was no electrode showing significant between-groups differences in the alpha I band. Then the same electrodes as for alpha II were taken to create alpha I scatter plots. Another statistical test was conducted on electrodes-averaged data and results of this final test are reported in the results section.

Before conducting between-groups statistical tests normality of distribution was assessed with Kolmogorov-Smirnov test. If measures of both groups exhibited normal distribution an independent sample t-test was used. Otherwise, Mann-Whitney U-test was used. To assess the relationship between EEG and clinical variables, Pearson correlation

coefficient was used. A criterion of $p=0.05$ (two-tailed) was set for all statistical tests. Results are reported as mean \pm standard error of the mean (SEM).

4.3 Study III: Results

4.3.1 Synchronization strength

Patients exhibited lower power of alpha II band ($p=0.038$; **Fig. 4.2A**) and weaker alpha II functional connectivity ($p=0.042$; **Fig. 4.3A**) indicating that strength of both, local and global (distant) neural synchronization is disturbed.

4.3.2 Temporal stability of synchronization: active- and waiting-periods

Patients exhibited disturbed temporal dynamic of neural synchronization in the alpha II band. The probability of long alpha II active-periods ($p=0.015$; **Fig. 4.2B**) and long waiting-periods ($p=0.011$; **Fig. 4.2C**) was significantly lower in patients than in control subjects. This indicates that synchronization in patients is more volatile, with shorter periods of stable strong/weak synchronization. This is confirmed by PLV, which also indicates lower probability of long alpha II active-periods ($p=0.021$; **Fig. 4.3B**) and waiting-periods ($p=0.004$; **Fig. 4.3C**). Yet, we also noticed that two electrodes (CP5, FC6) showed higher probability of long synchronized-periods in alpha I band in patients ($p=0.028$).

4.3.3 Higuchi fractal dimension (HFD)

Further evidence for altered temporal dynamic of neural synchronization in patients comes from HFD analysis. Time-series representing alpha II amplitude in patients were characterized by higher HFD ($p=0.002$; **Fig. 4.2D**). Similarly, PLV time series from patients exhibited higher HFD than those in control subjects ($p=0.023$; **Fig. 4.3D**). A higher HFD points towards a more random, noise-like character of synchronization dynamics in patients.

4.3.4 Detrended fluctuation analysis (DFA)

Finally, the third method quantifying temporal correlations in time-series, detrended fluctuation analysis (DFA), also indicates a weaker temporal patterns in patients data. Specifically, alpha II amplitude envelopes were characterized by lower DFA exponents in patients ($p=0.005$; **Fig. 4.2E**). However, at a single electrode (FC1) the alpha I DFA exponent

was higher in patients group ($p=0.046$). Weaker temporal correlations in alpha II synchronization were found also for PLV time-series ($p=0.009$; **Fig. 4.3E**). Therefore, in line with two other methods used, DFA analysis indicated that dynamics of synchronization in patients exhibits weaker temporal correlations and more noise-like character.

4.3.5 Comparison to surrogate data

The three methods used to study temporal patterns were applied to surrogate data, i.e. filtered white noise, where no true temporal structure was expected. All three methods indicate that in patients temporal dynamic of alpha II power was similar to temporal dynamic of white noise (**Fig. 4.2B, 4.2C, 4.2D, 4.2E**). This indicated that alpha II synchronization pattern in patients possess no temporal structure, or the pattern exhibits a very random, noise-like character.

4.3.6 Amplitude-matched data

Although, from a mathematical point of view, the three methods used were by definition amplitude-independent, from the physiological point of view it is still possible that a decrease in alpha power is tightly linked to changes in the temporal network structure in patients (but see: Linkenkaer-Hansen et al., 2007). Therefore, I sought further confirmation that between-groups differences in temporal dynamic cannot be accounted for by differences in power. To this end amplitude-matched datasets were created by choosing epochs with high mean amplitude for patients and low mean amplitude for controls (see: methods section). In this way I was able to confirm that disturbance of temporal dynamics of alpha II in patients ($p=0.014$; **Fig. 4.4**) is indeed independent of power decreases.

4.3.7 Correlations with vision measures

Alpha band oscillatory activity was related to visual capabilities of patients as measured by perimetry (**Fig. 4.5**). Higher amplitudes in the alpha II band were related to better detection abilities in static perimetry ($r=0.52$, $p=0.021$). But also measures of temporal dynamic were related to patients' vision. Specifically, a larger visual field as assessed by kinetic perimetry was associated with longer waiting-periods ($r=0.47$, $p=0.041$), whereas better detection in static perimetry was related to both, lower HFD ($r=-0.54$, $p=0.017$) and longer waiting-periods ($r=0.54$, $p=0.014$). I did not find correlations between PLV and vision measures.

Local synchronization (power)

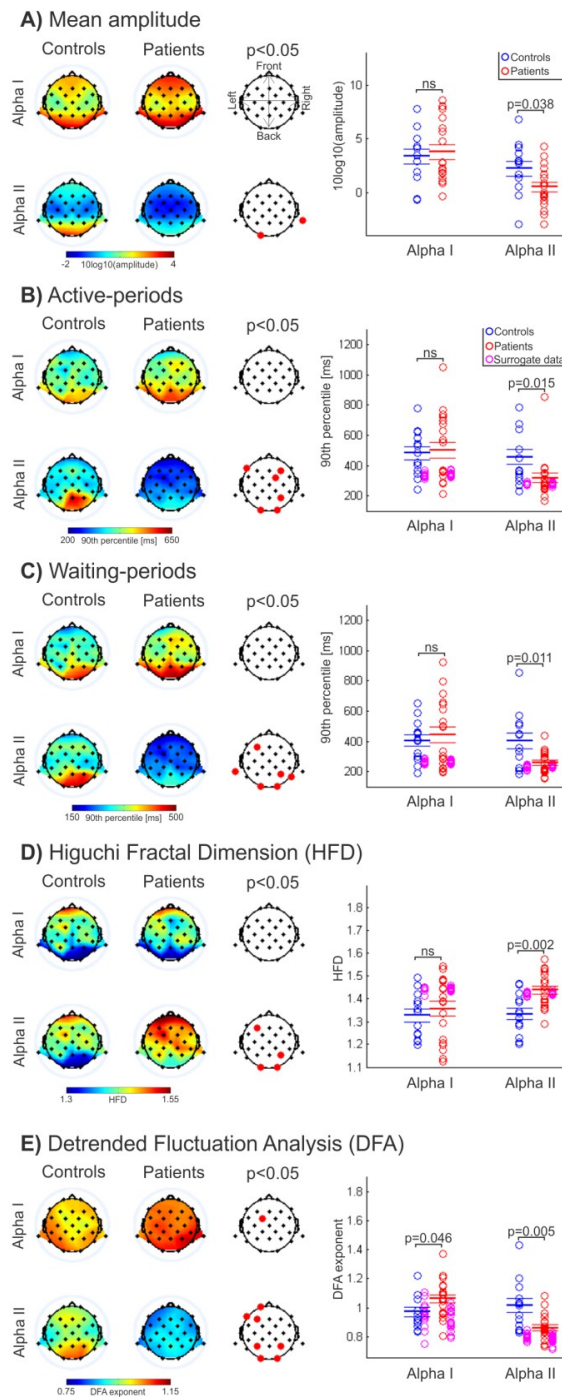


Figure 4.2. Amplitude and temporal dynamics of local synchronization. Topographic plots show values of calculated measures for all electrodes. Electrodes at which significant between-groups difference was found are marked in red (third column). On the right side scatter plots presenting data from all subjects. To create scatter plots data were averaged over all electrodes showing significant between-groups difference and retested statistically. The thick horizontal line indicates mean and thin horizontal lines indicate standard error of the mean (SEM).

Distant synchronization (PLV)

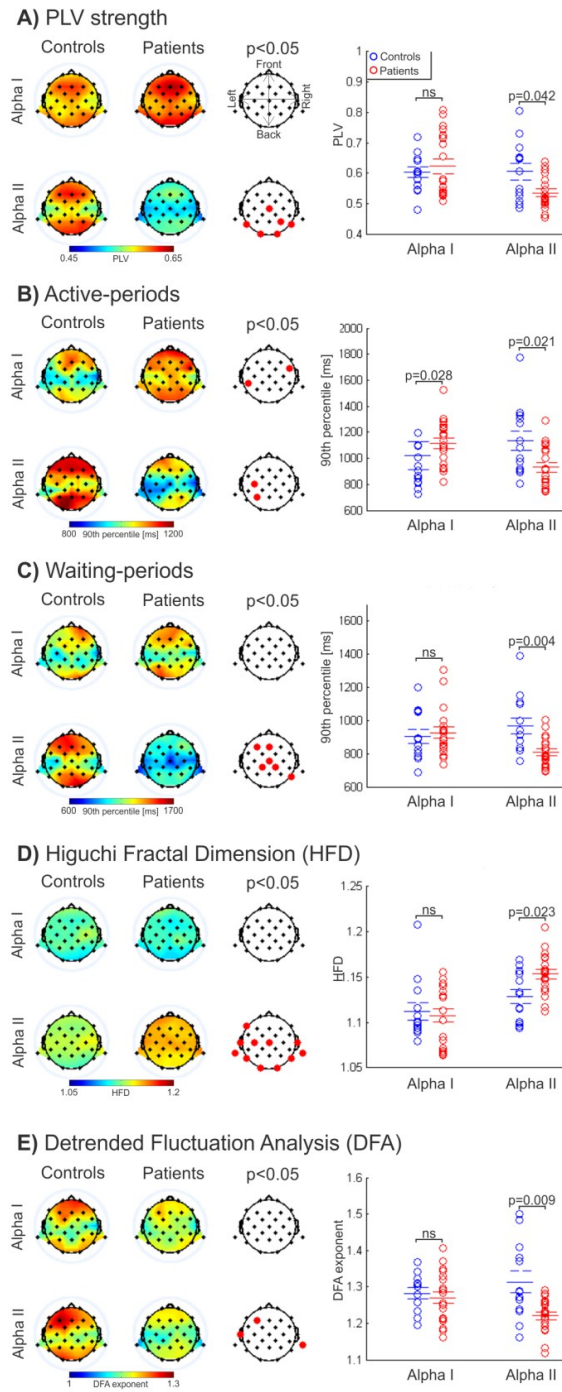


Figure 4.3. Strength and temporal dynamics of distant synchronization. Convention the same as in Figure 4.2.

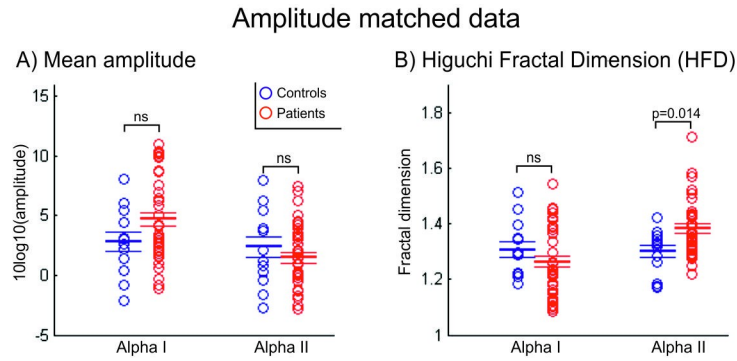


Figure 4.4. Analysis of amplitude-matched data. High-amplitude epochs were taken chosen from patients while low-amplitude epochs were chosen from controls to create data set with no between-groups difference in alpha activity amplitude (**A**). Still, HFD was higher in patients (**B**), which indicates that between-groups difference in temporal dynamics is independent from between-groups difference in alpha amplitude.

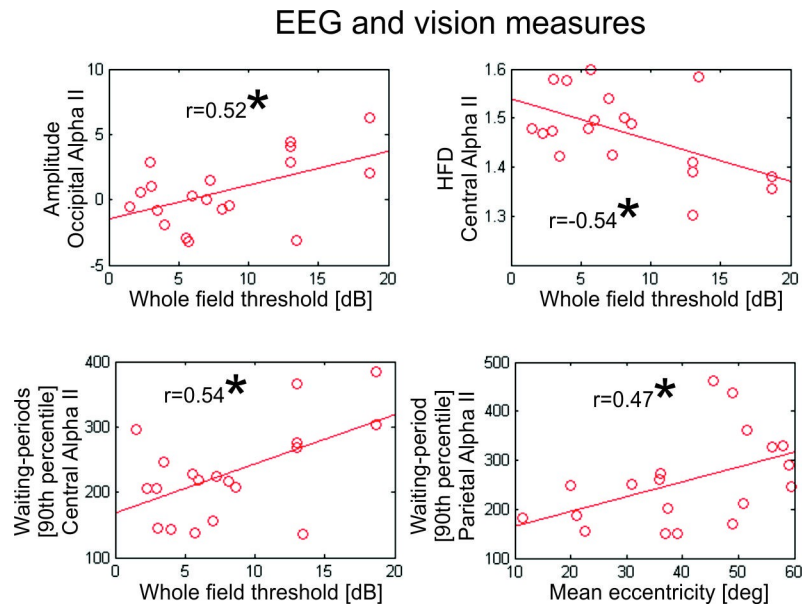


Figure 4.5. Correlation between EEG and vision measures. Data of all patients are presented. The red line represents the best linear fit to the data.

4.4 Study III: Discussion

Patients suffering from vision loss due to pre-chiasmatic visual system damage exhibit disturbed temporal patterns of spontaneous neural synchronization. Specifically, in line with our previous study investigating functional connectivity (Study I; Bola et al., 2014), the high-alpha band activity (alpha II; 11-14Hz) was altered. In patients the temporal patterns of high-alpha band synchronization exhibit a less complex, more random and noise-like structure.

Importantly, greater complexity of spontaneous alpha synchronization was related to better perceptual capabilities of patients.

4.4.1 Temporal patterns – looking at brain activity from a new angle

What is the relevance of studying temporal patterns of synchronization in vision loss patients? The activity of neural networks exhibits complex spatio-temporal properties. Most of the hitherto conducted neuroimaging studies focused on how the spatial representation of the visual field changes after damage (review: Wandell and Smirnakis, 2009; Sabel et al., 2011a). Indeed, the representation of visual input is spatially precise given its strict retinotopic organization. Therefore, any deviation from the optimal pattern is indicative of disorganization or reorganization and will likely have functional consequences. Similarly, brain functional networks exhibit specific spatial reorganization, i.e. the deviation from the optimal small-world structure is associated with various pathological conditions (review: Stam and van Straaten, 2012).

Yet, since perceptual and cognitive processes typically involve the rapid binding of stimulus features and various operations which are executed in parallel (such as attention, saccades, multisensory integration, and movement execution), neural processes must be coordinated not only in space but also in time. This temporal aspect is also reflected in the resting-state where brain activity fluctuates in a highly complex manner (Linkenkaer-Hansen et al., 2001; Stam and de Bruin, 2004; Nikulin and Brismar, 2004; Poil et al., 2008; Kitzbühler et al., 2009). Temporal complexity of spontaneous activity develops with age (Smit et al., 2011) and is relevant for behavior (Smit et al., 2013; Palva et al., 2013). Therefore, loss of temporal complexity or any deviation from the optimal *temporal* pattern might be indicative of changes in the underlying neural circuits and are as important to know about as deviations from the typical *spatial* pattern. Indeed, measures of temporal complexity emerge as a potential biomarker of various brain disorders such as depression (Linkenkaer-Hansen et al., 2005), Alzheimer's disease (Montez et al., 2009), schizophrenia (Nikulin et al., 2012), epilepsy (Parish et al., 2004, Monto et al., 2007), and stroke (Zappasodi et al., 2014). Thus, by studying temporal dynamics of neural activity in patients we are now able to take into account a new dimension of the brain pathophysiological activity, which might be no less important than the spatial patterns of activity and connectivity.

4.4.2 Disturbance of temporal patterns as another aspect of diaschisis

Because the subjects studied suffered from pre-chiasmatic (peripheral) lesion and the cortex was not injured, we assume that the disturbance of spontaneous synchronization is caused by prolonged lack of visual input, not by direct tissue damage. This is in line with the concept of diaschisis, defined as neurophysiological changes that occur distant to a focal brain lesion (von Monakow, 1914; review: Carrera and Tononi, 2014). Therefore, my study shows for the first time that brain lesion induced diaschisis might also be manifested by disturbance of the temporal patterns. Given that neural communication relies on precise temporal relations (synchronization), temporal measures might actually provide even more sensitive markers of diaschisis and disrupted communication than activation levels alone.

Yet, the physiological interpretation of the present results is still a challenge because few studies inform us about the basic mechanisms of temporal dynamics of synchronization. It is not known, for example, which visual system changes account for the observed EEG findings, e.g. whether it is anterograde degeneration or plasticity and reorganization of neural circuits. Crucially, in the present study temporal complexity of alpha synchronization was related to patients' perceptual capabilities – higher complexity was associated with better vision. This is in line with the hypothesis that greater temporal complexity, indicating that a system's greater flexibility, is advantageous for the function (Goldberger et al., 2002).

4.4.3 Using EEG to study brain reorganization

In the present study I used EEG which is typically not considered the right tool to study lesion-induced reorganization because of its poor spatial resolution. Indeed, signals recorded at each electrode represent the sum of activity from large cortical neuron assemblies and hence cannot be easily attributed to one anatomical location. Yet, due to superior temporal resolution EEG revealed another aspect of visual network alterations after pre-chiasmatic damage, namely disturbance of temporal dynamics. As we show here, this is functionally meaningful because the EEG network measures at rest were correlated with results of performance in simple vision tests (detection rate in perimetry). Thus, although EEG does not allow precise spatial localization of activity, the “holistic” measure of visual network activity might actually be an equal, if not superior, correlate of perceptual impairments.

4.4.4 Conclusions

Study III revealed that in vision loss patients the temporal patterns of brain activity are less complex, more random and noise-like. This provides another insight into diaschisis mechanisms after sensory loss, as not only activity levels and spatial patterns of activation are disturbed, but also precise temporal relations.

5. General discussion

The present series of studies was conducted to investigate the brain mechanisms of vision loss and restoration in patients with visual system damage. Firstly, we demonstrated that patients suffer from subtle perceptual deficits in the visual field considered to be intact (Bola et al., 2013a). I called this phenomenon “sightblind” (Bola et al., 2013b) and hypothesized that it might be caused by disturbance of brain functional networks in vision loss. Thus, in the two subsequent studies I investigated spatial and temporal patterns of brain activity and connectivity using EEG (Bola et al., 2014; Bola et al., submitted). Vision loss patients exhibited disturbed activation patterns when compared to age-matched control group. Importantly, EEG measures were related to patients’ vision – the stronger brain synchronization the better vision. The same was true when brain synchronization was modulated by rtACS to induce vision restoration – greater post-treatment increase in synchronization was associated with greater vision restoration (Bola et al., 2014). Therefore, we argue that not only the extent of tissue loss determined perceptual capabilities of patients, but also the state of brain functional networks. Understanding the networks’ role in vision loss might help us to understand acquired blindness better and pave the way to develop new ways of vision restoration.

5.1 Brain visual network in vision loss - diaschisis

Sensory damage leads to profound changes in the deafferented downstream brain structures which might include both, passive degeneration and plastic reorganization of neural circuits (Chen et al., 2002; Merabet and Pascual-Leone, 2009). Sensory lesions have been studied also in the visual system. Here, damage to the retina and/or optic nerve results in anterograde degeneration of structures along the visual pathway, including LGN and V1 (Boucard et al., 2009; Plank et al., 2011; Bogorodzki et al., 2014; review: Gupta and Yücel, 2007). Further, lesion-induced plasticity at the border of the deafferented visual cortex region has been extensively investigated (review: Wandell and Smirnakis, 2009; Sabel et al., 2011a). But not much is known about possible macro-scale changes on the level of large-scale brain networks in patients with vision loss. Apparently, extrastriate visual regions reorganize to facilitate processing of incomplete input (Werring et al., 2000; Toosy et al., 2002, 2005). Further, changes in strength of functional connections between specific visual brain regions

were found in optic neuritis (Gallo et al. 2012) and glaucoma patients (Dai et al. 2013; Song et al. 2014).

The hitherto conducted studies employed fMRI and thus studied brain activity and connectivity only indirectly. Since neuronal coherence is considered the mechanism of brain communication (Fries, 2005) I hypothesized that prolonged deafferentation might disturb the visual networks' synchronization. I expected to observe this synchronization breakdown also in the resting-state. Indeed, synchronization of brain visual network was found to be disturbed in patients. This was indicated by specific alterations in alpha band activity, namely weaker oscillatory activity, less clustered spatial patterns of functional connectivity networks, and less complex, more random and noise-like temporal patterns of synchronization.

Patients included in the present study suffered from peripheral, pre-chiasmatic visual system damage. Therefore, changes in functional state of brain cortical networks cannot be ascribed to the damage itself, i.e. are not a direct consequence of the lesion. I rather interpret these changes as an example of “diaschisis” defined as neurophysiological effects occurring distant to a focal brain lesion (von Monakow, 1914; review: Carrera and Tononi, 2014). Such remote effects of local, circumscribed lesions were also demonstrated in the motor system (review: Grefkes and Fink, 2011). That diaschisis might occur in the visual system after pre-chiasmatic damage was demonstrated by earlier fMRI studies in glaucoma (Dai et al., 2012) and optic neuritis patients (Toosy et al., 2002, 2005; Werring et al., 2000).

Future studies need to elucidate processes taking place in the deafferented LGN and visual cortex which are responsible for changes observed in the EEG. Because alpha activity is believed to arise from the interactions between visual cortex and thalamus (review: Hughes and Crunelli, 2005), therefore alpha synchronization deficits might indicate disrupted LGN-V1 communication. On the other hand, oscillatory activity is often related to inhibitory circuits (review: Buzsaki and Wang, 2012). Similarly, complex temporal fluctuations of synchronization amplitude depend on the presence of inhibition (Gonzalez et al., 2012). Nevertheless, to determine the specific mechanisms will likely require animal models experiments and therefore is beyond the scope of this thesis.

5.2 Plastic reorganization in vision loss

Another open question is whether active reorganization and plasticity take place in visual system of patients who lost vision late in the adulthood. In human fMRI and EEG studies reorganization and plasticity are believed to occur when functional activity or connectivity in patients is stronger than in control subjects. A number of previous studies reported functional reorganization in vision loss patients defined in such way (Toosy et al., 2005; Werring et al., 2000; Dai et al., 2012). But here we did not find any signs of compensations. Rather the observed changes were interpreted as a sign of deficits and deterioration.

From the studies on completely blind subjects we know that there is massive plasticity and reorganization of visual circuits when these are deprived of retinal input (review: Pascual-Leone et al., 2005; Voss, 2013). But it is well established that such pronounced changes typically take place only when vision is lost early in life, i.e. before the critical period, but in subjects who lost sight in adulthood plasticity is limited. Considering that subjects blinded by optic neuropathies (e.g. glaucoma or AMD) are typically in late adulthood it is not clear whether spontaneous compensatory plasticity takes place in visual system. Yet, it is important to keep in mind that the current definition of reorganization when investigating neuroimaging data might be too narrow in scope. It might be actually difficult to find what the signs of reorganization and compensation are in such a disturbed system where compensation might come in forms not expected so far.

5.3 Spontaneous brain activity in neurological patients

In the present study resting-state EEG data recorded with subjects maintaining their eyes closed were analyzed. Such recordings represent spontaneous, intrinsic brain activity. But why do we care about spontaneous activity of brain networks in brain damage patients? It is known that perception, cognition, and action depend on the state of brain functional networks linking widespread anatomical areas (Siegel et al., 2012). The current view is that task-related processing merely modifies (perturbs) the spontaneous network activity and therefore spontaneous, resting-state activation patterns constitute good predictors of perception and action (Harmelech and Malach, 2013). Indeed, in patients suffering from motor or attentional impairments caused by stroke the resting-state activity and functional connectivity predict the behavioral capabilities (He et al., 2007b; Carter et al., 2010; Castellanos et al., 2010; Assenza et al., 2013; review: Grefkes and Fink, 2011). Although acquired blindness, e.g. due to glaucoma, is a pressing clinical problem, it is not clear how

spontaneous activity of brain visual networks is related to perception in patients that suffer from vision loss.

Here I focused on resting-state activity recorded with subjects maintaining their eyes closed. But how visual network activity can be characterized without any overt visual task? It is well-established that the visual system at rest is not silent but that brain visual circuits generate rhythmic oscillations in the 7-14Hz range called alpha rhythm (Hughes and Crunelli, 2005). Thus, studying resting-state alpha band synchronization is a reasonable way to probe functioning and efficiency of the visual system requiring no presentation of a visual stimulus. The advantage of this approach is that the interpretation of any EEG responses is not limited to one specific task, but the task-independent structure of the visual system during the “resting-state” might be a more fundamental measure of visual network integrity. Importantly, I recorded “eyes-closed” EEGs in a dark room so that any between-groups differences could not be attributed to differences in the degree of visual input during EEG recording, i.e. the reduced retinal input to visual structures of the brain in patients could then not account for any network changes.

Further, several studies indicate that the classically defined alpha band (7-14Hz) is not a homogeneous phenomenon but that it should be divided into low-alpha (alpha I) and high-alpha (alpha II) which play different functional roles (Klimesch, 1999). Indeed, our analyses revealed that only high-alpha band functional activity and connectivity are impaired in patients with vision loss. But the specific roles of the alpha sub-bands are not well understood and further basic studies are needed to interpret the exclusive high-alpha deficit in vision loss.

5.4 Network synchronization and perception: areas of residual vision (ARV)

Both, spatial and temporal patterns of brain synchronization were related to perception in patients, i.e. the stronger synchronization the better vision. How can the relationship between network synchronization and vision impairments be explained? It has been shown that the instantaneous state of brain networks (i.e. at the stimulus onset) might either facilitate or hamper perception. Under difficult perceptual conditions, when the stimulus is weak and noisy with poor signal-to-noise ratio (e.g. a stimulus at threshold, an incomplete figure), the instantaneous network state might make a difference between seeing and not seeing (Babiloni et al., 2006; Hanslmayr et al., 2007; van Dijk et al., 2008; Busch et al., 2009; Weisz et al., 2014). Because in patients the visual input is reduced and/or noisy, I propose that the network

state plays a key role in patients' perception. Based on my findings I argue that in patients the network state is suboptimal for input processing, as indicated by disturbed synchronization and functional connectivity. This might hamper perception even beyond the direct consequences of anatomical damage.

Importantly, in patients with pre-chiasmatic visual system damage the visual field defect is typically not clear-cut, but there are extensive "areas of residual vision" (ARV; Sabel et al., 2011a). In ARVs, also known as "relative defects", residual perception is still present but it is unreliable and imprecise (increased thresholds, slowed reaction times, reduce acuity etc.). It was proposed that ARV likely correspond to the partially damaged areas of the retina and optic nerve (Sabel et al. 2011a). Therefore, when a stimulus is presented in ARVs the bottom-up signal reaching visual cortex might have a poor signal-to-noise ratio. In this situation, the instantaneous state of the cortical networks might play the key role in ARV vision, perhaps even more so than when vision is intact. This hypothesis might be directly tested in an experiment involving visual stimulus-related EEG analysis.

The importance of network-state and top-down influences for patients' vision was proved by behavioral studies investigating the role of spatial attention in ARV perception. Detection in ARV was improved when attention was cued to the location of presentation before the stimulus onset (Poggel et al., 2006). Attention training has also prolonged effects on perception and plasticity as vision restoration training combining stimuli presentation (bottom-up input) with attentional cueing (top-down influence) is more effective than the training employing stimuli presentation alone (Poggel et al., 2004). This is in line with the view that attention and instantaneous network state strongly modulate perception under difficult perceptual conditions.

5.5 Network synchronization and perception: "sightblindness"

Furthermore, if the large-scale networks are in a suboptimal state this may affect the whole visual field in a non-retinotopic manner, including presumably "intact" regions. Thus, patients might be "sightblind" (Bola et al., 2013b), i.e. they might experience perceptual deficits in temporal processing and feature integration even in the visual field regions believed to be "intact" (Poggel et al., 2011; Bola et al., 2013a). Indeed, patients often report certain subjective impairments such as slowing of visual processing, foggy vision, and glare which are not of refraction origin of the eye optics (unpublished observations). In the first study

presented in this thesis I conducted a detailed analysis of patients' perceptual abilities in the "intact" visual field. Specifically, we investigated visual processing speed of simple stimuli as measured by reaction time (RT). Patients exhibited lower processing speed than age-matched controls. Further, two factors were related to the processing speed: (i) distance to the scotoma border and (ii) size of the scotoma. The former factor was interpreted as a retinotopic (local) influence of the lesion which might be a manifestation of intrinsic V1 reorganization close to the lesion border. The latter factor was interpreted as global influence of the lesion, likely a manifestation of the visual network disturbance beyond V1. Indeed, in further analyses I found network correlate of the intact field processing. Specifically, slower reaction-time in the intact visual field sectors was related to weaker alpha band functional connectivity (Bola et al., 2014). I believe that also other types of visual impairments could possibly be attributed to permanently disturbed large-scale brain networks, including abnormal patterns of eye movements (Kanjee et al., 2012) or attentional problems (Loughman et al., 2007). Interestingly, perceptual deficits might include other domains, beyond vision, as glaucoma patients suffer from auditory processing deficits as well (Rance et al., 2012; O'Hare et al., 2012), and this might also be an expression of a global, network-wide disturbance of synchronization.

5.6 Network synchronization as a target for vision restoration treatments

If network synchronization is as one of the factors affecting patients' perception, improving such synchronized network activity might be one avenue to take towards vision restoration. Then stronger synchronization alone can improve detection and perception, even if the anatomical tissue loss cannot be reversed. It would be like a receiver better tuned into a faint signal.

Indeed, using non-invasive brain stimulation techniques, e.g. rtACS that sends pulsed currents to the retina, vision can be improved in patients (Sabel et al., 2011b; Fedorov et al., 2011; Schmidt et al., 2012). In addition to improved detection in perimetry patients' subjective vision-related quality of life, as measured by questionnaires, increased as well (Gall et al., 2011). Here we proved that rtACS indeed affects brain visual circuits and results in increase in theta and alpha bands power and coherence. The increase in alpha band coherence was related to improvements in vision tests, i.e. patients with greater alpha increase improved more in perimetry.

This shows that affecting brain cortical circuits to restore vision is a feasible approach. Interestingly, the rtACS induced improvements are observed mainly in the ARV (unpublished observations), which is in line with the hypothesis that the synchronized network state modulates perception in ARVs. But cortical circuits might be modulated also by other techniques. Plow et al. (2012) used DCS to increase excitability of the visual cortex of patients who, at the same time, trained with VRT. Bottom-up input (visual training) combined with neuromodulation (DCS) led to better therapeutic results than the training alone (similarly as in studies on VRT combined with attentional cueing; Poggel et al., 2004). Another approach to neuromodulation is neurofeedback. Recently Nan et al. (2013) reported that healthy subjects who trained to enhance their alpha activity improved their peripheral vision. This relation between alpha activity and vision is in agreement with our findings and the neurofeedback approach might be employed in the future to improve vision in vision loss patients.

5.7 Methodological considerations and limitations

Several methodological limitations of the present work are worth mentioning, particularly because considering them in the future might help to design better studies.

Firstly, higher perceptual functions were not tested in this study, only tests of simple visual functions (e.g. detection) were available. It would be interesting to see whether higher perceptual functions like contour integration or movement detection are related to brain networks' synchronization. Because these functions might require more extensive network activity correlations with EEG measures might actually be stronger.

Secondly, the neurophysiological effects should be further tested by employing high density EEG combined with source reconstruction methods. As already mentioned poor spatial resolution and volume conduction are the biggest disadvantages of EEG and might affect functional connectivity estimates. Source reconstruction techniques, for instance LORETA or Minimum Norm Estimate are thought to at least partially address the volume conduction problem (review: Palva and Palva, 2012). Yet, these methods require high-density EEG to give accurate estimates of cortical activity and here data recorded with only 30 channels were analyzed. Another way to deal with the problem would be to use measures insensitive to volume conduction, e.g. imaginary part of coherence (Nolte et al., 2004).

Thirdly, one might point out the need to use multiple comparisons correction (MCC e.g. Bonferroni) because multiple outcome measures were used (e.g. five EEG bands in the Study II). Yet, one of the assumptions behind MCC is that the measures used are independent of each other. However, in case of power/coherence of particular EEG bands it is not the case, as these are strongly correlated, i.e. dependent. Further, as the cut-off in case of the corrected p depends on the number of comparisons, forcing to use a correction provokes manipulation of results. For instance, instead of dividing alpha into two sub-bands one might have analyzed only broad alpha band, and additionally do not report beta results. That would help to keep the cut off relatively high. However, I preferred to present all the results. Finally, it is important to keep in mind that using correction for multiple comparisons might lead to inappropriate conclusions from the study as well, by rejecting factors which, in fact, play an important role in a particular phenomenon (increasing probability of type II error). For a discussion of arguments against correction please see: Feise, 2002; Bender and Lange, 2001.

Finally, we reported *correlations* between perceptual and neurophysiological measures. Therefore, one should not make inferences about causality, i.e. that high EEG alpha power *causes* better vision. Yet there are reports indicating that this might be the case, e.g. in the study of Nan et al. (2013) subjects trained with alpha-neurofeedback to enhance alpha-band activity and that caused improvements of peripheral perception. This shows that alpha band increase might be the cause and not the consequence of better vision.

6. Network-state dependent vision loss – a new theoretical model

Considering findings of the present study, when viewed in conjunction with prior work others, I wish to propose a new theory to understand vision loss after visual system damage (**Fig. 6.1**). Traditionally, vision loss is treated as the direct consequence of missing bottom-up (retinofugal) input of visual signals to visual cortex or higher visual centers of the brain. Therefore, the scotoma (blind field) is considered the only cause of patients' subjective vision problems (Gall et al., 2009). Since the anatomical damage is permanent and cannot be reversed, vision restoration was typically considered impossible.

My new findings suggest that perception depends on both, bottom-up input and the state of the brain visual network synchronization. I propose that lesions of the visual pathway lead to vision loss by preventing bottom-up input from reaching visual cortex. But at the same time there are also indirect consequences, as prolonged vision loss (sensory deprivation) disturbs the functioning of the global brain network affecting both visual and non-visual brain centers. This includes disturbed local activity, within visual areas, but also distant functional connectivity between visual and other specialized systems (Dai et al., 2013; Bola et al., 2014). Therefore, patients' vision loss is a combination of reduced visual input plus the state of the visual brain networks that is in a suboptimal (insufficiently synchronized) state for input processing. This has the following implications:

- i) Impaired network's state hampers perception globally, in a non-retinotopic manner, resulting in subtle perceptual deficits of the visual field sectors considered to be "intact" (Poggel et al., 2011; Bola et al., 2013a; review: Bola et al., 2013b). Such global network disturbance might also lead to attentional deficits (Loughman et al., 2007), motion and shape processing impairments (McKendrick et al., 2005), and abnormal eye movements patterns (Kanjee et al., 2012), all of which contribute to the subjective vision loss in patients.
- ii) The state of the brain network has its most pronounced impact on those areas of the brain which are only partially damaged: areas of residual vision (ARV; Sabel et al., 2011a), also known as "relative defect". Here, the incoming (bottom-up) signals from the partially damaged retina or optic-nerve are weaker (fewer cells)

and more noisy (loss of synchronized firing) resulting in poor signal-to-noise ratio. Under such conditions the network state at the time of stimulus processing can make a difference between seeing or not seeing.

- iii) A disturbed network state might hamper or slow-down restoration of vision if only the bottom-up drive is restored, i.e. with retinal artificial implants (Merabet et al., 2005). Here, efforts must be made to also modify how those signals are processed by the brain network.
- iv) Brain synchronization becomes a potential target for vision restoration treatments as improving the network state is expected to result in perceptual improvements, e.g. alleviating the “intact” field deficits and improving vision in the ARV. The network state might be optimized for instance by neurofeedback training (Nan et al., 2013) or non-invasive brain stimulation (Sabel et al., 2011b; Plow et al., 2012; Bola et al. 2014).

Although the focus of the present study is on patients with pre-chiasmatic damage, visual cortex plasticity (Dilks et al., 2007; Papanikolaou et al., 2014), network reorganization (Bridge et al., 2008; Perez et al., 2013), and intact field deficits (Rizzo and Robin, 1996; Schadow et al., 2009; Cavezian et al., 2010) were observed also in patients with post-chiasmatic damage e.g. due to stroke. Thus, the implications of the proposed theoretical model might also apply to patients with post-chiasmatic or other lesions.

We believe our new understanding that partial blindness is a combination of reduce bottom-up input and a disturbed network state might guide researchers and clinicians to better understand the physiological basis of vision loss and help develop novel vision restoration methods.

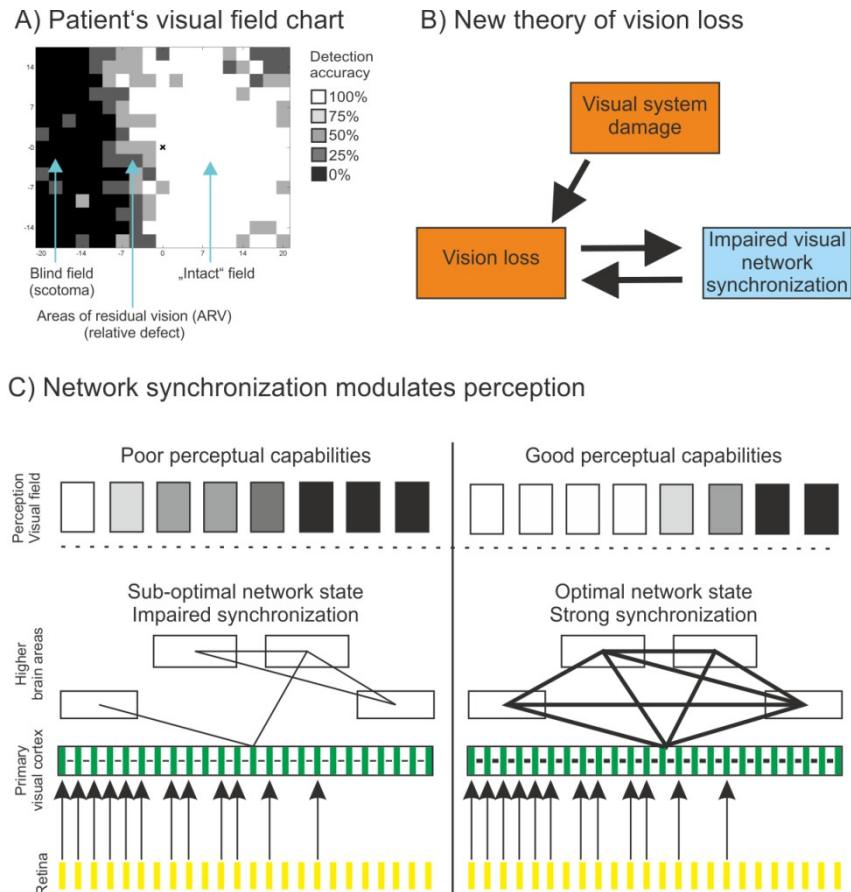


Figure 6.1. Vision loss is network-state dependent. The visual field of patients with acquired blindness typically can be divided into three areas (A): (i) intact field (good detection abilities, uninjured tissue); (ii) areas of residual vision (ARV; partial detections, partially damaged tissue); (iii) and blind field (no detection, completely damaged tissue). I argue that in addition to anatomical damage, visual network state defines patients' perceptual capabilities. Network state is disturbed by the loss of visual input and this, in turn, further aggravates vision loss (B). Therefore, patients with the same anatomical structure of the optic-nerve damage might exhibit different patterns of vision loss (C). If the network synchronization is disturbed patients' vision is more impaired than predicted based on the structure of the damage (left panel). But if the network is strongly synchronized, then patients' vision might be better than predicted based on the structure of the damage (right panel).

7. References

- Accardo, A., Affinito, M., Carrozzi, M., & Bouquet, F. (1997). Use of the fractal dimension for the analysis of electroencephalographic time series. *Biological Cybernetics*, 77(5), 339-350.
- Assenza, G., Zappasodi, F., Pasqualetti, P., Vernieri, F., & Tecchio, F. (2013). A contralesional EEG power increase mediated by interhemispheric disconnection provides negative prognosis in acute stroke. *Restorative Neurology and Neuroscience*, 31(2), 177-188.
- Babiloni, C., Vecchio, F., Bultrini, A., Romani, G. L., & Rossini, P. M. (2006). Pre-and poststimulus alpha rhythms are related to conscious visual perception: a high-resolution EEG study. *Cerebral Cortex*, 16(12), 1690-1700.
- Baker, C. I., Peli, E., Knouf, N., & Kanwisher, N. G. (2005). Reorganization of visual processing in macular degeneration. *The Journal of Neuroscience*, 25(3), 614-618.
- Bartolomei, F., Bosma, I., Klein, M., Baayen, J. C., Reijneveld, J. C., Postma, T. J., ... & Stam, C. J. (2006). How do brain tumors alter functional connectivity? A magnetoencephalography study. *Annals of Neurology*, 59(1), 128-138.
- Baseler, H. A., Gouws, A., Haak, K. V., Racey, C., Crossland, M. D., Tufail, A., ... & Morland, A. B. (2011). Large-scale remapping of visual cortex is absent in adult humans with macular degeneration. *Nature Neuroscience*, 14(5), 649-655.
- Bender, R., & Lange, S. (2001). Adjusting for multiple testing—when and how? *Journal of Clinical Epidemiology*, 54(4), 343-349.
- Boersma, M., Smit, D. J., de Bie, H., Van Baal, G. C. M., Boomsma, D. I., de Geus, E. J., ... & Stam, C. J. (2011). Network analysis of resting state EEG in the developing young brain: structure comes with maturation. *Human Brain Mapping*, 32(3), 413-425.
- Bogorodzki, P., Piątkowska-Janko, E., Szaflik, J., Szaflik, J. P., Gacek, M., & Grieb, P. (2014). Mapping Cortical Thickness of the Patients with Unilateral End-Stage Open Angle Glaucoma on Planar Cerebral Cortex Maps. *PloS One*, 9(4), e93682.

Bola, M., Gall, C., & Sabel, B. A. (2013a). The second face of blindness: processing speed deficits in the intact visual field after pre-and post-chiasmatic lesions. *PloS One*, 8(5), e63700.

Bola, M., Gall, C., & Sabel, B. A. (2013b). “Sightblind”: perceptual deficits in the “intact” visual field. *Frontiers in Neurology*, 4.

Bola, M., Gall, C., Moewes, C., Fedorov, A., Hinrichs, H., & Sabel, B. A. (2014). Brain functional connectivity network breakdown and restoration in blindness. *Neurology*, 83(6), 542-551.

Boucard, C. C., Hernowo, A. T., Maguire, R. P., Jansonius, N. M., Roerdink, J. B., Hooymans, J. M., & Cornelissen, F. W. (2009). Changes in cortical grey matter density associated with long-standing retinal visual field defects. *Brain*, awp119.

Bridge, H., Thomas, O., Jbabdi, S., & Cowey, A. (2008). Changes in connectivity after visual cortical brain damage underlie altered visual function. *Brain*, 131(6), 1433-1444.

Busch, N. A., Dubois, J., & VanRullen, R. (2009). The phase of ongoing EEG oscillations predicts visual perception. *The Journal of Neuroscience*, 29(24), 7869-7876.

Buzsáki, G., & Draguhn, A. (2004). Neuronal oscillations in cortical networks. *Science*, 304(5679), 1926-1929.

Caeyenberghs, K., Leemans, A., Heitger, M. H., Leunissen, I., Dhollander, T., Sunaert, S., ... & Swinnen, S. P. (2012). Graph analysis of functional brain networks for cognitive control of action in traumatic brain injury. *Brain*, 135(4), 1293-1307.

Calford, M. B., Wang, C., Taglianetti, V., Waleszczyk, W. J., Burke, W., & Dreher, B. (2000). Plasticity in adult cat visual cortex (area 17) following circumscribed monocular lesions of all retinal layers. *The Journal of Physiology*, 524(2), 587-602.

Carrera, E., & Tononi, G. (2014). Diaschisis: past, present, future. *Brain*, awu101.

Carter, A. R., Astafiev, S. V., Lang, C. E., Connor, L. T., Rengachary, J., Strube, M. J., ... & Corbetta, M. (2010). Resting interhemispheric functional magnetic resonance imaging connectivity predicts performance after stroke. *Annals of Neurology*, 67(3), 365-375.

Carter, A. R., Patel, K. R., Astafiev, S. V., Snyder, A. Z., Rengachary, J., Strube, M. J., ... & Corbetta, M. (2012). Upstream dysfunction of somatomotor functional connectivity after corticospinal damage in stroke. *Neurorehabilitation and Neural Repair*, *26*(1), 7-19.

Castellanos, N. P., Paúl, N., Ordóñez, V. E., Demuyneck, O., Bajo, R., Campo, P., ... & Maestú, F. (2010). Reorganization of functional connectivity as a correlate of cognitive recovery in acquired brain injury. *Brain*, *133*(8), 2365-2381.

Catani, M., Dell'Acqua, F., Bizzi, A., Forkel, S. J., Williams, S. C., Simmons, A., ... & Thiebaut de Schotten, M. (2012). Beyond cortical localization in clinico-anatomical correlation. *Cortex*, *48*(10), 1262-1287.

Cavézian, C., Gaudry, I., Perez, C., Coubard, O., Doucet, G., Peyrin, C., ... & Chokron, S. (2010). Specific impairments in visual processing following lesion side in hemianopic patients. *Cortex*, *46*(9), 1123-1131.

Chen, R., Cohen, L. G., & Hallett, M. (2002). Nervous system reorganization following injury. *Neuroscience*, *111*(4), 761-773.

Cowey, A. (2010). The blindsight saga. *Experimental Brain Research*, *200*(1), 3-24.

Dai, H., Morelli, J. N., Ai, F., Yin, D., Hu, C., Xu, D., & Li, Y. (2013). Resting-state functional MRI: Functional connectivity analysis of the visual cortex in primary open-angle glaucoma patients. *Human Brain Mapping*, *34*(10), 2455-2463.

de Haan, E. H., & Cowey, A. (2011). On the usefulness of ‘what’ and ‘where’ pathways in vision. *Trends in Cognitive Sciences*, *15*(10), 460-466.

Delorme, A., & Makeig, S. (2004). EEGLAB: an open source toolbox for analysis of single-trial EEG dynamics including independent component analysis. *Journal of Neuroscience Methods*, *134*(1), 9-21.

Dilks, D. D., Baker, C. I., Peli, E., & Kanwisher, N. (2009). Reorganization of visual processing in macular degeneration is not specific to the “preferred retinal locus”. *The Journal of Neuroscience*, *29*(9), 2768-2773.

Dilks, D. D., Serences, J. T., Rosenau, B. J., Yantis, S., & McCloskey, M. (2007). Human adult cortical reorganization and consequent visual distortion. *The Journal of Neuroscience*, 27(36), 9585-9594.

Engel, A. K., & Fries, P. (2010). Beta-band oscillations—signalling the status quo?. *Current opinion in Neurobiology*, 20(2), 156-165.

Engel, A. K., Fries, P., & Singer, W. (2001). Dynamic predictions: oscillations and synchrony in top-down processing. *Nature Reviews Neuroscience*, 2(10), 704-716.

Engel, A. K., Fries, P., & Singer, W. (2001). Dynamic predictions: oscillations and synchrony in top-down processing. *Nature Reviews Neuroscience*, 2(10), 704-716.

Fedorov, A., Jobke, S., Bersnev, V., Chibisova, A., Chibisova, Y., Gall, C., & Sabel, B. A. (2011). Restoration of vision after optic nerve lesions with noninvasive transorbital alternating current stimulation: a clinical observational study. *Brain Stimulation*, 4(4), 189-201.

Feise, R. J. (2002). Do multiple outcome measures require p-value adjustment? *BMC Medical Research Methodology*, 2(1), 8.

Felleman, D. J., & Van Essen, D. C. (1991). Distributed hierarchical processing in the primate cerebral cortex. *Cerebral Cortex*, 1(1), 1-47.

Fox, M. D., & Raichle, M. E. (2007). Spontaneous fluctuations in brain activity observed with functional magnetic resonance imaging. *Nature Reviews Neuroscience*, 8(9), 700-711.

Fries, P. (2005). A mechanism for cognitive dynamics: neuronal communication through neuronal coherence. *Trends in Cognitive Sciences*, 9(10), 474-480.

Friston, K. J. (1994). Functional and effective connectivity in neuroimaging: a synthesis. *Human Brain Mapping*, 2(1-2), 56-78.

Friston, K. J. (2011). Functional and effective connectivity: a review. *Brain Connectivity*, 1(1), 13-36.

Gall, C., Lucklum, J., Sabel, B. A., & Franke, G. H. (2009). Vision-and health-related quality of life in patients with visual field loss after postchiasmatic lesions. *Investigative Ophthalmology & Visual Science*, 50(6), 2765-2776.

Gall, C., Sgorzaly, S., Schmidt, S., Brandt, S., Fedorov, A., & Sabel, B. A. (2011). Noninvasive transorbital alternating current stimulation improves subjective visual functioning and vision-related quality of life in optic neuropathy. *Brain Stimulation*, 4(4), 175-188.

Gallo, A., Esposito, F., Sacco, R., Docimo, R., Bisecco, A., Della Corte, M., ... & Tedeschi, G. (2012). Visual resting-state network in relapsing-remitting MS with and without previous optic neuritis. *Neurology*, 79(14), 1458-1465.

Gilbert, C. D., & Wiesel, T. N. (1992). Receptive field dynamics in adult primary visual cortex. *Nature*, 356(6365), 150-152.

Goldberger, A. L., Amaral, L. A., Hausdorff, J. M., Ivanov, P. C., Peng, C. K., & Stanley, H. E. (2002). Fractal dynamics in physiology: alterations with disease and aging. *Proceedings of the National Academy of Sciences*, 99(suppl 1), 2466-2472.

Gonzalez, O. J. A., van Aerde, K. I., van Elburg, R. A., Poil, S. S., Mansvelder, H. D., Linkenkaer-Hansen, K., ... & van Ooyen, A. (2012). External drive to inhibitory cells induces alternating episodes of high-and low-amplitude oscillations. *PLoS Computational Biology*, 8(8), e1002666.

Grefkes, C., & Fink, G. R. (2011). Reorganization of cerebral networks after stroke: new insights from neuroimaging with connectivity approaches. *Brain*, awr033.

Grefkes, C., Nowak, D. A., Eickhoff, S. B., Dafotakis, M., Küst, J., Karbe, H., & Fink, G. R. (2008). Cortical connectivity after subcortical stroke assessed with functional magnetic resonance imaging. *Annals of Neurology*, 63(2), 236-246.

Gupta, N., & Yücel, Y. H. (2007). What changes can we expect in the brain of glaucoma patients?. *Survey of Ophthalmology*, 52(6), S122-S126.

Hallett, M. (2001). Plasticity of the human motor cortex and recovery from stroke. *Brain Research Reviews*, 36(2), 169-174.

Hanslmayr, S., Aslan, A., Staudigl, T., Klimesch, W., Herrmann, C. S., & Bäuml, K. H. (2007). Prestimulus oscillations predict visual perception performance between and within subjects. *Neuroimage*, *37*(4), 1465-1473.

Hardstone, R., Poil, S. S., Schiavone, G., Jansen, R., Nikulin, V. V., Mansvelder, H. D., & Linkenkaer-Hansen, K. (2012). Detrended fluctuation analysis: a scale-free view on neuronal oscillations. *Frontiers in Physiology*, *3*.

Harmelech, T., & Malach, R. (2013). Neurocognitive biases and the patterns of spontaneous correlations in the human cortex. *Trends in Cognitive Sciences*, *17*(12), 606-615.

Hawellek, D. J., Schepers, I. M., Roeder, B., Engel, A. K., Siegel, M., & Hipp, J. F. (2013). Altered intrinsic neuronal interactions in the visual cortex of the blind. *The Journal of Neuroscience*, *33*(43), 17072-17080.

He, B. J., Shulman, G. L., Snyder, A. Z., & Corbetta, M. (2007a). The role of impaired neuronal communication in neurological disorders. *Current Opinion in Neurology*, *20*(6), 655-660.

He, B. J., Snyder, A. Z., Vincent, J. L., Epstein, A., Shulman, G. L., & Corbetta, M. (2007b). Breakdown of functional connectivity in frontoparietal networks underlies behavioral deficits in spatial neglect. *Neuron*, *53*(6), 905-918.

He, B. J., Zempel, J. M., Snyder, A. Z., & Raichle, M. E. (2010). The temporal structures and functional significance of scale-free brain activity. *Neuron*, *66*(3), 353-369.

Hernowo, A. T., Boucard, C. C., Jansonius, N. M., Hooymans, J. M., & Cornelissen, F. W. (2011). Automated morphometry of the visual pathway in primary open-angle glaucoma. *Investigative Ophthalmology & Visual Science*, *52*(5), 2758-2766. Lee et al., 2014

Hernowo, A. T., Prins, D., Baseler, H. A., Plank, T., Gouws, A. D., Hooymans, J. M., ... & Cornelissen, F. W. (2013). Morphometric analyses of the visual pathways in macular degeneration. *Cortex*, *56*, 99-110.

Hess, R. F., & Pointer, J. S. (1989). Spatial and temporal contrast sensitivity in hemianopia: a comparative study of the sighted and blind hemifields. *Brain*, *112*(4), 871-894.

Higuchi, T. (1988). Approach to an irregular time series on the basis of the fractal theory. *Physica D: Nonlinear Phenomena*, 31(2), 277-283.

Hilgetag, C. C., Burns, G. A., O'Neill, M. A., Scannell, J. W., & Young, M. P. (2000). Anatomical connectivity defines the organization of clusters of cortical areas in the macaque and the cat. *Philosophical Transactions of the Royal Society of London. Series B: Biological Sciences*, 355(1393), 91-110.

Hipp, J. F., Engel, A. K., & Siegel, M. (2011). Oscillatory synchronization in large-scale cortical networks predicts perception. *Neuron*, 69(2), 387-396.

Hughes, S. W., & Crunelli, V. (2005). Thalamic mechanisms of EEG alpha rhythms and their pathological implications. *The Neuroscientist*, 11(4), 357-372.

Hummel, F. C., & Cohen, L. G. (2006). Non-invasive brain stimulation: a new strategy to improve neurorehabilitation after stroke?. *The Lancet Neurology*, 5(8), 708-712.

Hummel, F., Celnik, P., Giraux, P., Floel, A., Wu, W. H., Gerloff, C., & Cohen, L. G. (2005). Effects of non-invasive cortical stimulation on skilled motor function in chronic stroke. *Brain*, 128(3), 490-499.

Kaas, J. H., Krubitzer, L. A., Chino, Y. M., Langston, A. L., Polley, E. H., & Blair, N. (1990). Reorganization of retinotopic cortical maps in adult mammals after lesions of the retina. *Science*, 248(4952), 229-231.

Kanjee, R., Yücel, Y. H., Steinbach, M. J., González, E. G., & Gupta, N. (2012). Delayed saccadic eye movements in glaucoma. *Eye*, 4, 63-8.

Kasten, E., Wüst, S., Behrens-Baumann, W., & Sabel, B. A. (1998). Computer-based training for the treatment of partial blindness. *Nature Medicine*, 4(9), 1083-1087.

Keck, T., Mrsic-Flogel, T. D., Afonso, M. V., Eysel, U. T., Bonhoeffer, T., & Hübener, M. (2008). Massive restructuring of neuronal circuits during functional reorganization of adult visual cortex. *Nature Neuroscience*, 11(10), 1162-1167.

Keck, T., Scheuss, V., Jacobsen, R. I., Wierenga, C. J., Eysel, U. T., Bonhoeffer, T., & Hübener, M. (2011). Loss of sensory input causes rapid structural changes of inhibitory neurons in adult mouse visual cortex. *Neuron*, *71*(5), 869-882.

Kitzbichler, M. G., Smith, M. L., Christensen, S. R., & Bullmore, E. (2009). Broadband criticality of human brain network synchronization. *PLoS Computational Biology*, *5*(3), e1000314.

Klimesch, W. (1999). EEG alpha and theta oscillations reflect cognitive and memory performance: a review and analysis. *Brain Research Reviews*, *29*(2), 169-195.

Kuhn, T. S. (1962). *The Structure of Scientific Revolutions*. University of Chicago press.

Lachaux, J. P., Rodriguez, E., Martinerie, J., & Varela, F. J. (1999). Measuring phase synchrony in brain signals. *Human Brain Mapping*, *8*(4), 194-208.

Langer, N., Pedroni, A., Gianotti, L. R., Hänggi, J., Knoch, D., & Jäncke, L. (2012). Functional brain network efficiency predicts intelligence. *Human Brain Mapping*, *33*(6), 1393-1406.

Linkenkaer-Hansen, K., Monto, S., Rytsälä, H., Suominen, K., Isometsä, E., & Kähkönen, S. (2005). Breakdown of long-range temporal correlations in theta oscillations in patients with major depressive disorder. *The Journal of Neuroscience*, *25*(44), 10131-10137.

Linkenkaer-Hansen, K., Nikouline, V. V., Palva, J. M., & Ilmoniemi, R. J. (2001). Long-range temporal correlations and scaling behavior in human brain oscillations. *The Journal of Neuroscience*, *21*(4), 1370-1377.

Liu, T., Cheung, S. H., Schuchard, R. A., Glielmi, C. B., Hu, X., He, S., & Legge, G. E. (2010). Incomplete cortical reorganization in macular degeneration. *Investigative Ophthalmology & Visual Science*, *51*(12), 6826-6834.

Liu, Y., Yu, C., Liang, M., Li, J., Tian, L., Zhou, Y., ... & Jiang, T. (2007). Whole brain functional connectivity in the early blind. *Brain*, *130*(8), 2085-2096.

Loughman, J., Davison, P., & Flitcroft, I. (2007). Open angle glaucoma effects on preattentive visual search efficiency for flicker, motion displacement and orientation pop-out tasks. *British Journal of Ophthalmology*, *91*(11), 1493-1498.

McKendrick, A. M., Badcock, D. R., & Morgan, W. H. (2005). The detection of both global motion and global form is disrupted in glaucoma. *Investigative Ophthalmology & Visual Science*, *46*(10), 3693-3701.

Merabet, L. B., & Pascual-Leone, A. (2009). Neural reorganization following sensory loss: the opportunity of change. *Nature Reviews Neuroscience*, *11*(1), 44-52.

Merabet, L. B., Rizzo, J. F., Amedi, A., Somers, D. C., & Pascual-Leone, A. (2005). What blindness can tell us about seeing again: merging neuroplasticity and neuroprostheses. *Nature Reviews Neuroscience*, *6*(1), 71-77.

Montez, T., Poil, S. S., Jones, B. F., Manshanden, I., Verbunt, J. P., van Dijk, B. W., ... & Linkenkaer-Hansen, K. (2009). Altered temporal correlations in parietal alpha and prefrontal theta oscillations in early-stage Alzheimer disease. *Proceedings of the National Academy of Sciences*, *106*(5), 1614-1619.

Monto, S., Vanhatalo, S., Holmes, M. D., & Palva, J. M. (2007). Epileptogenic neocortical networks are revealed by abnormal temporal dynamics in seizure-free subdural EEG. *Cerebral Cortex*, *17*(6), 1386-1393.

Müller, I., Poggel, D., Kenkel, S., Kasten, E., & Sabel, B. (2003). Vision restoration therapy after brain damage: Subjective improvements of activities of daily life and their relationship to visual field enlargements. *Visual Impairment Research*, *5*(3), 157-178.

Nan, W., Wan, F., Lou, C. I., Vai, M. I., & Rosa, A. (2013). Peripheral Visual Performance Enhancement by Neurofeedback Training. *Applied Psychophysiology and Biofeedback*, *38*(4), 285-291.

Newman, M. E. (2003). The structure and function of complex networks. *SIAM Review*, *45*(2), 167-256.

Nikulin, V. V., & Brismar, T. (2004). Long-range temporal correlations in alpha and beta oscillations: effect of arousal level and test–retest reliability. *Clinical Neurophysiology*, *115*(8), 1896-1908.

Nikulin, V. V., Jönsson, E. G., & Brismar, T. (2012). Attenuation of long-range temporal correlations in the amplitude dynamics of alpha and beta neuronal oscillations in patients with schizophrenia. *Neuroimage*, *61*(1), 162-169.

Nolte, G., Bai, O., Wheaton, L., Mari, Z., Vorbach, S., & Hallett, M. (2004). Identifying true brain interaction from EEG data using the imaginary part of coherency. *Clinical Neurophysiology*, *115*(10), 2292-2307.

Nurminen, L., Kilpeläinen, M., Laurinen, P., & Vanni, S. (2009). Area summation in human visual system: psychophysics, fMRI, and modeling. *Journal of Neurophysiology*, *102*(5), 2900-2909.

O'Hare, F., Rance, G., Crowston, J. G., & McKendrick, A. M. (2012). Auditory and visual temporal processing disruption in open angle glaucoma. *Investigative Ophthalmology & Visual Science*, *53*(10), 6512-6518.

Palagina, G., Eysel, U. T., & Jancke, D. (2009). Strengthening of lateral activation in adult rat visual cortex after retinal lesions captured with voltage-sensitive dye imaging in vivo. *Proceedings of the National Academy of Sciences*, *106*(21), 8743-8747.

Palva, J. M., Zhigalov, A., Hirvonen, J., Korhonen, O., Linkenkaer-Hansen, K., & Palva, S. (2013). Neuronal long-range temporal correlations and avalanche dynamics are correlated with behavioral scaling laws. *Proceedings of the National Academy of Sciences*, *110*(9), 3585-3590.

Palva, S., & Palva, J. M. (2007). New vistas for α -frequency band oscillations. *Trends in Neurosciences*, *30*(4), 150-158.

Palva, S., & Palva, J. M. (2012). Discovering oscillatory interaction networks with M/EEG: challenges and breakthroughs. *Trends in Cognitive Sciences*, *16*(4), 219-230.

Papanikolaou, A., Keliris, G. A., Papageorgiou, T. D., Shao, Y., Krapp, E., Papageorgiou, E., ... & Smirnakis, S. M. (2014). Population receptive field analysis of the

primary visual cortex complements perimetry in patients with homonymous visual field defects. *Proceedings of the National Academy of Sciences*, 111(16), E1656-E1665.

Paramei, G. V., & Sabel, B. A. (2008). Contour-integration deficits on the intact side of the visual field in hemianopia patients. *Behavioural Brain Research*, 188(1), 109-124.

Parish, L. M., Worrell, G. A., Cranstoun, S. D., Stead, S. M., Pennell, P., & Litt, B. (2004). Long-range temporal correlations in epileptogenic and non-epileptogenic human hippocampus. *Neuroscience*, 125(4), 1069-1076.

Pascual-Leone, A., Amedi, A., Fregni, F., & Merabet, L. B. (2005). The plastic human brain cortex. *Annual Reviews in Neuroscience*, 28, 377-401.

Peng, C. K., Buldyrev, S. V., Havlin, S., Simons, M., Stanley, H. E., & Goldberger, A. L. (1994). Mosaic organization of DNA nucleotides. *Physical Review E*, 49(2), 1685.

Pereda, E., Quiroga, R. Q., & Bhattacharya, J. (2005). Nonlinear multivariate analysis of neurophysiological signals. *Progress in Neurobiology*, 77(1), 1-37.

Perez, C., Peyrin, C., Cavézan, C., Coubard, O., Caetta, F., Raz, N., ... & Chokron, S. (2013). An fMRI investigation of the cortical network underlying detection and categorization abilities in hemianopic patients. *Brain Topography*, 26(2), 264-277.

Pievani, M., de Haan, W., Wu, T., Seeley, W. W., & Frisoni, G. B. (2011). Functional network disruption in the degenerative dementias. *The Lancet Neurology*, 10(9), 829-843.

Plank, T., Frolo, J., Brandl-Rühle, S., Renner, A. B., Hufendiek, K., Helbig, H., & Greenlee, M. W. (2011). Gray matter alterations in visual cortex of patients with loss of central vision due to hereditary retinal dystrophies. *Neuroimage*, 56(3), 1556-1565.

Plow, E. B., Obretenova, S. N., Fregni, F., Pascual-Leone, A., & Merabet, L. B. (2012). Comparison of visual field training for hemianopia with active versus sham transcranial direct cortical stimulation. *Neurorehabilitation and Neural Repair*, 26(6), 616-626.

Poggel, D. A., Kasten, E., & Sabel, B. A. (2004). Attentional cueing improves vision restoration therapy in patients with visual field defects. *Neurology*, 63(11), 2069-2076.

Poggel, D. A., Kasten, E., Müller-Oehring, E. M., Bunzenthal, U., & Sabel, B. A. (2006). Improving residual vision by attentional cueing in patients with brain lesions. *Brain Research, 1097*(1), 142-148.

Poggel, D. A., Treutwein, B., & Strasburger, H. (2011). Time will tell: deficits of temporal information processing in patients with visual field loss. *Brain Research, 1368*, 196-207.

Poggel, D. A., Treutwein, B., Calmanti, C., & Strasburger, H. (2012). The Tölz Temporal Topography Study: Mapping the visual field across the life span. Part I: The topography of light detection and temporal-information processing. *Attention, Perception, & Psychophysics, 74*(6), 1114-1132.

Poil, S. S., van Ooyen, A., & Linkenkaer-Hansen, K. (2008). Avalanche dynamics of human brain oscillations: relation to critical branching processes and temporal correlations. *Human Brain Mapping, 29*(7), 770-777.

Polanía, R., Paulus, W., Antal, A., & Nitsche, M. A. (2011). Introducing graph theory to track for neuroplastic alterations in the resting human brain: a transcranial direct current stimulation study. *Neuroimage, 54*(3), 2287-2296.

Pöppel, E., Held, R., & Frost, D. (1973). Residual visual function after brain wounds involving the central visual pathways in man. *Nature, 243*, 295-296.

Qing, G., Zhang, S., Wang, B., & Wang, N. (2010). Functional MRI signal changes in primary visual cortex corresponding to the central normal visual field of patients with primary open-angle glaucoma. *Investigative Ophthalmology & Visual Science, 51*(9), 4627-4634.

Qiu, A., Rosenau, B. J., Greenberg, A. S., Hurdal, M. K., Barta, P., Yantis, S., & Miller, M. I. (2006). Estimating linear cortical magnification in human primary visual cortex via dynamic programming. *Neuroimage, 31*(1), 125-138.

Rance, G., O'Hare, F., O'Leary, S., Starr, A., Ly, A., Cheng, B., ... & Crowston, J. (2012). Auditory processing deficits in individuals with primary open-angle glaucoma. *International Journal of Audiology, 51*(1), 10-15.

Raz, N., Dotan, S., Benoliel, T., Chokron, S., Ben-Hur, T., & Levin, N. (2011). Sustained motion perception deficit following optic neuritis Behavioral and cortical evidence. *Neurology*, 76(24), 2103-2111.

Raz, N., Dotan, S., Chokron, S., Ben-Hur, T., & Levin, N. (2012). Demyelination affects temporal aspects of perception: an optic neuritis study. *Annals of Neurology*, 71(4), 531-538.

Rizzo, M., & Robin, D. A. (1996). Bilateral effects of unilateral visual cortex lesions in human. *Brain*, 119(3), 951-963.

Rizzo, M., & Robin, D. A. (1996). Bilateral effects of unilateral visual cortex lesions in human. *Brain*, 119(3), 951-963.

Rubinov, M., & Sporns, O. (2010). Complex network measures of brain connectivity: uses and interpretations. *Neuroimage*, 52(3), 1059-1069.

Sabel, B. A., Fedorov, A. B., Naue, N., Borrmann, A., Herrmann, C., & Gall, C. (2011b). Non-invasive alternating current stimulation improves vision in optic neuropathy. *Restorative Neurology and Neuroscience*, 29(6), 493-505.

Sabel, B. A., Henrich-Noack, P., Fedorov, A., & Gall, C. (2011a). Vision restoration after brain and retina damage: the “residual vision activation theory”. *Progress in Brain Research*, 192, 199-262.

Salvador, R., Suckling, J., Coleman, M. R., Pickard, J. D., Menon, D., & Bullmore, E. D. (2005). Neurophysiological architecture of functional magnetic resonance images of human brain. *Cerebral Cortex*, 15(9), 1332-1342.

Sandmann, P., Dillier, N., Eichele, T., Meyer, M., Kegel, A., Pascual-Marqui, R. D., ... & Debener, S. (2012). Visual activation of auditory cortex reflects maladaptive plasticity in cochlear implant users. *Brain*, awr329.

Schadow, J., Dettler, N., Paramei, G. V., Lenz, D., Fründ, I., Sabel, B. A., & Herrmann, C. S. (2009). Impairments of Gestalt perception in the intact hemifield of hemianopic patients are reflected in gamma-band EEG activity. *Neuropsychologia*, 47(2), 556-568.

Schepers, I. M., Hipp, J. F., Schneider, T. R., Röder, B., & Engel, A. K. (2012). Functionally specific oscillatory activity correlates between visual and auditory cortex in the blind. *Brain*, *135*(3), 922-934.

Schmidt, S., Mante, A., Rönnefarth, M., Fleischmann, R., Gall, C., & Brandt, S. A. (2013). Progressive enhancement of alpha activity and visual function in patients with optic neuropathy: a two-week repeated session alternating current stimulation study. *Brain Stimulation*, *6*(1), 87-93.

Schumacher, E. H., Jacko, J. A., Primo, S. A., Main, K. L., Moloney, K. P., Kinzel, E. N., & Ginn, J. (2008). Reorganization of visual processing is related to eccentric viewing in patients with macular degeneration. *Restorative Neurology and Neuroscience*, *26*(4), 391-402.

Seth, A. K. (2010). A MATLAB toolbox for Granger causal connectivity analysis. *Journal of Neuroscience Methods*, *186*(2), 262-273.

Shafi, M. M., Westover, M. B., Fox, M. D., & Pascual-Leone, A. (2012). Exploration and modulation of brain network interactions with noninvasive brain stimulation in combination with neuroimaging. *European Journal of Neuroscience*, *35*(6), 805-825.

Shepherd, R. B. (2001). Exercise and training to optimize functional motor performance in stroke: driving neural reorganization? *Neural Plasticity*, *8*(1-2), 121-129.

Siegel, M., Donner, T. H., & Engel, A. K. (2012). Spectral fingerprints of large-scale neuronal interactions. *Nature Reviews Neuroscience*, *13*(2), 121-134.

Siegel, M., Donner, T. H., Oostenveld, R., Fries, P., & Engel, A. K. (2008). Neuronal synchronization along the dorsal visual pathway reflects the focus of spatial attention. *Neuron*, *60*(4), 709-719.

Singer, W., & Gray, C. M. (1995). Visual feature integration and the temporal correlation hypothesis. *Annual Review of Neuroscience*, *18*(1), 555-586.

Smirnakis, S. M., Brewer, A. A., Schmid, M. C., Tolia, A. S., Schüz, A., Augath, M., ... & Logothetis, N. K. (2005). Lack of long-term cortical reorganization after macaque retinal lesions. *Nature*, *435*(7040), 300-307.

Smit, D. J., De Geus, E. J., van de Nieuwenhuijzen, M. E., van Beijsterveldt, C. E., van Baal, G. C. M., Mansvelder, H. D., ... & Linkenkaer-Hansen, K. (2011). Scale-free modulation of resting-state neuronal oscillations reflects prolonged brain maturation in humans. *The Journal of Neuroscience*, *31*(37), 13128-13136.

Smit, D. J., Linkenkaer-Hansen, K., & de Geus, E. J. (2013). Long-range temporal correlations in resting-state alpha oscillations predict human timing-error dynamics. *The Journal of Neuroscience*, *33*(27), 11212-11220.

Song, Y., Mu, K., Wang, J., Lin, F., Chen, Z., Yan, X., ... & Zhang, H. (2014). Altered Spontaneous Brain Activity in Primary Open Angle Glaucoma: A Resting-State Functional Magnetic Resonance Imaging Study. *PloS One*, *9*(2), e89493.

Sporns, O. (2013). Network attributes for segregation and integration in the human brain. *Current Opinion in Neurobiology*, *23*(2), 162-171.

Sporns, O., & Zwi, J. D. (2004). The small world of the cerebral cortex. *Neuroinformatics*, *2*(2), 145-162.

Stam, C. J. (2004). Functional connectivity patterns of human magnetoencephalographic recordings: a 'small-world' network?. *Neuroscience Letters*, *355*(1), 25-28.

Stam, C. J., & de Bruin, E. A. (2004). Scale-free dynamics of global functional connectivity in the human brain. *Human Brain Mapping*, *22*(2), 97-109.

Stam, C. J., & Van Straaten, E. C. W. (2012). The organization of physiological brain networks. *Clinical Neurophysiology*, *123*(6), 1067-1087.

Stam, C. J., De Haan, W., Daffertshofer, A., Jones, B. F., Manshanden, I., Van Walsum, A. V. C., ... & Scheltens, P. (2009). Graph theoretical analysis of magnetoencephalographic functional connectivity in Alzheimer's disease. *Brain*, *132*(1), 213-224.

Toosy, A. T., Hickman, S. J., Miszkiel, K. A., Jones, S. J., Plant, G. T., Altmann, D. R., ... & Thompson, A. J. (2005). Adaptive cortical plasticity in higher visual areas after acute optic neuritis. *Annals of Neurology*, *57*(5), 622-633.

Toosy, A. T., Werring, D. J., Bullmore, E. T., Plant, G. T., Barker, G. J., Miller, D. H., & Thompson, A. J. (2002). Functional magnetic resonance imaging of the cortical response to photic stimulation in humans following optic neuritis recovery. *Neuroscience Letters*, *330*(3), 255-259.

Uhlhaas, P. J., & Singer, W. (2012). Neuronal dynamics and neuropsychiatric disorders: toward a translational paradigm for dysfunctional large-scale networks. *Neuron*, *75*(6), 963-980.

Van Den Heuvel, M. P., & Hulshoff Pol, H. E. (2010). Exploring the brain network: a review on resting-state fMRI functional connectivity. *European Neuropsychopharmacology*, *20*(8), 519-534.

van den Heuvel, M. P., Stam, C. J., Kahn, R. S., & Pol, H. E. H. (2009). Efficiency of functional brain networks and intellectual performance. *The Journal of Neuroscience*, *29*(23), 7619-7624.

Van Dijk, H., Schoffelen, J. M., Oostenveld, R., & Jensen, O. (2008). Prestimulus oscillatory activity in the alpha band predicts visual discrimination ability. *The Journal of Neuroscience*, *28*(8), 1816-1823.

Van Essen, D. C., Anderson, C. H., & Felleman, D. J. (1992). Information processing in the primate visual system: an integrated systems perspective. *Science*, *255*(5043), 419-423.

Varela, F., Lachaux, J. P., Rodriguez, E., & Martinerie, J. (2001). The brainweb: phase synchronization and large-scale integration. *Nature Reviews Neuroscience*, *2*(4), 229-239.

von Monakow C. Die Localization im Grosshirn und der Abbau der Funktion durch kortikale Herde. Wiesbaden, Germany: JF Bergmann; 1914.

Voss, P. (2013). Sensitive and critical periods in visual sensory deprivation. *Frontiers in Psychology*, *4*.

Waleszczyk, W. J., Wang, C., Young, J. M., Burke, W., Calford, M. B., & Dreher, B. (2003). Laminar differences in plasticity in area 17 following retinal lesions in kittens or adult cats. *European Journal of Neuroscience*, *17*(11), 2351-2368.

Wandell, B. A., & Smirnakis, S. M. (2009). Plasticity and stability of visual field maps in adult primary visual cortex. *Nature Reviews Neuroscience*, *10*(12), 873-884.

Watts, D. J., & Strogatz, S. H. (1998). Collective dynamics of 'small-world' networks. *Nature*, *393*(6684), 440-442.

Weiskrantz, L., Warrington, E. K., Sanders, M. D., & Marshall, J. (1974). Visual capacity in the hemianopic field following a restricted occipital ablation. *Brain*, *97*(4), 709-728.

Weisz, N., Wühle, A., Monittola, G., Demarchi, G., Frey, J., Popov, T., & Braun, C. (2014). Prestimulus oscillatory power and connectivity patterns predispose conscious somatosensory perception. *Proceedings of the National Academy of Sciences*, *111*(4), E417-E425.

Werring, D. J., Bullmore, E. T., Toosy, A. T., Miller, D. H., Barker, G. J., MacManus, D. G., ... & Thompson, A. J. (2000). Recovery from optic neuritis is associated with a change in the distribution of cerebral response to visual stimulation: a functional magnetic resonance imaging study. *Journal of Neurology, Neurosurgery & Psychiatry*, *68*(4), 441-449.

Yamahachi, H., Marik, S. A., McManus, J. N., Denk, W., & Gilbert, C. D. (2009). Rapid axonal sprouting and pruning accompany functional reorganization in primary visual cortex. *Neuron*, *64*(5), 719-729.

Yu, S., Huang, D., Singer, W., & Nikolić, D. (2008). A small world of neuronal synchrony. *Cerebral Cortex*, *18*(12), 2891-2901.

Zaehle, T., Rach, S., & Herrmann, C. S. (2010). Transcranial alternating current stimulation enhances individual alpha activity in human EEG. *PLoS One*, *5*(11), e13766.

Zappasodi, F., Olejarczyk, E., Marzetti, L., Assenza, G., Pizzella, V., & Tecchio, F. (2014). Fractal Dimension of EEG Activity Senses Neuronal Impairment in Acute Stroke. *PloS One*, *9*(6), e100199.

8. Selbständigkeitserklärung

Michal Bola, Magister in Psychologie

+48 513 939 616

Ernst-Lehmann Str. 2/335

39106 Magdeburg

michalbola@gmail.com

Erklärung

Hiermit erkläre ich, dass ich die von mir eingereichte Dissertation zum dem Thema „Breakdown and restoration of brain synchronization in blindness“ selbständig verfasst, nicht schon als Dissertation verwendet habe und die benutzten Hilfsmittel und Quellen vollständig angegeben wurden.

Weiterhin erkläre ich, dass ich weder diese noch eine andere Arbeit zur Erlangung des akademischen Grades doctor rerum naturalium (Dr. rer. nat.) an anderen Einrichtungen eingereicht habe.

Magdeburg, 24.11.2014

Michal Bola